Aus dem

Institut für Muskuloskelettale Medizin

Klinikum der Ludwig-Maximilians-Universität München

Influence of different knee prosthesis designs on tibiofemoral kinematics and stability: A biomechanical study using human cadaveric knees and a six-degrees-of-freedom joint motion simulator

Dissertation

zum Erwerb des Doktorgrades der Humanbiologie

an der Medizinischen Fakultät

der Ludwig-Maximilians-Universität München

vorgelegt von

Saskia Anna Brendle

aus

Aalen

2025

Mit Genehmigung der Medizinischen Fakultät der

Ludwig-Maximilians-Universität München

Erstes Gutachten:	Prof. Dr. Dr. Thomas M. Grupp
Zweites Gutachten:	Prof. Dr. Steffen Peldschus
Drittes Gutachten:	Prof. Dr. Stefan Piltz
Dekan:	Prof. Dr. med. Thomas Gudermann
Tag der mündlichen Prüfung:	13.11.2025

Affidavit

LMU LUDWIG-MAXIMILIANS-UNIVERSITÄT MÜNCHEN

Dekanat Medizinische Fakultät
Promotionsbüro

Eidesstattliche Versicherung

Brendle, Saskia Anna

Name, Vorname

Ich erkläre hiermit an Eides statt, dass ich die vorliegende Dissertation mit dem Thema:

Influence of different knee prosthesis designs on tibiofemoral kinematics and stability: A biomechanical study using human cadaveric knees and a six-degrees-of-freedom joint motion simulator

selbständig verfasst, mich außer der angegebenen keiner weiteren Hilfsmittel bedient und alle Erkenntnisse, die aus dem Schrifttum ganz oder annähernd übernommen sind, als solche kenntlich gemacht und nach ihrer Herkunft unter Bezeichnung der Fundstelle einzeln nachgewiesen habe.

Ich erkläre des Weiteren, dass die hier vorgelegte Dissertation nicht in gleicher oder in ähnlicher Form bei einer anderen Stelle zur Erlangung eines akademischen Grades eingereicht wurde.

Tuttlingen, den 21.11.2025
Ort, Datum

Saskia Anna Brendle
Unterschrift Doktorandin/Doktorand

Congruency of submitted versions

LMU LUDWIG-MAXIMILIANS-UNIVERSITÄT MÜNCHEN

Dekanat Medizinische Fakultät
Promotionsbüro

Erklärung zur Übereinstimmung der gebundenen Ausgabe der Dissertation mit der elektronischen Fassung

Brendle, Saskia Anna

Name, Vorname

Hiermit erkläre ich, dass die elektronische Version der eingereichten Dissertation mit dem Titel:

Influence of different knee prosthesis designs on tibiofemoral kinematics and stability: A biomechanical study using human cadaveric knees and a six-degrees-of-freedom joint motion simulator

in Inhalt und Formatierung mit den gedruckten und gebundenen Exemplaren übereinstimmt.

Tuttlingen, den 21.11.2025
Ort, Datum

Saskia Anna Brendle
Unterschrift Doktorandin/Doktorand

Table of content

List of abbreviations

°	Degree
3D	Three-dimensional
ACL	Anterior cruciate ligament
AP	Anterior-posterior
BMI	Body mass index
CAD	Computer aided design
CR	Cruciate-retaining
CS	Cruciate-sacrificing
CT	Computed tomography
FE	Flexion-extension
FFC	Flexion facet centers
Hz	Hertz
IE	Internal-external
LFC	Lateral flexion facet center
MFC	Medial flexion facet center
ML	Medial-lateral
mm	Millimeter
MP	Medial-pivot
MS	Medial-stabilized
N	Newton
Nm	Newtonmeter
OA	Osteoarthritis
PCL	Posterior cruciate ligament
PD	Proximal-distal
PS	Posterior-stabilized
RMSE	Root mean square error
TKA	Total knee arthroplasty
UC	Ultra-congruent
VV	Varus-valgus

List of figures

List of publications

Publications as part of the cumulative dissertation

Brendle SA, Krueger S, Grifka J, Müller PE, Grupp TM. A new methodology for the accurate measurement of tibiofemoral kinematics in human cadaveric knees: An evaluation of the anterior–posterior laxity pre- and post-cruciate ligament resection. *Life* 2024, *14*, 877. https://doi.org/10.3390/life14070877

Brendle SA, Krueger S, Fehrenbacher J, Grifka J, Müller PE, Mihalko WM, Richter B, Grupp TM. Kinematic patterns of different loading profiles before and after total knee arthroplasty: A cadaveric study. *Bioengineering* 2024, *11*, 1064. https://doi.org/10.3390/bioengineering11111064

Brendle SA, Krueger S, Grifka J, Müller PE, Mihalko WM, Richter B, Grupp TM. Constraint of different knee implant designs under anterior−posterior shear forces and internal−external rotation moments in human cadaveric knees. *Bioengineering* 2025, *12*, 87. https://doi.org/10.3390/bioengineering12010087

Additional publications

Henke P, Meier J, Ruehrmund L, Brendle SA, Krueger S, Grupp TM, Lutter C, Woernle C, Bader R, Kebbach M. Modeling of the native knee with kinematic data derived from experiments using the VIVO™ joint simulator: A feasibility study. *BioMedical Engineering OnLine* 2024, *23.* https://doi.org/10.1186/s12938-024-01279-z

Behn A, Brendle SA, Ehrnsperger M, Zborilova M, Grupp TM, Grifka J, **Schäfer N, Grässel S.** Filtered and unfiltered lipoaspirates reveal novel molecular insights and therapeutic potential for osteoarthritis treatment. *Front. Cell Dev. Biol.* 2025, 13:1534281. https://doi.org/10.3389/fcell.2025.1534281

Podium presentations

Brendle SA, Krueger S, Grifka J, Müller PE, Grupp TM. Tibiofemoral gaps of human cadaveric knees before and after sacrificing both cruciate ligaments. *28th Congress of the European Society of Biomechanics,* Maastricht, Netherlands. 2023.

Krueger S, Brendle SA, Benz K, Merckle C, Grupp TM. Influence of biomechanical loading on the physical behavior of a hydrogel after injection into native human knees. *28th Congress of the European Society of Biomechanics,* Maastricht, Netherlands. 2023.

Brendle SA, Krueger S, Grifka J, Müller PE, Grupp TM. Condylar motion of human cadaveric knees before and after sacrificing both cruciate ligaments. *34th Annual Congress of the International Society of Technology in Arthroplasty,* New York, USA. 2023.

Brendle SA, Dupraz I, Krueger S, Grifka J, Müller PE, Grupp TM. Comparison of two methods used to assess gaps in total knee arthroplasty. *34th Annual Congress of the International Society of Technology in Arthroplasty,* New York, USA. 2023.

Henke P, Meier J, Ruehrmund L, Brendle SA, Krueger S, Grupp TM, Woernle C, Lutter C, Bader R, Kebbach M. Generierung eines muskuloskelettalen Mehrkörpermodells des Tibiofemoralgelenks basierend auf experimentellen Untersuchungen am Humanpräparat mittels 6-Freiheitsgrad Gelenksimulator. *10th Congress of the International Federation for the Promotion of Mechanism and Machine Science*, Rostock, Germany. 2024.

Brendle SA, Krueger S. Optimize your lab testing performance for medical devices. *Zeiss Quality Innovation Days.* 2024.

Grupp TM, Puente Reyna AL, Schierjott RA, Pfaff A, Rusch S, Brendle SA, Mulliez MA, Holderied M, Weiss JB, Hettich G, Ortigas Vásquez A, Dohm J, Sauer A, Renaudot R, Taylor WR, Richter B, Krueger S, Schwiesau J, Maas A, Schilling C. Overview biomechanical research laboratories & current innovations – Il laboratorio di biomeccanica & innovazioni attuali. *Scientific Dialogue Italian Surgeon Product Course 25th THI-Aesculap collaboration*, Tuttlingen, Germany. 2024.

Brendle SA, Krueger S, Grifka J, Müller PE, Mihalko WM, Richter B, Grupp TM. Anterior-posterior constraint of two different knee inlay designs in mid-flexion. *35th Congress of the International Society of Technology in Arthroplasty,* Nashville, USA. 2024.

Richter B, Altermann B, Maas A, Sauer A, Krueger S, Dupraz I, Brendle SA, Giurea A, Hasegawa M, Minoda Y, Windhagen H, Mihalko WM, Grupp TM. Conception, biomechanical formation and validation of a unique knee system platform design for primary and revision knee arthroplasty in regard to tibio-femoral kinematics. *32nd Annual Meeting of the European Orthopaedic Research Society,* Aalborg, Denmark. 2024.

Grupp TM, Taylor WR, Larrainzar-Garijo R, Müller PE, Ochs BG, Windhagen H, McHugh G, Schierjott-Hermle RA, Richter B, Brendle SA, Renaudot R, Maas A. Future perspectives in navigated total knee arthroplasty - individual alignment, functional phenotypes & biomechanical evidence. *32nd Annual Meeting of the European Orthopaedic Research Society,* Aalborg, Denmark. 2024.

Grupp TM, Taylor WR, Larrainzar-Garijo R, Müller PE, Ochs BG, McHugh G, Windhagen H, Schierjott-Hermle RA, Richter B, Brendle SA, Renaudot R, Maas A. Perspectives in navigated total knee arthroplasty - Individual alignment, functional phenotypes & biomechanical evidence. *"Pheno4U-TKA – Intraoperative technology to assess & select patient gait patterns" Scientific Dialogue & Dinner Meeting.* South Brisbane, Australia. 2024.

Grupp TM, Arno S, Richter B, Taylor WR, Larrainzar-Garijo R, Mueller PE, Ochs BG, Windhagen H, Gerdesmeyer L, McHugh G, Schierjott RA, Brendle SA, Renaudot R, Maas A. Pheno4U-TKA & oneKNEE - Entdecke die Zukunft der personalisierten Knieendoprothetik – Symposium Chair "Endoprothetik der Zukunft – zwischen personalisierter Versorgung und Fließband". *AE-Kongress,* Dresden, Germany. 2024.

Grupp TM, Taylor WR, Larrainzar-Garijo R, Mueller PE, Woiczinski M, Ochs BG, Windhagen H, Gerdesmeyer L, McHugh G, Richter B, Schierjott RA, Brendle SA, Renaudot R, Maas A. "Kontroverse Debatten Navigation & Robotik" – Langfristige Forschungsstrategie und konsequente Datenanalyse aus Biomechanik und funktionaler Phänotypisierung – die Navigation hat Zukunft! "Tägliche Herausforderugen & Aktuelle Entwicklungen in der Knieendoprothetik". *Hamburg-Schleswig-Holsteiner Symposium für Knie-Endoprothetik*, Hamburg, Germany. 2025.

Grupp TM, Taylor WR, Larrainzar-Garijo R, Mueller PE, Woiczinski M, Ochs BG, Windhagen H, Gerdesmeyer L, McHugh G, Richter B, Schierjott RA, Brendle SA, Renaudot R, Maas A. "Phänotypisierung in der personalisierten Knieendoprothetik" – Pheno4U®-TKA - Individuelles Alignment & biomechanische Evidenz. *Winglet TV Event,* München, Germany. 2025.

Grupp TM, Taylor WR, Larrainzar-Garijo R, Mueller PE, Woiczinski M, Ochs BG, Windhagen H, Gerdesmeyer L, McHugh G, Richter B, Schierjott RA, Brendle SA, Renaudot R, Maas A. "Phänotypisierung in der personalisierten Knieendoprothetik" – Zukunftsvision und weitere Stufen Pheno4U®-TKA. *Winglet TV Event,* München, Germany. 2025.

Grupp TM, Taylor WR, Larrainzar-Garijo R, Mueller PE, Woiczinski M, Ochs BG, Windhagen H, Gerdesmeyer L, McHugh G, Richter B, Schierjott RA, Brendle SA, Renaudot R, Maas A. Phenotypes in personalised total knee arthroplasty – Pheno4U®-TKA – Individual alignment & biomechanical evidence and future perspectives & next steps Pheno4U®-TKA. *Guest Lecture London Health Science Center University Hospital, University of Western Ontario*, London, Canada. 2025.

Grupp TM, Taylor WR, Larrainzar-Garijo R, Mueller PE, Woiczinski M, Ochs BG, Windhagen H, Gerdesmeyer L, McHugh G, Richter B, Schierjott RA, Brendle SA, Renaudot R, Maas A. Phenotypes in personalised total knee arthroplasty – Pheno4U®-TKA – Individual alignment & biomechanical evidence and future perspectives & next steps Pheno4U®-TKA. *Guest Lecture London Bone & Joint Institute by invitation of Assoc. Prof. Ryan Willing & Assoc. Prof. Louis Miguel Ferreira*, University of Western Ontario, London, Canada. 2025.

Grupp TM, Taylor WR, Larrainzar-Garijo R, Mueller PE, Woiczinski M, Ochs BG, Windhagen H, Mihalko WM, McHugh G, Richter B, Ortigas-Vásquez A, Sauer A, Brendle SA, Renaudot R, Maas A. Perspective Talk - ICORS Symposium "Advancing clinical impact of movement analysis and patient activity - Monitoring combining wearables, AI, computer vision & data-driven approaches" − Pre-/intra-op knee kinematic and ligament stability evaluation integrated in the workflow towards functional phenotypes in total knee arthroplasty. *Annual Meeting of the Orthopaedic Research Society*, Phoenix, USA. 2025.

Poster presentations

Brendle SA, Krueger S, Grupp TM. A novel approach to measure tibiofemoral kinematics in human cadaveric knees with intact capsule. *28th Congress of the European Society of Biomechanics,* Maastricht, Netherlands. 2023.

Brendle SA, Krueger S, Grifka J, Müller PE, Grupp TM. Influence of the cruciate ligaments on tibiofemoral gaps. *Annual Meeting of the Orthopaedic Research Society,* Long Beach, USA. 2024.

Brendle SA, Krueger S, Grifka J, Müller PE, Grupp TM. Condylar motion patterns during passive knee flexion are not only a result of osteoarthrosis. *Annual Meeting of the Orthopaedic Research Society,* Long Beach, USA. 2024.

Brendle SA, Krueger S, Grifka J, Müller PE, Mihalko WM, Richter B, Grupp TM. Influence of a post-cam mechanism on femoral rollback of human cadaveric knees. *35th Congress of the International Society of Technology in Arthroplasty,* Nashville, USA. 2024.

Contribution to the publications

The contributions of the co-authors to the three publications of this cumulative dissertation are submitted separately. All authors agreed that the publications are used within this dissertation and must not be part of another doctoral thesis.

Contribution to publication I

Within the first publication, the author of this dissertation (SB) was in charge of the conception and design of the study. She developed and validated the new methodology for precise measurement of tibiofemoral kinematics in human cadaveric knees using Mimics (Materialise, Leuven, Belgium) and 3-matic medical (Materialise, Leuven, Belgium), as well as MATLAB (MathWorks Inc., Natick, MA, USA), ARAMIS 12M (Carl Zeiss GOM Metrology GmbH, Braunschweig, Germany) and a six-degrees-of-freedom joint motion simulator (VIVO, Advanced Mechanical Technologies Inc., Watertown, MA, USA). Furthermore, she carried out the preparation of the cadaveric specimens and the complete experimental test series. She was fully responsible for the data collection, analysis, statistical evaluation and interpretation of the results. To this end, she developed complex custom MATLAB scripts. In addition, SB was responsible for the literature review, drafting of the manuscript, the submission and review process.

Contribution to publication II

Within the second publication, SB was responsible for the design of the study and the methodology. Furthermore, she planned the implantation of the TKA components and assisted during the surgery. SB conducted the entire experimental test series and was fully responsible for the data collection, analysis, statistical evaluation and interpretation of the results. For this, she created complex MATLAB scripts. In addition, she was in charge of the literature review, drafting of the manuscript, as well as for the submission and review process.

Contribution to publication III

For the third publication, SB was responsible for the study design and the methodology. She carried out the entire experimental test series and was in charge of the data collection, analysis, statistical evaluation and interpretation of the results. Furthermore, she conducted the literature review, drafted the manuscript, and managed the submission and review process.

1 Abstract (English)

Background

Total knee arthroplasty (TKA) is an effective treatment for patients with severe knee osteoarthritis. Despite continuous advances in implant design and good long-term results, numerous studies point out that up to 20% of patients remain dissatisfied after TKA. As one of the major goals of TKA is to restore the physiological knee function, it is hypothesized that the ability of the prosthesis to recreate the native tibiofemoral kinematics and stability plays a crucial role in enhancing patient satisfaction. However, the influence of different TKA designs on tibiofemoral kinematics and stability within individual ligament conditions remains unclear.

Objective

To enable the selection of the optimal implant design for individual patients within a more personalized approach, this dissertation primarily aimed to investigate the effects of different TKA designs on tibiofemoral kinematics and stability within individual ligament situations under highly controlled experimental conditions.

Materials and methods

In the first step, a new methodology was developed to accurately measure the tibiofemoral kinematics in human cadaveric knees using a six-degrees-of-freedom joint motion simulator. In the second step, the new methodology was used to apply passive and complex active loading profiles to thirteen fresh-frozen human cadaveric knees in the native condition and after implantation of symmetrical implants with and without a post-cam mechanism (PS and CR/CS). Finally, the constraint of different TKA designs (CR/CS, MS and PS) was investigated during anterior-posterior shear forces and internal-external rotation moments at different flexion angles.

Results

The new methodology allowed the accurate tracking of landmark-based femoral and tibial coordinate systems and their corresponding bone geometries with good control accuracy and kinematic reproducibility. The comparison between different TKA designs and the native condition during passive and complex active loading scenarios revealed that neither TKA design was superior in restoring the mean native kinematics. However, both TKA designs were capable of restoring the individual kinematic behaviour of the native knees during passive and complex active loading conditions. During anterior-posterior shear forces and internal-external rotation

moments, it was found that despite variations in ligament conditions and individual implant positioning, both symmetrical designs exhibited a similar anterior-posterior range of motion for the medial and lateral condyles, whereas the medial-stabilized implant design showed less anterior-posterior translation medially.

Conclusion and outlook

Overall, the results of this dissertation highlight the importance of individual kinematic analyses to select the most appropriate TKA design for a specific patient and provide valuable insights into the stability and kinematic performance of different TKA designs. This knowledge forms the basis for developing more effective and personalized treatment strategies for patients undergoing TKA and thereby helps to improve patient satisfaction.

2 Zusammenfassung (Deutsch)

Hintergrund

Die totale Knie Arthroplastik (TKA) ist eine wirksame Behandlung für Patienten mit schwerer Gonarthrose. Trotz kontinuierlicher Weiterentwicklung der Implantatdesigns und guter Langzeitergebnisse zeigen zahlreiche Studien, dass bis zu 20 % der Patienten nach einer TKA unzufrieden sind. Da die Wiederherstellung der physiologischen Kniefunktion eines der Hauptziele der TKA ist, wird angenommen, dass die Fähigkeit der Prothese, die native tibio-femorale Kinematik und Stabilität nachzubilden, eine entscheidende Rolle bei der Verbesserung der Patientenzufriedenheit spielt. Der Einfluss unterschiedlicher TKA-Designs auf die tibio-femorale Kinematik und Stabilität unter individuellen Bandverhältnissen ist bisher jedoch nicht bekannt.

Zielsetzung

Um die Auswahl des optimalen Implantatdesigns für einzelne Patienten in einem personalisierten Ansatz zu ermöglichen, zielte diese Dissertation hauptsächlich darauf ab, den Einfluss verschiedener TKA-Designs auf die tibio-femorale Kinematik und Stabilität bei individuellen Bandbedingungen unter hochkontrollierten experimentellen Bedingungen zu untersuchen.

Material und Methoden

Im ersten Schritt wurde eine neue Methodik entwickelt, um die tibio-femorale Kinematik in humanen Kniepräparaten mit Hilfe eines Gelenksimulators mit sechs Freiheitsgraden präzise zu ermitteln. Im zweiten Schritt wurde die neue Methodik angewendet, um die Kinematik von dreizehn humanen Kniepräparaten unter passiven und komplexen aktiven Belastungsszenarien im nativen Zustand und nach der Implantation von symmetrischen Implantaten mit und ohne Post-Cam-Mechanismus (PS und CR/CS) zu analysieren. Schließlich wurde der „Constraint“ verschiedener TKA-Designs (CR/CS, MS und PS) unter anterior-posterioren Scherkräften und internen-externen Rotationsmomenten bei verschiedenen Flexionswinkeln untersucht.

Ergebnisse

Die neue Methodik ermöglichte die genaue Verfolgung der landmarkenbasierten femoralen und tibialen Koordinatensysteme und der entsprechenden Knochengeometrien mit guter Regelgenauigkeit und kinematischer Reproduzierbarkeit. Der Vergleich verschiedener TKA-Designs mit dem nativen Zustand während passiver und komplexer aktiver Belastungsszenarien

zeigte, dass kein TKA-Design bei der Wiederherstellung der mittleren nativen Kinematik überlegen war. Beide TKA-Designs waren jedoch in der Lage, das individuelle kinematische Verhalten der nativen Knie während passiver und komplexer aktiver Belastungsbedingungen wiederherzustellen. Während der Applikation anterior-posteriorer Scherkräfte und interner-externer Rotationsmomente wurde festgestellt, dass trotz Variationen in den Bandbedingungen und der individuellen Implantatpositionierung beide symmetrischen Designs einen ähnlichen anterior-posterioren Bewegungsumfang für die medialen und lateralen Kondylen aufwiesen, während das medial stabilisierte Implantatdesign medial eine geringere anterior-posteriore Translation zeigte.

Fazit und Ausblick

Insgesamt unterstreichen die Ergebnisse dieser Dissertation die Bedeutung individueller kinematischer Analysen für die Auswahl des am besten geeigneten TKA-Designs für einen bestimmten Patienten und liefern wertvolle Einblicke in die Stabilität und das kinematische Verhalten verschiedener TKA-Designs. Dieses Wissen bildet die Grundlage, um effektive und personalisierte Behandlungsstrategien für Patienten, die sich einer TKA unterziehen, zu entwickeln und die Patientenzufriedenheit zu verbessern.

3 Introduction

3.1 The human knee joint

The knee is the largest joint in the human body and consists of two partial joints within a single joint capsule: the patellofemoral and tibiofemoral joints (1–3). In the tibiofemoral joint, the medial and lateral condyles of the distal femur slide on the proximal tibial plateau, creating a six-degrees-of-freedom motion system (Figure 1). Rotational movement consists of flexion–extension, adduction−abduction and internal−external. Translational movement is possible in the medial–lateral and anterior−posterior directions, as well as by compression and distraction of the knee joint (proximal−distal translation) (3–5). Thus, in terms of function, the knee is a gliding hinge joint (1–3, 5).

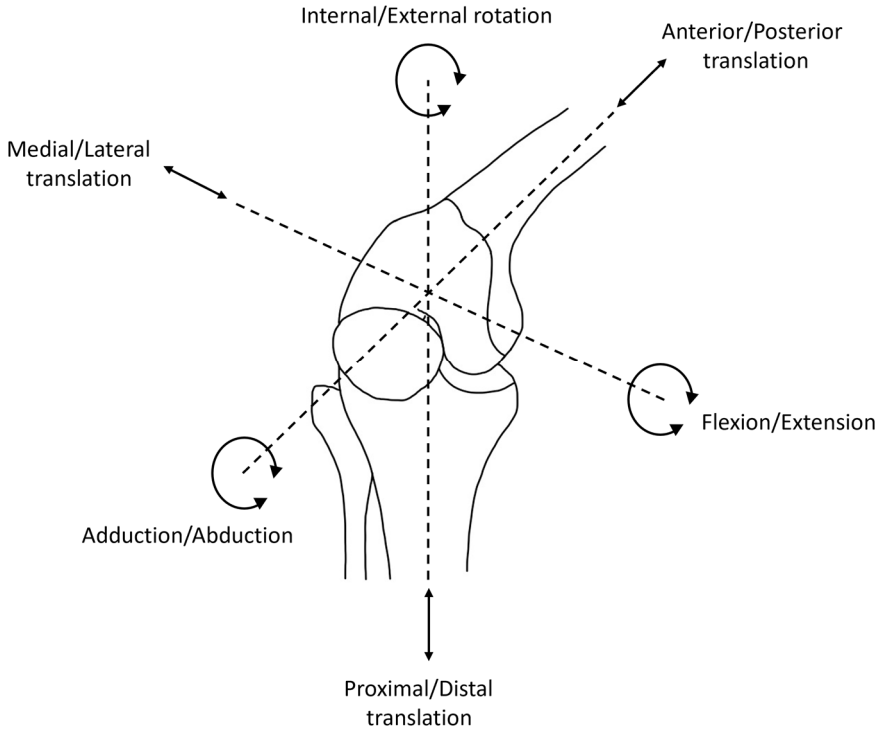

Figure 1. The tibiofemoral joint creates a six-degrees-of-freedom motion system. Translational movement is possible in the medial-lateral, anterior-posterior and proximal-distal directions. Rotational movement consists of flexion-extension, adduction-abduction and internal-external. Adapted from (4).

A number of ligaments and other structures allow for high mobility while providing passive stability to the knee joint in all directions (3, 4). The menisci compensate the femorotibial incongruence, cushion compressive loads, increase the joint stability and reduce friction during movement (3–5). Knee stability is further enhanced by the cruciate ligaments, which prevent

anterior and posterior displacement of the tibia, and the medial and lateral collateral ligaments, which provide stability against adduction and abduction as well as internal and external rotation (1, 3, 5). In addition, the ventral and dorsal muscle groups surrounding the knee have a stabilizing effect on the joint (1, 3).

3.2 Knee osteoarthritis

Osteoarthritis (OA) is the most common degenerative disorder of the knee and one of the leading causes of disability (6). It affects hundreds of millions of people worldwide (7–9), with a prevalence of more than 30% in people over the age of 65 (10) and is characterized by the progressive degeneration of articular cartilage. In advanced stages, complete destruction of the cartilage occurs and the adjacent bone responds with the formation of osteophytes and subchondral sclerosis. At this point, patients experience restricted joint mobility, stiffness, and severe pain due to bone friction (9). Initial conservative management is targeted towards symptom control and may include physiotherapy and medication. If these methods do not sufficiently improve the patient's quality of life, joint replacement surgery may be considered (11, 12).

3.3 Total knee arthroplasty

Total knee arthroplasty (TKA) is an effective treatment for patients with end-stage knee osteoarthritis. The goal of TKA is to relieve pain, restore the physiological joint function, and consequently improve the patient's quality of life. During the procedure, the bony surfaces of the distal femur and the proximal tibia are replaced with metal components, and a polyethylene tibia inlay is typically used as a bearing that is attached to the tibial plateau. Surgeons can choose between different TKA designs, with varying degrees of congruence, resulting in different kinematics and stability (13–17) (Figure 2). The most commonly used implants are symmetrical designs that preserve the posterior cruciate ligament (PCL) during implantation, known as cruciate retaining (CR) implants (18, 19). These designs have been established for years and have shown promising long-term results (18, 20). Cruciate retaining/sacrificing (CR/CS) designs can be used with or without an intact PCL and provide stability through a steeper anterior ramp. In contrast, posterior-stabilized (PS) implants substitute the PCL with a post-cam mechanism. Medial-stabilized (MS) and medial-pivot (MP) designs are more recent innovations that have been increasingly used in the last few years (18–20). These designs are characterized by a higher conformity of the medial compartment compared to the lateral compartment to mimic the kinematic pattern of the healthy knee (21–24).

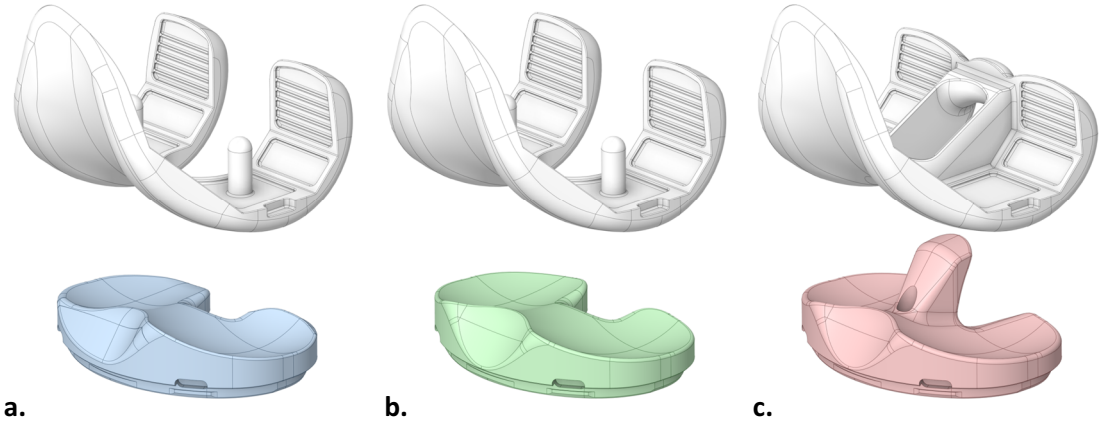

Figure 2. Illustration of different knee implant designs. (a) Medial-stabilized (MS), (b) cruciate retaining/sacrificing (CR/CS) and (c) posterior-stabilized (PS) femoral component and tibia inlay designs for a right knee (oneKNEE®, Aesculap AG, Tuttlingen, Germany). All inlay designs can be fixed to the same tibial component.

Despite continuous advances in implant design and good implant survival rates (18, 20), studies indicate that up to 20% of patients are dissatisfied with the results of their TKA (25–32). Patients report persistent pain, reduced joint mobility, or unmet expectations (27, 32–34). Factors influencing patient satisfaction are multifaceted and range from preoperative to surgical and postoperative rehabilitation factors (25–30, 35). Surgical factors include the precision of surgical techniques and the selection of the optimal implant type and alignment strategy. As the fundamental objective of TKA is the restoration of physiological knee function, it is hypothesized that the ability of the prothesis to replicate the native tibiofemoral kinematics and stability enhances patient satisfaction (36, 37). Nevertheless, given the high inter-individual variability of the knee, selecting the most appropriate implant design and alignment strategy remains a challenge (16, 38). With the capabilities of modern navigation and robotic systems and the growing importance of personalized medicine in orthopaedics, efforts are being made to tailor treatments to the individual needs and characteristics of patients (37, 39). However, the influence of different knee prothesis designs on tibiofemoral kinematics and stability within individual ligamentous conditions is not yet fully understood.

3.4 *In vitro* studies

Biomechanical *in vitro* studies using human cadaveric specimens play a central role in the development and optimization of knee implants. These preclinical investigations allow detailed analysis of the mechanical behaviour of implant designs and fixation methods under controlled

conditions (40, 41). By using standardized testing protocols in combination with complex joint motion simulators, different design parameters and surgical techniques can be systematically assessed and compared (13, 17, 42, 43). In addition, biomechanical *in vitro* studies offer insights into the functional behaviour of the knee joint that are unattainable *in vivo* due to ethical constraints (44, 45). Furthermore, these investigations serve as a basis for the development of validated computer models for further simulating the *in vivo* situation and enable a deeper understanding of the complex biomechanical interactions in the knee joint (46). For this reason, findings from *in vitro* studies are essential to improve surgical outcomes after TKA.

To date, many *in vitro* kinematic analyses have been performed using mechanical knee rigs, which use muscle forces to induce movement (13, 42, 43, 45). However, this methodology inherently lacks independent control over individual degrees of freedom, limiting the ability to accurately reproduce passive joint mechanics. In particular, scenarios without active muscle force contributions, such as the assessment of passive joint laxity or passive flexion as performed intraoperatively, cannot be precisely replicated. However, this capability is relevant to research questions in the field of intraoperative navigation and robotics. Furthermore, the reliance on muscle-driven systems limits the complexity of the applied loading conditions, typically restricting analyses to deep knee bend and precluding the investigation of more complex loading scenarios, such as level walking or stair ascent. Moreover, kinematic data acquisition in current methodologies is often limited to the tracking of coordinate systems, without a direct link to the corresponding bone geometries (13, 43, 47, 48). This indirect approach impairs detailed characterization of the relative position of the medial and lateral femoral condyles with respect to the proximal tibia and may be a potential cause for misinterpretation of normal movement. In addition, precise control of force application along anatomically relevant axes is compromised, reducing data comparability and repeatability.

3.5 Research questions and objectives

To enable more individual approaches and select the optimal implant design and alignment strategy for an individual patient to improve patient satisfaction after TKA, a more comprehensive understanding of the biomechanics of the native knee and the influence of different TKA designs is essential. Acquiring this fundamental knowledge requires investigations within a highly controlled environment. Therefore, the main objective of this dissertation was to investigate the influence of different knee prothesis designs on the tibiofemoral kinematics and stability of human cadaveric knees in a six-degrees-of-freedom joint motion simulator during various activities.

Given the constraints of existing methodologies used for *in vitro* kinematic analyses, the first objective of this dissertation focused on the development of a new methodology to accurately measure the tibiofemoral kinematics in human cadaveric knees. The **first publication**, entitled "A new methodology for the accurate measurement of tibiofemoral kinematics in human cadaveric knees: an evaluation of the anterior-posterior laxity pre- and post-cruciate ligament resection" introduced the new workflow, validated relevant parameters and showed a potential application. The strength of this innovative approach is the accurate tracking of landmark-based femoral and tibial coordinate systems and their corresponding bone geometries within a controlled environment by combining a 3D measurement system and a six-degrees-of-freedom joint motion simulator. The 3D fitting integrated in this workflow allows for a precise and reproducible placement of the landmark-based coordinate systems even with a closed knee capsule (Figure 3) (49, 50).

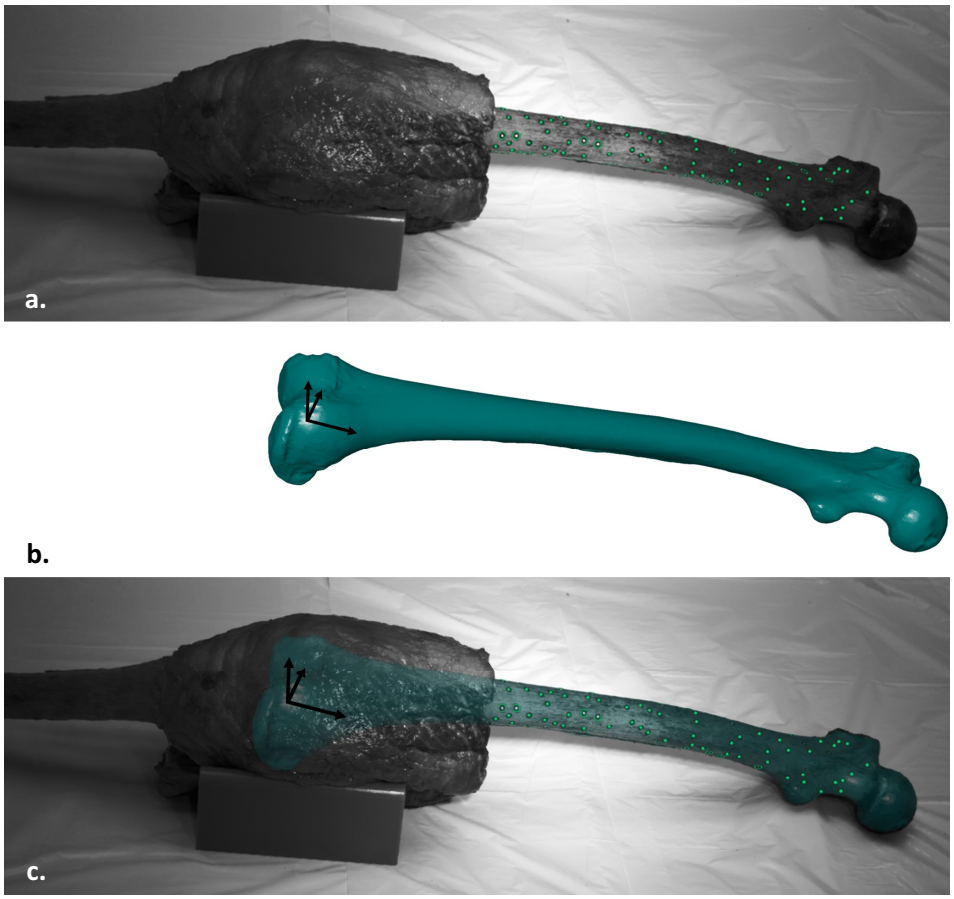

Figure 3. Illustration of the 3D fitting procedure for the femur. (a) Cadaveric femur with measuring points marked in green. (b) Segmented computed tomography (CT) scan shown in blue, containing a landmark-based femoral coordinate system. (c) Cadaveric femur with 3D-fitted segmented CT scan in blue. Adapted from (51).

Furthermore, the 3D fitting procedure enables the controlled positioning of the knee specimen in the joint motion simulator by aligning the landmark-based coordinate systems of the knee with the axes of the joint motion simulator (Figure 4). The new workflow therefore provides a basis for consistent force application across different specimens and tracking of the resulting kinematics, with the possibility to apply both passive and complex loading profiles. In addition, the six-degrees-of-freedom joint motion simulator demonstrated good control accuracy, as well as kinematic reproducibility, further validating the robustness of this approach.

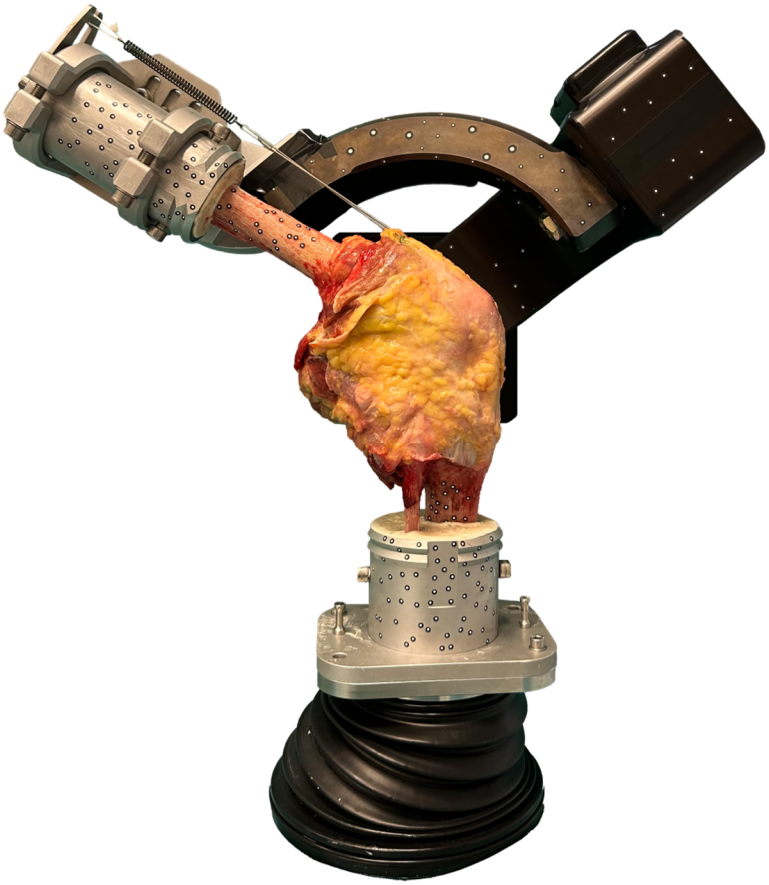

Figure 4. Experimental setup showing the knee specimen mounted on the six-degrees-of-freedom joint motion simulator. Adapted from (51).

In the **second publication**, entitled “Kinematic patterns of different loading profiles before and after total knee arthroplasty: a cadaveric study”, the new workflow was used to identify differences in the kinematics during complex active and passive movements, in the native condition and with two different TKA designs. As previously stated, modern surgical navigation and robotic systems enable the intraoperative assessment of passive knee kinematics and stability and provide real-time feedback on various parameters, enabling adjustments to implant type, positioning, and overall alignment during surgery (37, 39, 52–61). For this reason,

intraoperative kinematic analysis could be used to implement a more personalized approach and assist the surgeon in restoring the physiological knee function by selecting the most appropriate implant design for each patient, as the only opportunity for adjustment is during surgery. However, it remains to be clarified whether passive movements can reveal kinematic differences between the native knee and different TKA designs (39, 55). Furthermore, it is necessary to understand whether there is an association between passive knee kinematics and knee kinematics during complex active activities of daily living. To date, it has been challenging to draw clear conclusions about kinematic differences between passive and complex active activities, primarily due to the numerous influencing factors, including the diverse methods used to measure kinematics during different activities (39, 52, 56). This shows the importance of a highly controlled environment for valid comparison between different conditions and loading profiles to eliminate the problem of large individual and technical differences. Therefore, passive flexion and stair ascent loading profiles were applied to thirteen cadaveric knees in the native condition and after implantation of two different TKA designs to determine which design better replicates the native kinematics of the knee and whether the kinematic patterns of passive and complex active loading scenarios lead to the same choice of implant design.

As instability is one of the main causes for revision after total knee arthroplasty (18, 19, 62, 63), it is important to focus not only on kinematics but also ensure adequate stability while selecting the most appropriate implant design to restore physiological knee function in a more personalized approach. For this reason, the surgeon needs to understand how much stability a particular implant design provides at different flexion angles. To accurately compare the anterior-posterior constraints of different implant designs, a highly controlled environment and precise force application are essential. Moreover, it is important to evaluate not only the implant itself but also its behaviour under clinically relevant conditions imposed by the surrounding ligament structures. However, *in vivo* studies do not allow for the comparative evaluation of different implant designs within the same ligamentous situation under controlled force application (35, 55, 64–70). Therefore, the workflow developed within this dissertation was used to characterize the constraint of three different TKA designs during anterior–posterior shear forces and internal–external rotation moments at various flexion angles in thirteen human cadaveric knees, what resulted in the **third publication**, entitled “Constraint of different knee implant designs under anterior−posterior shear forces and internal−external rotation moments in human cadaveric knees”.

3.6 Conclusion

This dissertation aimed to provide a better understanding of the influence of different knee prothesis designs on the tibiofemoral kinematics and stability of human cadaveric knees in a six-degrees-of-freedom joint motion simulator during various activities. To this end, a new methodology was developed to accurately measure tibiofemoral kinematics in human cadaveric knees by tracking the relative positions of landmark-based femoral and tibial coordinate systems and their corresponding bone geometries. This methodology has been used to investigate the kinematics during passive and complex active loading scenarios as well as the constraint of different implant designs within individual ligament situations under highly controlled experimental conditions. The results highlight the importance of individual kinematic analyses to select the most appropriate TKA design for each patient and help to understand how much stability a particular implant design provides at different flexion angles, thereby providing a basis for further investigations towards a more personalized approach to address the specific needs of individual patients and improve surgical outcomes after TKA.

4 Publications

4.1 Publication I: A new methodology for the accurate measurement of tibiofemoral kinematics in human cadaveric knees: An evaluation of the anterior-posterior laxity pre- and post-cruciate ligament resection

Authors:	Saskia A. Brendle, Sven Krueger, Joachim Grifka, Peter E. Müller, Thomas M. Grupp
Journal:	Life – Special Issue: Advances in Knee Biomechanics
Volume:	14
Pages:	15
Year:	2024
DOI:	https://doi.org/10.3390/life14070877
Impact factor:	3.2 (according to InCites Journal Citation Reports 2023)

life

MDPI

Article

A New Methodology for the Accurate Measurement of Tibiofemoral Kinematics in Human Cadaveric Knees: An Evaluation of the Anterior–Posterior Laxity Pre- and Post-Cruciate Ligament Resection

Saskia A. Brendle [1,2,*], Sven Krueger [1], Joachim Grifka [3], Peter E. Müller [2] and Thomas M. Grupp [1,2]

[1] Research & Development, Aesculap AG, 78532 Tuttlingen, Germany
[2] Department of Orthopaedic and Trauma Surgery, Musculoskeletal University Center Munich (MUM), Campus Grosshadern, LMU Munich, 81377 Munich, Germany
[3] Department of Orthopaedics, Asklepios Klinikum, 93077 Bad Abbach, Germany
* Correspondence: saskia.brendle@aesculap.de

Abstract: Anterior–posterior (AP) stability is an important measure of knee performance after total knee arthroplasty (TKA). To improve the stabilizing effect of implants designed to compensate for the loss of the cruciate ligaments, it is important to understand the tibiofemoral contact situation within the native ligamentous situation of the knee and how it changes after cruciate ligament resection. This in vitro study introduces a new approach to accurately measure the tibiofemoral kinematics in a six-degrees-of-freedom joint motion simulator by tracking landmark-based coordinate systems and their corresponding bone geometries. The tibiofemoral contact situation was investigated by projecting the medial and lateral flexion facet centers onto the tibial plateau under AP shear forces across various flexion angles in thirteen knees. Tests were conducted pre- and post-cruciate ligament resection. Post-cruciate ligament resection, the femoral condyles shifted closer to or even exceeded the posterior border of the tibial plateau, but only slightly closer to the anterior border. This study presents a new methodology for measuring the tibiofemoral kinematics that can be applied to multiple loading profiles. It provides a basis for further investigations, including passive or active muscle forces, to enhance the design of total knee protheses and improve surgical outcomes.

Keywords: knee; biomechanics; cadaveric study; anterior–posterior stability; cruciate ligaments

Citation: Brendle, S.A.; Krueger, S.; Grifka, J.; Müller, P.E.; Grupp, T.M. A New Methodology for the Accurate Measurement of Tibiofemoral Kinematics in Human Cadaveric Knees: An Evaluation of the Anterior–Posterior Laxity Pre- and Post-Cruciate Ligament Resection. *Life* **2024**, *14*, 877. https://doi.org/10.3390/life14070877

Academic Editor: Panagiotis Georgianos

Received: 11 June 2024
Revised: 8 July 2024
Accepted: 12 July 2024
Published: 14 July 2024

1. Introduction

The decision to sacrifice or preserve the posterior cruciate ligament (PCL) in total knee arthroplasty (TKA) remains debated and depends mainly on the surgeon's preference. In cases where the PCL is insufficient or absent, posterior-stabilized (PS) or ultra-congruent (UC) implants can be used. PS implants substitute the PCL with a post-cam mechanism, whereas UC implants provide stability through conformity. While some studies have shown that neither UC nor PS implants provide anterior–posterior (AP) stability in all the positions of flexion [1,2], other studies have reported good clinical results for both PS and UC implants [3–6]. Nevertheless, instability is still one of the most common indications for revision after TKA [7–9]. Since AP stability is an important measure of functional knee performance, understanding the tibiofemoral contact situation within the native ligamentous situation and its changes after cruciate ligament resection is crucial to analyze where the implant needs to provide a stabilizing effect to compensate for the loss of both cruciate ligaments. Biomechanical in vitro studies provide high accuracy and control, offering insights into the AP stability of the knee joint unattainable in vivo due to ethical constraints [10–19]. However, many studies lack detailed investigation of the position of the medial and lateral femoral condyles on the proximal tibia during AP shear forces, particularly without cruciate ligaments. This gap is due to the limitations of current

methodologies, which often fail to connect coordinate systems to the corresponding bone geometries [11,13,18]. In addition, many studies were performed using mechanical knee rigs [11,15,16], which use muscle forces to induce movement and therefore cannot actively control each degree of freedom separately to reproduce scenarios without muscles, such as passive laxity measurements or passive knee flexion as performed intraoperatively, or by applying manual force [13], which has limited reproducibility. In addition, the application of forces during testing is an important aspect to ensure comparability between measurements. As the relationship between coordinate systems and bone geometries is often unknown prior to testing, force application along reliable axes cannot be controlled.

Therefore, the primary objective of this study was to develop a new methodology and testing workflow for controlled force application and accurate tracking of landmark-based femoral and tibial coordinate systems and their corresponding bone geometries in human cadaveric knees during static and dynamic testing in a six-degrees-of-freedom joint motion simulator. The secondary objective was to show an application of this workflow by simulating clinical knee examinations as performed intraoperatively and evaluating the positions of the medial and lateral femoral condyles on the tibial plateau during anterior and posterior shear forces pre- and post-cruciate ligament resection. The hypothesis was that, in the native condition in deep flexion, the lateral femoral condyle approaches subluxation at the posterior border of the envelope of laxity, whereas the medial femoral condyle does not. Post-cruciate ligament resection, we anticipated the positions of the femoral condyles to move close to the anterior and posterior border of the tibial plateau.

2. Materials and Methods

2.1. Specimens

Thirteen fresh-frozen human cadaveric lower right extremities, preserved from the femoral head to the malleoli, were included in this study. The donors had a mean age of 66.62 ± 9.97 years and a mean body mass index (BMI) of 23.31 ± 8.02. The sample included three females and ten males. Medical records indicated no pre-existing knee disorders or surgical interventions. Ethical approval was obtained from the ethics committee of the Ludwig Maximilian University of Munich (No. 20-0856).

2.2. Coordinate Systems

Computed tomography (CT) scans (Siemens SOMATOM Perspective, Siemens Healthineers, Erlangen, Germany) were obtained for each specimen. The scans were segmented using Mimics 24.0 (Materialise, Leuven, Belgium), and the anatomic landmarks were identified with 3-matic medical 16.0 (Materialise, Leuven, Belgium) to define the femoral and tibial coordinate systems and further relevant axes.

For the femur, the flexion axis was defined by connecting the centers of two spheres fitted in the posterior condyles (medial flexion facet center (MFC) and lateral flexion facet center (LFC) [20,21], whereas the midpoint between the medial sulcus and the lateral prominence was specified as the origin of the femoral coordinate system. The center of the hip was determined by fitting a sphere in the femoral head. By connecting this point to the origin of the femoral coordinate system, the mechanical axis was identified [21]. The AP axis of the femoral coordinate system resulted from these two axes and pointed anteriorly. The femoral joint line was defined as a tangent through the most distal points of the medial and lateral condyles. For the tibia, a cone fit was applied in between the tibial tuberosity and the malleoli to identify the mechanical axis [22]. The proximal exit point of this axis was used as the origin of the tibial coordinate system. The AP axis of the tibial coordinate system was defined by a line connecting the attachment point of the PCL and the medial third of the tuberosity [23]. The medial–lateral axis of the tibial coordinate system resulted from the cross-product of the other two axes and pointed laterally. The tibial joint line was defined as a tangent through the most distal points on the medial and lateral tibial plateau [24]. Figure 1 illustrates the femoral and tibial coordinate systems.

Life **2024**, *14*, 877

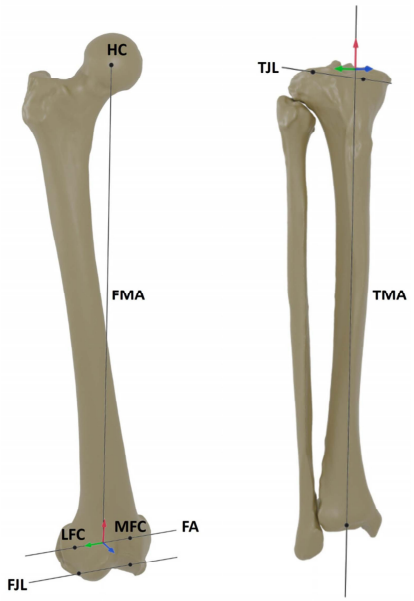

(**a**) (**b**)

Figure 1. Anatomic landmarks and (**a**) femoral and (**b**) tibial coordinate systems. Anterior–posterior axes are marked in blue, medial–lateral axes are marked in green and proximal–distal (mechanical) axes are marked in red. FA = flexion axis, FJL = femoral joint line, FMA = femoral mechanical axis, HC = hip center, LFC = lateral flexion facet center, MFC = medial flexion facet center, TJL = tibial joint line, TMA = tibial mechanical axis.

2.3. Specimen Preparation

Each specimen was thawed for 24 h at 7 °C before the experiment. The proximal and distal segments of the leg were skeletonized, preserving the knee joint capsule and surrounding soft tissue, including the ligaments, muscles and tendons, up to 100 mm superior and 50 mm inferior to the knee joint space. The GOM measuring points (1.5 mm, Carl Zeiss GOM Metrology GmbH, Braunschweig, Germany) were attached to the cleaned bone surfaces and the 3D point clouds of each bone were acquired using ARAMIS 12M (Carl Zeiss GOM Metrology GmbH, Braunschweig, Germany) by rotating the specimen stepwise around its mechanical axis. The 3D fittings of the femur and tibia were performed by aligning the segmented CT scans containing the landmark-based coordinate systems with the previously acquired 3D point clouds of each bone (Figure 2). To ensure accurate alignment, visual and quantitative inspections of the 3D fittings were conducted from different perspectives. The quantitative inspections were performed by palpating each bone at a minimum of six points with a touch probe (1 mm, PM 3, Carl Zeiss GOM Metrology GmbH, Braunschweig, Germany) and measuring the distance to the matched segmented CT scan. The mean deviations should not exceed $\pm$ 1 mm. After successful fitting, the 3D fitting information was saved and the specimens were transected 250 mm proximally and 150 mm distally to the knee joint space. The intramedullary canals were cleaned and closed with Play-Doh before potting into fast-cast resin (Gößl und Pfaff, Brautlach, Germany).

For accurate measurement of the kinematics, it was necessary to place the femur in the joint motion simulator in such a way that the femoral coordinate system was aligned with the upper coordinate system of the joint motion simulator. For this purpose, the upper coordinate system was virtually assigned to the custom-made aluminum femur pot, as its fixed position in the joint motion simulator is known. This was achieved by performing a

Life **2024**, *14*, 877

3D fitting of the femur pot by aligning its computer-aided design (CAD) file containing the upper coordinate system of the joint motion simulator to the femur pot. To embed the femur, the specimen and the femur pot were placed in an embedding fixture. A 2D point cloud of the femur pot and the residual femur was acquired and the previously created 3D-fitting files of femur pot and femur were loaded again. Due to the unique point patterns, it was possible to realign the 3D-fitting files to the new 2D point cloud. In this way, the accurate 3D information of the complete femur and the according coordinate system was available, even after the femur was cut. The femur was adjusted while tracking the measuring points such that the femoral coordinate system was within ± 0.5 mm and $\pm 1^{\circ}$ relative to the upper coordinate system of the joint motion simulator. After successful alignment, the proximal femur was embedded in the femur pot and attached to the custom-made aluminum fixture mounted on the upper actuator of the joint motion simulator. To embed the tibia, the upper actuator was held in position and an axial compression force of 100 N was applied to the specimen, with all the other forces and moments maintained at 0 N/Nm. In order to embed the tibia at 0° flexion, the mechanical axis of the tibia was aligned with the mechanical axis of the femur in the sagittal plane while tracking their coordinate systems using measurement points on the tibia and the tibia pot in combination with the previously created 3D-fitting files. The tibia and fibula were then potted together in a custom-made aluminum tibia pot that was fixed on the lower actuator of the joint motion simulator.

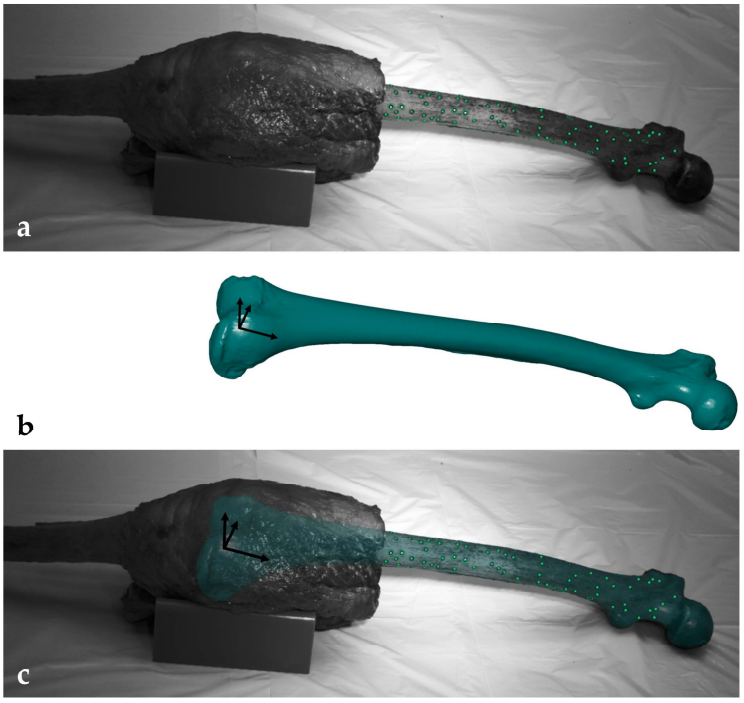

Figure 2. (**a**) Cadaveric femur with measuring points (green). (**b**) Segmented computed tomography (CT) scan (blue) with landmark-based femoral coordinate system. (**c**) Cadaveric femur with 3D-fitted segmented CT scan (blue).

2.4. Experimental Testing

Testing was conducted using a six-degrees-of-freedom joint motion simulator (VIVO, Advanced Mechanical Technologies Inc., Watertown, MA, USA). The six degrees of freedom were implemented by two actuators: the upper (femoral) actuator and the lower

(tibial) actuator. The simulator's upper actuator performed flexion–extension and varus–valgus rotations, while the lower actuator managed medial–lateral, anterior–posterior, proximal–distal translations, and internal–external rotation. Each degree of freedom could be controlled in force or displacement mode independently. The forces and motions are expressed in accordance with the conventions of Grood and Suntay [25]. Figure 3 provides an overview of the experimental setup.

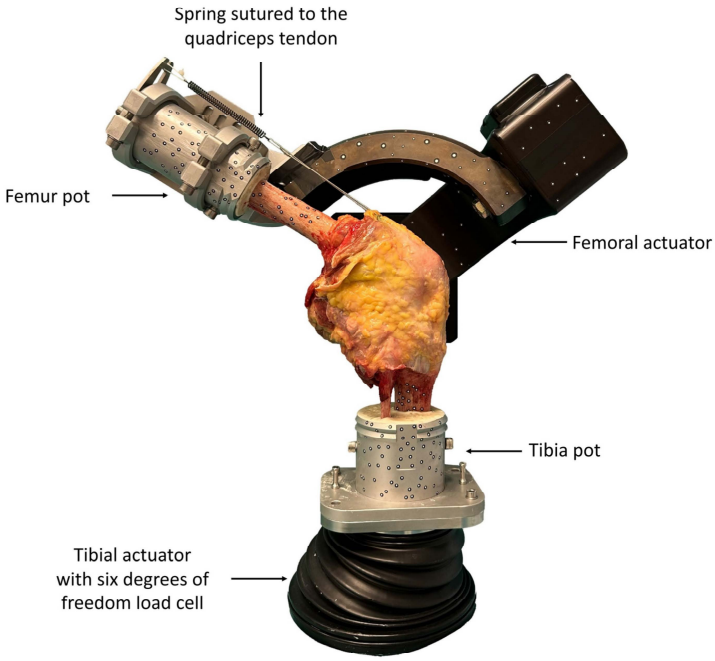

Figure 3. Experimental setup with the knee specimen mounted on the six-degrees-of-freedom joint motion simulator at 60° flexion.

To transfer the absolute joint position of the specimen to the joint motion simulator, a reference position was recorded under an axial compression force of 100 N at 0° flexion, with all the other forces and moments maintained at 0 N/Nm. At the same time, the previously generated 3D-fitting information of the segmented CT scans were again projected onto the residual bones using the remaining measuring point patterns. Based on this information, the relative position of the femoral and tibial coordinate systems was recorded and transferred to the joint motion simulator. Afterwards, the specimens were subjected to laxity testing. In order to characterize the passive AP laxity of each knee in the native condition, cyclic AP shear forces of ±80 N were applied as a ramp profile for 4 cycles at different flexion angles (0°, 30°, 60° and 90°) at a frequency of 0.04 Hz while maintaining an axial compression force of 200 N and all the other forces and moments at 0 N/Nm. The imposed loads were chosen to reflect those applied during clinical examination of joint laxity and were within the range of forces used in comparable studies [11,15,16]. After the native measurements, the cruciate ligaments were transected and the measurements were repeated. For both conditions, the knee capsule was opened using a medial parapatellar approach and closed with surgical sutures (Number 1 Vicryl, B. Braun, Melsungen, Germany) to ensure that only the effects of the cruciate ligament resection were investigated and to exclude the effects of opening the capsule. During testing, the relative position of the femoral and tibial coordinate systems and the resulting loads were sampled at 100 Hz by the joint motion simulator. To simulate the passive tension of the patella tendon in flexion, as present during

Life **2024**, *14*, 877

the intraoperative clinical examination, a spring with an increasing force of up to 50 N at 90° flexion was sutured to the quadriceps tendon with a line of action parallel to the anatomical axis of the femur. Furthermore, the specimens were kept moist by spraying the tissue with sodium chloride solution in order to mitigate the effects of tissue drying during the experimental testing. Figure 4 outlines the entire test process.

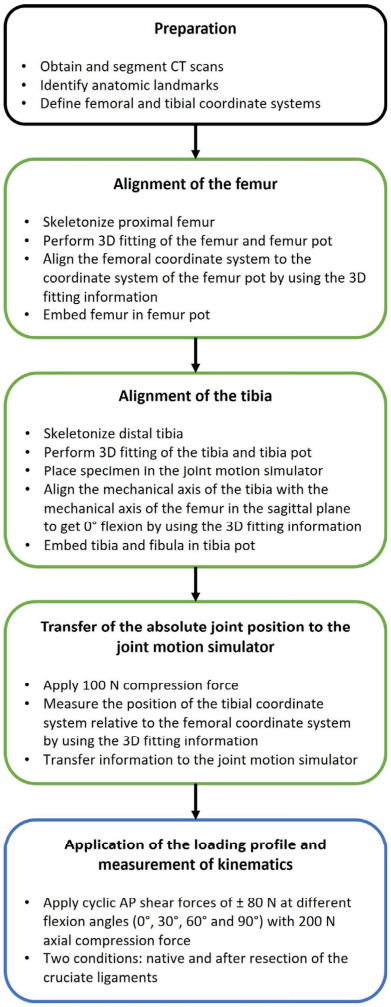

Figure 4. Flowchart illustrating the key steps in the entire test process. The preparation is marked in black. The workflow to ensure accurate measurement of the tibiofemoral kinematics is marked in green. The application of the loading profile and measurement of the kinematics is marked in blue.

2.5. Data Analysis

Data were analyzed using MATLAB (Version R2023a, MathWorks Inc., Natick, MA, USA). The first and last cycles of each measurement were removed from the data analysis to prevent potential data loss due to the start and stop behavior. Furthermore, the kinematic output of the second and third cycles showed excellent agreement (Table 1), and therefore, only data from a single cycle of each experiment were investigated. To evaluate the control accuracy, the root mean square error (RMSE) of all six controlled degrees of freedom was calculated by taking the square root of the mean of the squared differences between the

target and the actual values for all the measurements. The mean deviation between the bone and the segmented CT scan was calculated, ensuring accuracy within ±1 mm. Furthermore, the MFC and LFC of each knee were projected onto the articular surface of the proximal tibia at different flexion angles (0°, 30°, 60° and 90°) at the first time reaching the maximum anterior and posterior force, respectively, reflecting the corresponding positions of the medial and lateral condyles on the tibial plateau (Figure 5). Subsequently, the positions were normalized to the AP width of the articular surface of the respective tibia, which was defined as the distance between the most anterior and the most posterior point of the medial compartment of the tibia.

Table 1. Root mean square error (RMSE) of the kinematic output between the second and third cycles of all the measurements for medial–lateral (ML), anterior–posterior (AP), proximal–distal (PD), flexion–extension (FE), varus–valgus (VV) and internal–external (IE) directions.

ML Translation [mm]	AP Translation [mm]	PD Translation [mm]	FE Rotation [°]	VV Rotation [°]	IE Rotation [°]
0.07	0.11	0.04	0.01	0.03	0.16

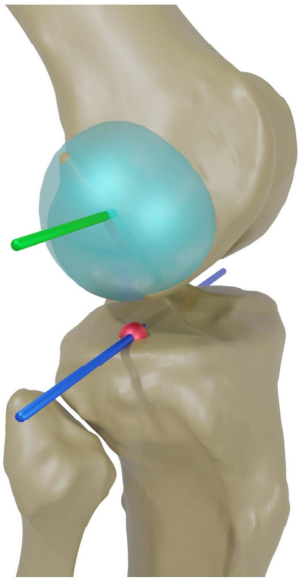

Figure 5. Schematic illustration of the fitted spheres (light blue) in the posterior condyles and the projection (blue) of the flexion axis (green) as well as the medial and lateral flexion facet centers (MFC and LFC, red) ono the tibial plane.

Three specimens were removed from the data analysis due to exceeding the motion limits of the joint motion simulator or joint luxation. The statistical analyses were performed using Minitab (Version 21.2, Minitab GmbH, Munich, Germany). The significance of the differences between the positions in the native condition and the condition after resection of the cruciate ligaments was determined for each condyle at the flexion angles of 0°, 30°, 60° and 90° using Wilcoxon signed-rank tests with the significance level set at $p \leq 0.05$. The results are displayed with boxplots on a normalized tibia.

3. Results

3.1. Accuracy of 3D Fittings

Quantitative inspections of the 3D fittings using a touch probe revealed a mean deviation of $|0.27 \pm 0.21|$ mm between the real bone and the 3D-fitted segmented CT scan

(Figure 6). Most deviations were negative, indicating that the segmented CT scan slightly protruded beyond the real bone at these locations.

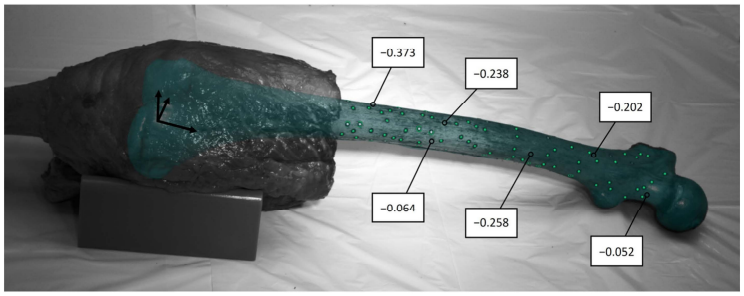

Figure 6. Cadaveric femur with measuring points (green), 3D-fitted segmented CT scan (blue) and deviations between the real bone and the 3D-fitted segmented CT scan at specific points. All the deviations are displayed in mm.

3.2. Control Accuracy

The RMSE of the control error of all six degrees of freedom for all the measurements is summarized in Table 2. The RMSEs of the flexion–extension (FE) angle, varus–valgus (VV) and internal–external (IE) moments, and the proximal–distal (PD) force were small. The largest errors were observed in the medial–lateral (ML) and AP directions. Figure 7 shows one cycle of the target and the actual curves of all six controlled degrees of freedom for all the specimens in the native condition at 0° flexion. Again, the good control accuracy of the FE angle, as well as the VV and IE moments, and the PD force can be seen. The largest deviations from the target curve were observed for the AP and ML. However, the target AP forces of ±80 N were achieved for all the specimens.

Table 2. RMSE of the control error for all the measurements for the medial–lateral (ML), anterior–posterior (AP), proximal–distal (PD), flexion–extension (FE), varus–valgus (VV) and internal–external (IE) directions.

ML Force Error [N]	AP Force Error [N]	PD Force Error [N]	FE Angle Error [°]	VV Moment Error [Nm]	IE Moment Error [Nm]
10.77	10.99	2.46	0.01	0.18	0.24

3.3. Influence of the Cruciate Ligaments on the Anterior–Posterior Laxity

Figure 8 shows the AP positions of the projected MFC and LFC at various flexion angles under the maximum anterior and posterior shear force acting on the tibia, pre- and post-cruciate ligament resection. The boxplots based on a normalized tibia illustrate these positions with the medians, quartiles, ranges and outliers. Significant differences ($p \leq 0.05$) are marked with an asterisk.

In the native condition, the median position of the medial condyle under anterior force was located in the posterior third of the tibia at 0° flexion (0.28), shifted slightly anteriorly at 30° flexion (0.31), and reached its most posterior position at 90° flexion (0.20). Under posterior force, the medial condyle's median position was located 0.41 from the posterior border of the tibial plateau at 0° of flexion, moved anteriorly at 30° flexion (0.48), and returned to near its initial position at higher flexion angles. The median position of the lateral condyle in the native condition was more anterior than the medial condyle for both anterior (0.39) and posterior (0.60) force at 0° flexion and shifted posteriorly throughout the arc of flexion, already exceeding the posterior border of the tibial plateau at 90° flexion with the maximum anterior force (−0.06). The lateral condyle thus showed a noticeably greater change in position during flexion than the medial condyle, which can be interpreted as a medial pivoting kinematic.

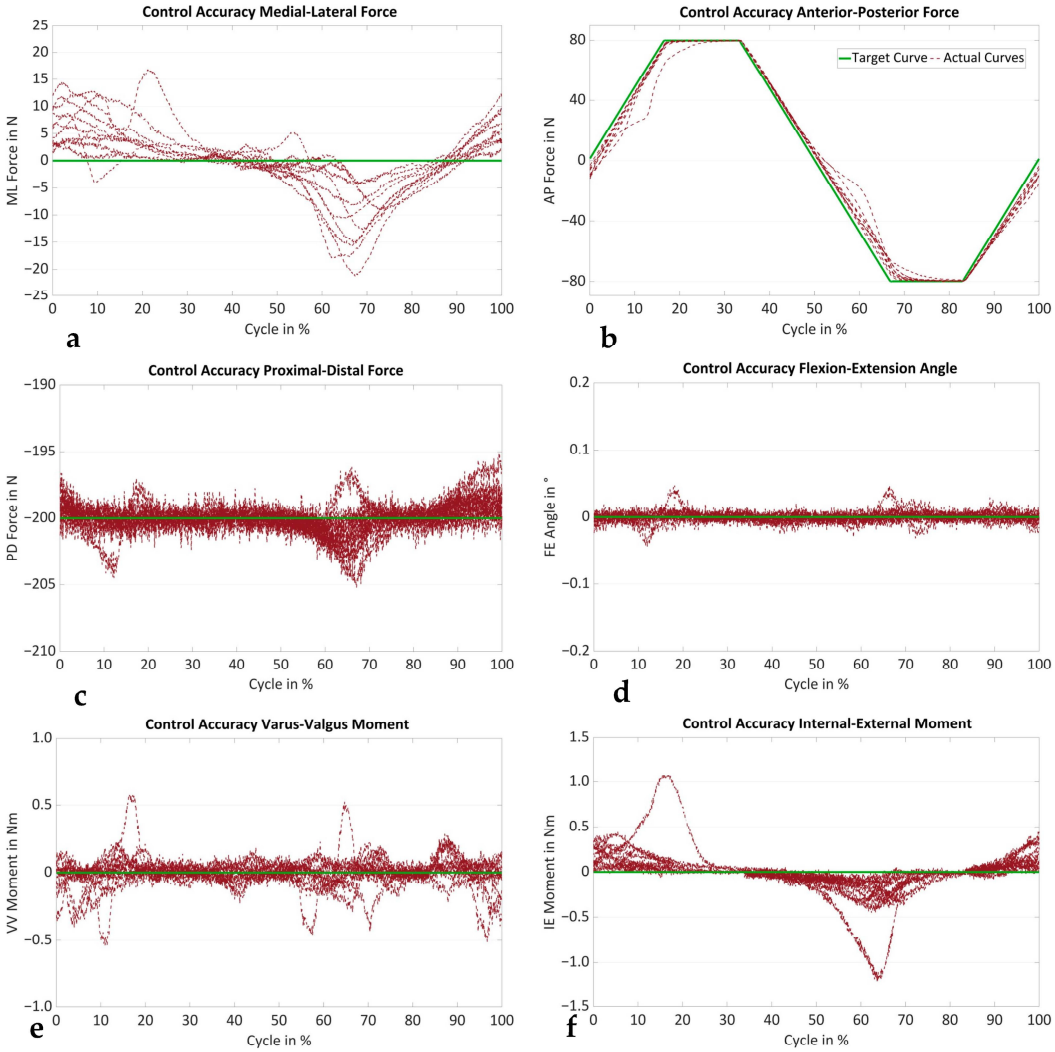

Figure 7. Target curve (green) and actual curves (red) of the (**a**) medial–lateral (ML) force, (**b**) anterior–posterior (AP) force, (**c**) proximal–distal (PD) force, (**d**) flexion–extension (FE) angle, (**e**) varus–valgus (VV) moment and (**f**) internal–external (IE) moment of all the specimens (n = 10) in the native condition at 0° flexion, showing the control accuracy.

After cruciate ligament resection, the median position of the medial condyle shifted significantly more posteriorly under anterior force at all the flexion angles: 0° (0.21, p = 0.006), 30° (0.08, p = 0.006), 60° (0.13, p = 0.006), and 90° (0.10, p = 0.006). The median position of the lateral condyle also shifted posteriorly and was significantly more posterior than in the native condition at 0° (0.31, p = 0.006), 30° (0.01, p = 0.006), 60° (−0.08, p = 0.006) and 90° (−0.14, p = 0.008) of flexion. Under posterior force, the medial condyle's median position was significantly more anterior at 0° (0.43, p = 0.006) and 90° (0.47, p = 0.032) of flexion, while the lateral condyle showed significant anterior shifts at 0° (0.63, p = 0.008), 60° (0.39, p = 0.008) and 90° (0.34, p = 0.006).

Life **2024**, *14*, 877

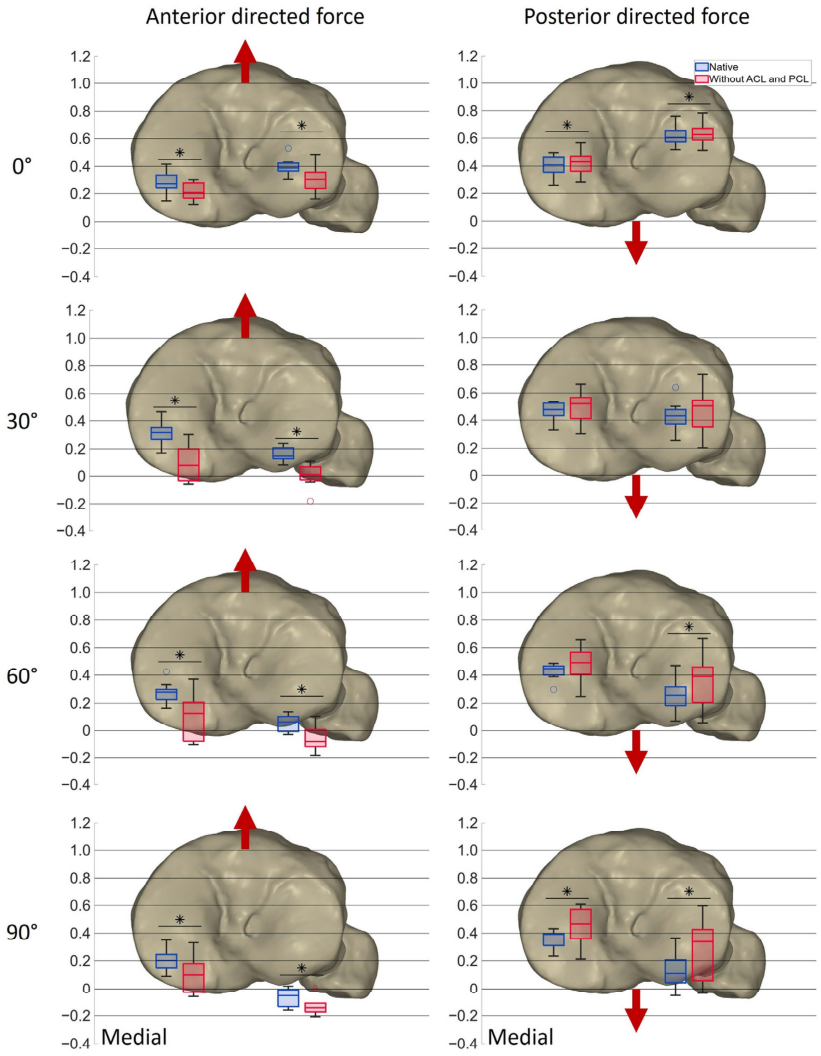

Figure 8. Boxplots showing the median (n = 10), first and third quartile, range and outliers of the AP positions of the projected MFC and LFC at different flexion angles at the maximum anterior and posterior force, respectively, in the native condition (blue) and after resection of the cruciate ligaments (red) on a normalized tibia. Red arrows indicate the direction of the shear force applied on the tibia. Significant differences are marked with an asterisk ($p \leq 0.05$).

The results suggest that resection of the cruciate ligaments significantly alters the anterior–posterior stability of the knee, with both femoral condyles showing increased posterior displacement under anterior force and varied behavior under posterior force. The increased length of the boxplots after resection of the cruciate ligaments indicates greater variability, especially at higher flexion angles.

4. Discussion

In this study, a new workflow was developed for accurately tracking landmark-based femoral and tibial coordinate systems and their corresponding bone geometries in human

cadaveric knees during static and dynamic testing using a six-degrees-of-freedom joint motion simulator.

A reliable method to define coordinate systems is crucial in kinematic assessments, as different coordinate systems can lead to significant variations in the results and interpretations of normal movement [26,27]. For this reason, landmark-based coordinate systems are recommended for measuring tibiofemoral kinematics [26]. However, accurate and reliable placement of landmark-based coordinate systems in cadaveric knees is challenging due to soft tissue covering the landmarks. Moreover, if the landmarks are palpated using a touch probe, from which a coordinate system is finally formed, the exact relationship between the bone and the coordinate system is not known. In the workflow developed in the scope of this study, the landmarks are selected in 3D models of the bones using geometrical primitives that have been shown to have a good inter-observer reliability [22,28], allowing for precise and reproduceable placement. In addition, the accuracy of the subsequent 3D fitting can be analyzed by measuring the deviation between the bone and the fitted segmented CT scan using a touch probe. Small deviations may result from the quality of the CT scan, segmentation errors or the possibility of scraping bone during preparation. The high accuracy of the 3D fitting in this study and the knowledge of the relative positions of the femoral and tibial bone geometries enable multiple analyses, such as projecting the flexion axis and flexion facet centers (FFCs) onto the tibial plane. This method approximates the tibiofemoral contact pattern [16,29,30] and is valid to describe the kinematic behavior of the knee [31], especially for single radius implant designs [32]. Fitting of the spheres into the posterior condyles in the present study revealed that the specimens mainly had a constant radius of curvature.

Another important aspect during static and dynamic testing is the application of forces. If the exact relationship between the bone and the coordinate system is not known before testing, it cannot be ensured that the forces during testing are applied along the same axes when comparing different specimens. In the workflow developed in this study, not only the location of the tibial coordinate system with respect to the femoral coordinate system but also their location relative to the bones is known. This is a major advantage of the method, as it enables the controlled application of forces and moments through the origin of the tibial coordinate system with the line of action parallel to the Grood and Suntay axes [25,33]. This ensures consistent and reliable force application across different specimens. Furthermore, the six-degrees-of-freedom joint motion simulator allows for independent control of each degree of freedom, making it possible to reproduce scenarios without muscle forces, such as passive laxity measurements or passive knee flexion as performed intraoperatively. This capability is relevant for navigation and robotics research. In addition, it is possible to apply passive knee flexion with a controlled preload or even complex loading scenarios like level walking based on the CAMS knee dataset [34]. Moreover, the simulator can be modified by adding virtual ligament models and actively controlled quadriceps and hamstrings forces [17,33,35]. Previous studies have shown that adding the muscle load significantly affects the resulting kinematics [17,36]. Depending on the research question, it may therefore be more appropriate to perform active instead of passive movements. The present study focused mainly on characterizing the tibiofemoral contact situation within the ligamentous situation. For this reason, passive movements were chosen, since forces across the joint reduce the contribution of the soft tissue and increase the contribution of the articular surfaces [37]. However, the results may be different when loading the knee with hamstrings and quadriceps force [36]. Nevertheless, this workflow provides a basis for reliable force application and tracking of the resulting kinematics, regardless of which loading profile is applied. In addition, the six-degrees-of-freedom joint motion simulator demonstrated good control accuracy for the loading profile used in this study, as well as kinematic reproducibility, as evidenced by the excellent agreement of the kinematic output between two cycles. However, the control parameters may need to be adjusted for more complex loading profiles.

In order to accomplish the secondary objective of the present study, the new workflow was used to evaluate the positions of the medial and lateral femoral condyles on the tibial plateau during anterior and posterior shear forces in the native knee and after resection of both cruciate ligaments. In the native condition, the lateral femoral condyles moved posteriorly on the tibial plateau with increasing flexion under both anterior- and posterior-directed forces. The medial femoral condyles moved slightly anteriorly until 30° of flexion under posterior-directed force and then continued moving posteriorly until 90° of flexion. The results support the hypothesis that with anterior-directed force in deep flexion, the lateral femoral condyle approaches the posterior border of the tibial plateau, while the medial femoral condyle remains more anterior. Moreover, the results are in accordance with a previous study [16] and reflect the medial pivoting characteristics that can be observed during the neutral path of motion [16,29,30].

The second hypothesis regarding the position of the femoral condyles after resection of the cruciate ligaments could not be confirmed. The positions of the femoral condyles shifted closer to or even exceeded the posterior border of the tibial plateau, but only slightly closer to the anterior border. This implies that the implant primarily has to provide posterior stabilization to compensate for the loss of both cruciate ligaments. However, the AP position of the femoral condyles on the tibial plateau was shown to vary depending on the axial force and tibial slope [12,15]. Previous studies reported a more posterior position and less anterior translation with an increasing slope [12]. The anatomical tibial slope in the specimens, with a mean medial slope of $9.14 \pm 2.81°$ and higher lateral slopes in most cases, might explain why the femoral condyles are closer to the posterior tibial border. For this reason, the positions of the femoral condyles on the tibial plateau might be different with less slope, as would probably be the case after implantation of tibial total knee components. Depending on the prothesis and alignment technique, tibial components are usually implanted with less tibial slope than in the native situation, with recommendations ranging from 0° to 10° [38,39]. A study by Giffin et al. [12] showed that, even though more posterior translation of the femur was observed with increased slope, the overall AP translation remained the same. This implies that after resection of the cruciate ligaments, stabilization of the joint by the implant is necessary, even with less slope. Nevertheless, the stabilizing effect that the implant needs to provide may vary depending on the slope. Furthermore, various loading conditions may also lead to different results [36,40]. While this study mainly investigated the passive AP laxity within the ligamentous situation, the AP translation may vary during active movements including quadriceps and hamstrings force. For this reason, further research is needed to identify the stabilizing effects that implants must provide to compensate for the loss of both cruciate ligaments during various activities. Future studies should also consider the influence of different tibial slopes and physiological muscle loading to better understand the differences in knee kinematics pre- and post-implantation.

Several limitations should be taken into account when interpreting the results of the present study. First, this study investigated a limited number of human cadaveric specimens, which may not fully represent the variability found in living patients. Additionally, physiological muscle loading was not applied, and the patellar mechanism was only present to a limited extent by simulating the passive tension of the patella tendon in flexion, as present during intraoperative clinical examination. Therefore, the results may not be directly transferable to in vivo conditions and may only be representative of passive laxity tests as performed intraoperatively. However, it is essential to perform biomechanical in vitro studies to better understand the causes of a certain behavior, unattainable in vivo due to ethical constraints. Furthermore, AP laxity was not investigated beyond 90° of flexion due to the design constraints of the joint motion simulator; therefore, no conclusions can be drawn about laxity behavior at higher flexion angles. However, a large proportion of activities of daily living are covered with flexion angles of up to 90° [34]. Moreover, the order of the two different test conditions could not be changed. Time-dependent effects

can therefore not be eliminated. The limited number of tests and the resulting short test duration should minimize these effects [41].

5. Conclusions

This study introduced a new method to accurately measure the tibiofemoral kinematics using a six-degrees-of-freedom joint motion simulator and landmark-based coordinate systems. The method was employed to analyze the positions of the medial and lateral femoral condyles on the tibial plateau under AP shear forces, pre- and post-cruciate ligament resection. The findings indicated that post-resection, the femoral condyles' positions shifted close to or even exceeded the posterior border of the tibial plateau, but only slightly closer to the anterior border. In addition, the high accuracy of the 3D fittings, kinematic reproducibility and control accuracy were demonstrated. These findings highlight the method's potential for further investigations to enhance the design of total knee protheses and improve surgical outcomes.

Author Contributions: Conceptualization, S.A.B., S.K., J.G., P.E.M. and T.M.G.; methodology, S.A.B. and S.K.; software, S.A.B.; validation, S.A.B. and S.K.; formal analysis, S.A.B.; investigation, S.A.B. and S.K.; resources, S.A.B., S.K., J.G., P.E.M. and T.M.G.; data curation, S.A.B.; writing—original draft preparation, S.A.B.; writing—review and editing, S.K., J.G., P.E.M. and T.M.G.; visualization, S.A.B.; supervision, T.M.G.; project administration, T.M.G.; funding acquisition, T.M.G. All authors have read and agreed to the published version of the manuscript.

Funding: All of the authors (S.A.B., S.K., J.G., P.E.M., T.M.G.) were funded by B. Braun Aesculap AG, Tuttlingen, Germany. The funders had no role in the design of the study; in the collection, analyses, or interpretation of the data; and in writing the manuscript, or in the decision to publish the results.

Institutional Review Board Statement: This study was conducted in accordance with the Declaration of Helsinki and approved by the Ethics Committee of the Ludwig Maximilian University of Munich (#20-0856, 9 November 2020).

Informed Consent Statement: Not applicable.

Data Availability Statement: The data presented in this study are available on request from the corresponding author. The data are not publicly available due to ethical and privacy considerations associated with human cadaveric donor material.

Acknowledgments: The authors would like to thank Ana-Laura Puente-Reyna and Josef-Benedikt Weiß for their valuable support during this study.

Conflicts of Interest: Three of the authors (S.A.B., S.K., T.M.G.) are employees of B. Braun Aesculap AG, Tuttlingen, Germany. J.G. and P.E.M. are paid consultants at B. Braun Aesculap AG. The funders had no role in the design of the study; in the collection, analyses, or interpretation of the data; and in writing the manuscript, or in the decision to publish the results.

References

1. Fritzsche, H.; Beyer, F.; Postler, A.; Lützner, J. Different intraoperative kinematics, stability, and range of motion between cruciate-substituting ultracongruent and posterior-stabilized total knee arthroplasty. *Knee Surg. Sports Traumatol. Arthrosc.* **2018**, *26*, 1465–1470. [CrossRef] [PubMed]
2. Scott, D.F.; Hellie, A.A. Mid-Flexion, Anteroposterior Stability of Total Knee Replacement Implanted with Kinematic Alignment: A Randomized, Quantitative Radiographic Laxity Study with Posterior-Stabilized and Medial-Stabilized Implants. *J. Bone Jt. Surg. Am.* **2023**, *105*, 9–19. [CrossRef]
3. Lützner, J.; Beyer, F.; Lützner, C.; Riedel, R.; Tille, E. Ultracongruent insert design is a safe alternative to posterior cruciate-substituting total knee arthroplasty: 5-year results of a randomized controlled trial. *Knee Surg. Sports Traumatol. Arthrosc.* **2022**, *30*, 3000–3006. [CrossRef] [PubMed]
4. Kim, T.W.; Lee, S.M.; Seong, S.C.; Lee, S.; Jang, J.; Lee, M.C. Different intraoperative kinematics with comparable clinical outcomes of ultracongruent and posterior stabilized mobile-bearing total knee arthroplasty. *Knee Surg. Sports Traumatol. Arthrosc.* **2016**, *24*, 3036–3043. [CrossRef]
5. Lützner, J.; Beyer, F.; Dexel, J.; Fritzsche, H.; Lützner, C.; Kirschner, S. No difference in range of motion between ultracongruent and posterior stabilized design in total knee arthroplasty: A randomized controlled trial. *Knee Surg. Sports Traumatol. Arthrosc.* **2017**, *25*, 3515–3521. [CrossRef]

6. Hinarejos, P.; Leal-Blanquet, J.; Fraile-Suari, A.; Sánchez-Soler, J.; Torres-Claramunt, R.; Monllau, J.C. Increased posterior translation but similar clinical outcomes using ultracongruent instead of posterior stabilized total knee arthroplasties in a prospective randomized trial. *Knee Surg. Sports Traumatol. Arthrosc.* **2022**, *30*, 3041–3048. [CrossRef]
7. Krackow, K.A. Instability in total knee arthroplasty: Loose as a goose. *J. Arthroplast.* **2003**, *18*, 45–47. [CrossRef]
8. Sharkey, P.F.; Lichstein, P.M.; Shen, C.; Tokarski, A.T.; Parvizi, J. Why are total knee arthroplasties failing today--has anything changed after 10 years? *J. Arthroplast.* **2014**, *29*, 1774–1778. [CrossRef] [PubMed]
9. Wilson, C.J.; Theodoulou, A.; Damarell, R.A.; Krishnan, J. Knee instability as the primary cause of failure following Total Knee Arthroplasty (TKA): A systematic review on the patient, surgical and implant characteristics of revised TKA patients. *Knee* **2017**, *24*, 1271–1281. [CrossRef]
10. Borque, K.A.; Gold, J.E.; Incavo, S.J.; Patel, R.M.; Ismaily, S.E.; Noble, P.C. Anteroposterior Knee Stability During Stair Descent. *J. Arthroplast.* **2015**, *30*, 1068–1072. [CrossRef]
11. Bull, A.M.J.; Kessler, O.; Alam, M.; Amis, A.A. Changes in knee kinematics reflect the articular geometry after arthroplasty. *Clin. Orthop. Relat. Res.* **2008**, *466*, 2491–2499. [CrossRef] [PubMed]
12. Giffin, J.R.; Stabile, K.J.; Zantop, T.; Vogrin, T.M.; Woo, S.L.-Y.; Harner, C.D. Importance of tibial slope for stability of the posterior cruciate ligament deficient knee. *Am. J. Sports Med.* **2007**, *35*, 1443–1449. [CrossRef] [PubMed]
13. Ghosh, K.M.; Blain, A.P.; Longstaff, L.; Rushton, S.; Amis, A.A.; Deehan, D.J. Can we define envelope of laxity during navigated knee arthroplasty? *Knee Surg. Sports Traumatol. Arthrosc.* **2014**, *22*, 1736–1743. [CrossRef] [PubMed]
14. Moslemian, A.; Arakgi, M.E.; Roessler, P.P.; Sidhu, R.S.; Degen, R.M.; Willing, R.; Getgood, A.M.J. The Medial structures of the knee have a significant contribution to posteromedial rotational laxity control in the PCL-deficient knee. *Knee Surg. Sports Traumatol. Arthrosc.* **2021**, *29*, 4172–4181. [CrossRef] [PubMed]
15. Reynolds, R.J.; Walker, P.S.; Buza, J. Mechanisms of anterior-posterior stability of the knee joint under load-bearing. *J. Biomech.* **2017**, *57*, 39–45. [CrossRef] [PubMed]
16. Walker, P.S.; Arno, S.; Borukhoy, I.; Bell, C.P. Characterising knee motion and laxity in a testing machine for application to total knee evaluation. *J. Biomech.* **2015**, *48*, 3551–3558. [CrossRef] [PubMed]
17. Willing, R.; Moslemian, A.; Yamomo, G.; Wood, T.; Howard, J.; Lanting, B. Condylar-Stabilized TKR May Not Fully Compensate for PCL-Deficiency: An In Vitro Cadaver Study. *J. Orthop. Res.* **2019**, *37*, 2172–2181. [CrossRef] [PubMed]
18. Roth, J.D.; Howell, S.M.; Hull, M.L. Analysis of differences in laxities and neutral positions from native after kinematically aligned TKA using cruciate retaining implants. *J. Orthop. Res.* **2019**, *37*, 358–369. [CrossRef] [PubMed]
19. Grood, E.S.; Stowers, S.F.; Noyes, F.R. Limits of movement in the human knee. Effect of sectioning the posterior cruciate ligament and posterolateral structures. *J. Bone Jt. Surg. Am.* **1988**, *70*, 88–97. [CrossRef]
20. Yin, L.; Chen, K.; Guo, L.; Cheng, L.; Wang, F.; Yang, L. Identifying the Functional Flexion-extension Axis of the Knee: An In-Vivo Kinematics Study. *PLoS ONE* **2015**, *10*, e0128877. [CrossRef]
21. Victor, J.; van Doninck, D.; Labey, L.; van Glabbeek, F.; Parizel, P.; Bellemans, J. A common reference frame for describing rotation of the distal femur: A ct-based kinematic study using cadavers. *J. Bone Jt. Surg. Br.* **2009**, *91*, 683–690. [CrossRef]
22. Millar, S.C.; Arnold, J.B.; B Solomon, L.; Thewlis, D.; Fraysse, F. Development and evaluation of a method to define a tibial coordinate system through the fitting of geometric primitives. *Int. Biomech.* **2021**, *8*, 12–18. [CrossRef] [PubMed]
23. Insall, J.N. *Insall & Scott Surgery of the Knee*, 6th ed.; Elsevier: Philadelphia, PA, USA, 2018; ISBN 0323248829.
24. Kahn, T.L.; Soheili, A.; Schwarzkopf, R. Outcomes of total knee arthroplasty in relation to preoperative patient-reported and radiographic measures: Data from the osteoarthritis initiative. *Geriatr. Orthop. Surg. Rehabil.* **2013**, *4*, 117–126. [CrossRef] [PubMed]
25. Grood, E.S.; Suntay, W.J. A joint coordinate system for the clinical description of three-dimensional motions: Application to the knee. *J. Biomech. Eng.* **1983**, *105*, 136–144. [CrossRef] [PubMed]
26. Wu, G.; Cavanagh, P.R. ISB recommendations for standardization in the reporting of kinematic data. *J. Biomech.* **1995**, *28*, 1257–1261. [CrossRef] [PubMed]
27. Sauer, A.; Kebbach, M.; Maas, A.; Mihalko, W.M.; Grupp, T.M. The Influence of Mathematical Definitions on Patellar Kinematics Representations. *Materials* **2021**, *14*, 7644. [CrossRef] [PubMed]
28. Hancock, C.W.; Winston, M.J.; Bach, J.M.; Davidson, B.S.; Eckhoff, D.G. Cylindrical axis, not epicondyles, approximates perpendicular to knee axes. *Clin. Orthop. Relat. Res.* **2013**, *471*, 2278–2283. [CrossRef]
29. Iwaki, H.; Pinskerova, V.; Freeman, M.A. Tibiofemoral movement 1: The shapes and relative movements of the femur and tibia in the unloaded cadaver knee. *J. Bone Jt. Surg. Br.* **2000**, *82*, 1189–1195. [CrossRef]
30. Pinskerova, V.; Johal, P.; Nakagawa, S.; Sosna, A.; Williams, A.; Gedroyc, W.; Freeman, M.A.R. Does the femur roll-back with flexion? *J. Bone Jt. Surg. Br.* **2004**, *86*, 925–931. [CrossRef]
31. Scarvell, J.M.; Smith, P.N.; Refshauge, K.M.; Galloway, H.R.; Woods, K.R. Comparison of kinematic analysis by mapping tibiofemoral contact with movement of the femoral condylar centres in healthy and anterior cruciate ligament injured knees. *J. Orthop. Res.* **2004**, *22*, 955–962. [CrossRef]
32. Hull, M.L. Errors in using fixed flexion facet centers to determine tibiofemoral kinematics increase fourfold for multi-radius femoral component designs with early versus late decreases in the radius of curvature. *Knee* **2022**, *35*, 183–191. [CrossRef] [PubMed]

33. Henke, P.; Ruehrmund, L.; Bader, R.; Kebbach, M. Exploration of the Advanced VIVOTM Joint Simulator: An In-Depth Analysis of Opportunities and Limitations Demonstrated by the Artificial Knee Joint. *Bioengineering* **2024**, *11*, 178. [CrossRef] [PubMed]
34. Taylor, W.R.; Schütz, P.; Bergmann, G.; List, R.; Postolka, B.; Hitz, M.; Dymke, J.; Damm, P.; Duda, G.; Gerber, H.; et al. A comprehensive assessment of the musculoskeletal system: The CAMS-Knee data set. *J. Biomech.* **2017**, *65*, 32–39. [CrossRef] [PubMed]
35. Vakili, S.; Lanting, B.; Getgood, A.; Willing, R. Comparison of the Kinematics and Laxity of Total Knee Arthroplasty Bearing Designs Stabilized with Specimen-Specific Virtual Ligaments on a Joint Motion Simulator. *J. Biomech. Eng.* **2024**, *146*, 081005. [CrossRef] [PubMed]
36. Victor, J.; Labey, L.; Wong, P.; Innocenti, B.; Bellemans, J. The influence of muscle load on tibiofemoral knee kinematics. *J. Orthop. Res.* **2010**, *28*, 419–428. [CrossRef] [PubMed]
37. Wang, X.; Malik, A.; Bartel, D.L.; Wickiewicz, T.L.; Wright, T. Asymmetric varus and valgus stability of the anatomic cadaver knee and the load sharing between collateral ligaments and bearing surfaces. *J. Biomech. Eng.* **2014**, *136*, 081005. [CrossRef] [PubMed]
38. Shi, X.; Shen, B.; Kang, P.; Yang, J.; Zhou, Z.; Pei, F. The effect of posterior tibial slope on knee flexion in posterior-stabilized total knee arthroplasty. *Knee Surg. Sports Traumatol. Arthrosc.* **2013**, *21*, 2696–2703. [CrossRef] [PubMed]
39. Wittenberg, S.; Sentuerk, U.; Renner, L.; Weynandt, C.; Perka, C.F.; Gwinner, C. Bedeutung des tibialen Slopes in der Knieendoprothetik. *Orthopade* **2020**, *49*, 10–17. [CrossRef]
40. Oehme, S.; Moewis, P.; Boeth, H.; Bartek, B.; Lippert, A.; von Tycowicz, C.; Ehrig, R.; Duda, G.N.; Jung, T. PCL insufficient patients with increased translational and rotational passive knee joint laxity have no increased range of anterior-posterior and rotational tibiofemoral motion during level walking. *Sci. Rep.* **2022**, *12*, 13232. [CrossRef]
41. Dandridge, O.; Garner, A.; Jeffers, J.R.T.; Amis, A.A.; Cobb, J.P.; van Arkel, R.J. Validity of repeated-measures analyses of in vitro arthroplasty kinematics and kinetics. *J. Biomech.* **2021**, *129*, 110669. [CrossRef]

4.2 Publication II: Kinematic patterns of different loading profiles before and after total knee arthroplasty: A cadaveric study

Authors:	Saskia A. Brendle, Sven Krueger, Janno Fehrenbacher, Joachim Grifka, Peter E. Müller, William M. Mihalko, Berna Richter, Thomas M. Grupp
Journal:	Bioengineering – Special Issue: Joint Biomechanics and Implant Design
Volume:	11
Pages:	18
Year:	2024
DOI:	https://doi.org/10.3390/bioengineering11111064
Impact factor:	3.8 (according to InCites Journal Citation Reports 2023)

This publication was selected as the Cover Story of Volume 11, Issue 11 in Bioengineering.

bioengineering

Impact Factor 3.8
CiteScore 4.0
Indexed in PubMed

ISSN 2306-5354

Comparative Analysis of Kinematic Patterns of the Knee

Volume 11 · Issue 11 November 2024

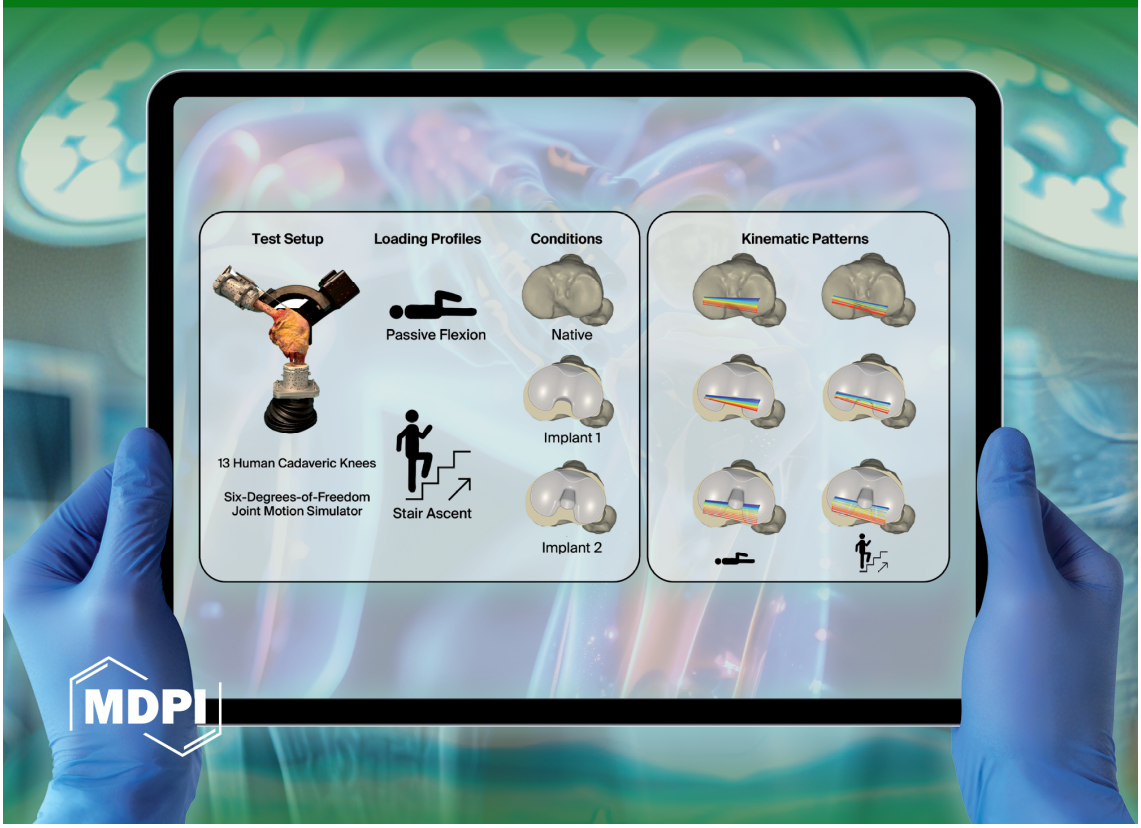

bioengineering

MDPI

Article

Kinematic Patterns of Different Loading Profiles Before and After Total Knee Arthroplasty: A Cadaveric Study

Saskia A. Brendle [1,2,*], Sven Krueger [1], Janno Fehrenbacher [1,3], Joachim Grifka [4], Peter E. Müller [2], William M. Mihalko [5], Berna Richter [1] and Thomas M. Grupp [1,2]

[1] Research & Development, Aesculap AG, 78532 Tuttlingen, Germany
[2] Department of Orthopaedic and Trauma Surgery, Musculoskeletal University Center Munich (MUM), Campus Grosshadern, LMU Munich, 81377 Munich, Germany
[3] Department of Mechanical and Process Engineering, Offenburg University of Applied Sciences, 77652 Offenburg, Germany
[4] Department of Orthopaedics, Asklepios Klinikum, 93077 Bad Abbach, Germany
[5] Campbell Clinic, Department of Orthopaedic Surgery & Biomedical Engineering, University of Tennessee Health Science Center, Memphis, TN 38104, USA
* Correspondence: saskia.brendle@aesculap.de

Abstract: One of the major goals of total knee arthroplasty (TKA) is to restore the physiological function of the knee. In order to select the appropriate TKA design for a specific patient, it would be helpful to understand whether there is an association between passive knee kinematics intraoperatively and during complex activities, such as ascending stairs. Therefore, the primary objective of this study was to compare the anterior–posterior (AP) range of motion during simulated passive flexion and stair ascent at different conditions in the same knees using a six-degrees-of-freedom joint motion simulator, and secondary, to identify whether differences between TKA designs with and without a post-cam mechanism can be detected during both activities, and if one design is superior in recreating the AP translation of the native knee. It was shown that neither TKA design was superior in restoring the mean native AP translation, but that both CR/CS and PS TKA designs may be suitable to restore the individual native kinematic pattern. Moreover, it was shown that passive and complex loading scenarios do not result in exactly the same kinematic pattern, but lead to the same choice of implant design to restore the general kinematic behavior of the native individual knee.

Keywords: knee; biomechanics; cadaveric study; kinematics; TKA design

Citation: Brendle, S.A.; Krueger, S.; Fehrenbacher, J.; Grifka, J.; Müller, P.E.; Mihalko, W.M.; Richter, B.; Grupp, T.M. Kinematic Patterns of Different Loading Profiles Before and After Total Knee Arthroplasty: A Cadaveric Study. *Bioengineering* **2024**, *11*, 1064. https://doi.org/10.3390/bioengineering11111064

Academic Editor: Ryan Willing

Received: 11 October 2024
Revised: 21 October 2024
Accepted: 24 October 2024
Published: 24 October 2024

1. Introduction

Total knee arthroplasty (TKA) is one of the most common procedures for the treatment of severe knee osteoarthritis [1–3]. Even though knee prostheses have improved greatly and became one of the most reliable joint replacements, numerous studies point out that only approximately 80% of the patients are satisfied with the results of their TKA [4–6]. It is hypothesized that the ability of the prosthesis to recreate the native tibiofemoral kinematics, especially the femoral rollback, is beneficial regarding patient satisfaction after TKA [7,8]. However, previous studies showed a high variability in the native knee kinematics, indicating the necessity for various TKA designs in order to restore physiological knee function [9]. For posterior cruciate ligament (PCL)-deficient TKA, surgeons can choose between inlay designs with or without a post-cam mechanism. It was shown that both inlay designs provide similar stability, but more potential complications were reported with the post-cam mechanism [10–12]. In addition, the post-cam mechanism could have an effect on tibiofemoral kinematics and result in a more pronounced femoral rollback [11,12].

Modern surgical navigation and robotic systems allow intraoperative measurement of knee joint kinematics and stability before and after implantation and provide real-time feedback on multiple parameters to adjust implant type, positioning and overall alignment

during surgery [8,13–19]. Therefore, the intraoperative kinematic analysis may assist in the selection of the TKA design and help surgeons get closer in restoring physiological knee function, since the only opportunity for adjustment of the kinematics is during surgery. However, it is not clear whether the differences in anterior–posterior (AP) translation between the native condition and different TKA designs can be detected intraoperatively during passive movements [13,17]. Furthermore, it is necessary to understand whether there is an association between passive knee kinematics measured during surgery and knee kinematics during complex activities of daily living. A previous study of Grassi et al. compared flexion–extension actively performed by the patient and passively performed by the surgeon using a navigation system [18]. They found that muscle contraction did not significantly affect the knee kinematics before and after TKA. Kono et al. reached the same conclusion in a cadaveric study [13]. Belvedere et al. showed that passive knee kinematics measured intraoperatively after TKA using a navigation system were predictive of postoperative kinematics measured using monoplane fluoroscopy during several complex weight-bearing activities [15,16]. Gasparutto et al. compared the passive knee kinematics during surgery with active knee kinematics during walking [14]. However, they could not draw any solid conclusions about differences between the activities because of too many influencing factors, such as the use of different methods to measure the kinematics during different activities. This shows the importance of a highly controlled environment for valid comparison between different conditions and loading profiles.

Therefore, the primary objective of this study was to compare the AP range of motion and position of the medial and lateral femoral condyles during passive flexion and a complex activity of daily living such as stair ascent, in the native condition, after resection of the cruciate ligaments and after implantation of two different TKA designs (with and without a post-cam mechanism) in the same knees. The secondary objective was to identify whether differences between the two different TKA designs can be detected during passive flexion and stair ascent, and if one design is superior in recreating the AP translation of the native knee. The hypothesis was that passive and complex loading scenarios show a comparable range of motion in the AP direction, especially after TKA. We anticipated that with the post-cam TKA design, the femoral posterior translation is higher compared to the TKA design without a post-cam mechanism. Furthermore, we hypothesized that no design is superior in restoring the mean native AP translation but for individual knees either the TKA design with or without a post-cam mechanism is superior in recreating the individual native kinematic pattern.

2. Materials and Methods

2.1. Specimen Preparation

This in vitro study used thirteen fresh-frozen human cadaveric lower right extremities, preserved from the femoral head to the malleoli. The samples included three females and ten males with a mean age of 67 ± 10 years and a mean body mass index of 23.3 ± 8.0 kg/m^2. Medical records did not indicate any pre-existing knee disorders, surgical interventions, or other relevant pathologies. No specimen had a severe varus or valgus deformity (≥10°). The mean native anatomical slope medially was 9.1 ± 2.8°. Ethical approval was obtained from the ethics committee of the Ludwig Maximilian University of Munich (No. 20-0856).

The specimen preparation and the general experimental setup were based on a methodology recently published by Brendle et al. [20]. Before the experiment, landmark-based femoral and tibial coordinate systems were generated by using segmented computed tomography (CT) scans of the specimens. Each specimen was thawed for 24 h at 7 °C and then prepared for testing. The proximal and distal segments of the leg were skeletonized, preserving soft tissue 100 mm superior and 50 mm inferior to the knee joint space. GOM measuring points (1.5 mm, Carl Zeiss GOM Metrology GmbH, Braunschweig, Germany) were attached to the clean bones and 3D fittings of femur and tibia were performed by aligning the segmented CT scans to the previously acquired 3D point clouds of each bone (ARAMIS 12M, Carl Zeiss GOM Metrology GmbH, Braunschweig, Germany). Subse-

Bioengineering **2024**, *11*, 1064

quently, the 3D fitting information was saved and the femur and tibia were transected and embedded in custom-made aluminum pots using fast-cast resin (Gößl und Pfaff, Brautlach, Germany) to allow fixation in a six-degrees-of-freedom joint motion simulator. Thereby, the femur was embedded such that the femoral coordinate system was aligned with the upper coordinate system of the joint motion simulator, whereas the tibia was embedded to achieve 0° flexion.

2.2. Implantation

The specimens underwent cruciate-sacrificing TKA without patella resurfacing by an experienced knee surgeon using oneKNEE TKA components (Aesculap AG, Tuttlingen, Germany). This TKA system allows the use of a femoral component and an inlay with or without a post-cam mechanism (PS or CR/CS) fixed to the same tibial component. First, a standard medial parapatellar arthrotomy and lateral dislocation of the patella were performed. After resection of osteophytes and menisci, a tibial cut was made using an extramedullary alignment guide. This was possible since the exact positions of the tibia and fibula in the tibia pot were known from the previous 3D fitting, and therefore the center of the malleoli could be reconstructed using custom-made fixtures specifically designed to match the alignment guide as shown in Figure 1.

Figure 1. Extramedullary alignment technique for the tibial cut with reconstruction of the center of the malleoli.

The tibial cut was made with a 0° slope, whereas a 3° posterior slope is integrated in the polyethylene inserts. The medial third of the tuberosity was used as a reference for the tibial rotation alignment. The femoral cut was made perpendicular to the mechanical axis of the femur using an intramedullary guide. Rotation of the femoral component was aligned as indicated by the soft-tissue strain at 90° knee flexion. Furthermore, a box preparation was conducted to allow the use of a PS femoral component. The trial components were positioned and the ligamentous situation was evaluated in flexion and extension to ensure proper implant alignment, knee balance, and function. Following this, the definite CR/CS components underwent a 3D fitting by aligning their computer-aided design (CAD) files to 3D point clouds of the femoral and tibial component. Afterwards, the components were inserted and the positions of the implants relative to the respective bones were measured

(ARAMIS 12M, Carl Zeiss GOM Metrology GmbH, Braunschweig, Germany). In a second step, the CR/CS femoral component and inlay were changed by a PS femoral component and inlay of the same size. The bone cuts remained unchanged.

2.3. Experimental Testing

Testing was performed on a six-degrees-of-freedom joint motion simulator (VIVO, Advanced Mechanical, Technologies Inc., Watertown, MA, USA), as illustrated in Figure 2. The femoral actuator provides flexion–extension and varus–valgus rotations, whereas the tibial actuator manages medial–lateral, anterior–posterior and proximal–distal translations, and internal-external rotations. The simulator allows independent control of each degree-of-freedom in either force or displacement mode. The forces and motions are expressed following the Grood and Suntay conventions [21].

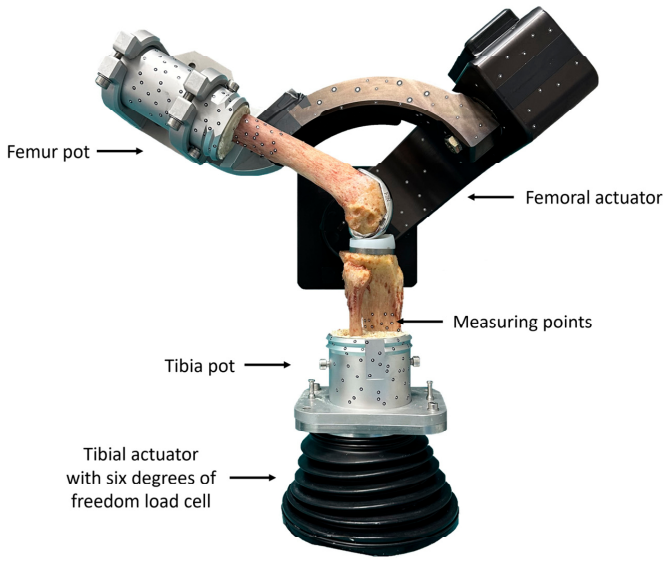

Figure 2. Experimental setup with the instrumented knee specimen mounted on the six-degrees-of-freedom joint motion simulator at 60° flexion. Soft tissue was removed for clarity, but left intact during actual testing.

After mounting the native specimen in the joint motion simulator, the previously generated 3D fitting information of the segmented CT scans were again projected onto the residual bones using the measuring points. In this way, the 3D information of the complete femur and tibia were available even after parts of the bones were resected. Based on this, the relative position of the femoral and tibial coordinate systems in the native condition was recorded and transferred to the joint motion simulator. Afterwards, the specimens were subjected to dynamic testing. The neutral path of motion of each knee was recorded by applying continuous knee flexion from 0° to 90° while maintaining an axial compression force of 50 N and all other forces/moments at 0 N/Nm. In addition, stair ascent was simulated by applying AVER75 loading data obtained from the Orthoload database [22]. The loads were reduced by 75% to prevent specimen damage considering the absence of muscle activity. The flexion angle was prescribed and all other degrees-of-freedom were controlled in force mode. Each loading profile was applied in the native condition, after resection of the cruciate ligaments and with both a CR/CS and a PS TKA design for four cycles at a frequency of 0.04 Hz. For all conditions, the knee capsule was opened using a medial parapatellar approach and closed with surgical sutures (Number 1 Vicryl, B. Braun, Melsungen, Germany). During testing, the relative position of the femoral and

tibial coordinate systems was recorded by the joint motion simulator. To mitigate the effects of tissue drying during testing, the specimens were kept moist with sodium chloride solution. Furthermore, the passive tension of the patella tendon was simulated by a spring sutured to the quadriceps tendon with an increasing force of up to 50 N at 90° flexion. Figure 3 illustrates the entire testing process.

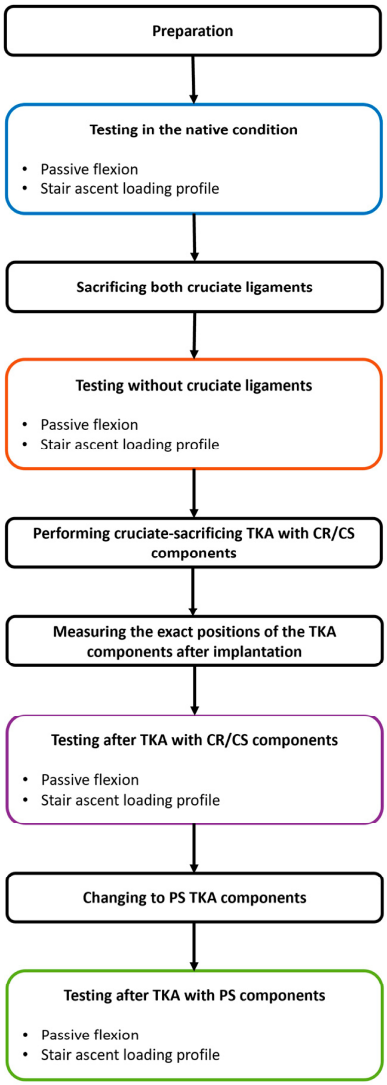

Figure 3. Illustration of the key steps of the entire testing process. TKA = total knee arthroplasty. CR/CS = TKA design without a post-cam mechanism. PS = TKA design with a post-cam mechanism.

2.4. Data Analysis

Data from a single cycle of each experiment were analyzed using MATLAB (Version R2023a, MathWorks Inc., Natick, MA, USA) [20]. Statistical analyses were performed using Minitab (Version 21.2, Minitab GmbH, Munich, Germany). For all analyses, the medial and lateral flexion facet centers (MFC and LFC) of the native femoral condyles were projected

onto the tibial plane at different timepoints. Subsequently, the positions were normalized to the anterior–posterior and medial–lateral width of the articular surface of the respective tibia, which were defined as the distance between the most anterior and posterior points of the medial articular surface and the most medial and lateral points of the proximal tibia, respectively. Thus, irrespectively of the different tibia size: 0 and 1 correspond to the most posterior and most anterior position, respectively.

The normalized AP range of motion (ROM) medially and laterally was analyzed for both movements in all conditions between 14° and 90° of flexion, as the flexion angles of the two loading profiles overlap in this range and, therefore, only the influence of the load situation and not that of the flexion angle was investigated. The significance of the differences between the normalized medial and lateral AP ROM during passive knee flexion and stair ascent was investigated for all conditions using Wilcoxon signed-rank tests with the level of significance set at $p \leq 0.05$. In addition, the projections of the MFC and LFC of all specimens at 14° flexion and at flexion angles between 15° and 90° are plotted in 5° increments on a normalized tibia for all loading profiles and conditions.

To investigate the differences between the native condition and the two TKA designs, the normalized medial and lateral AP translation of each specimen was calculated for the entire loading profiles in the different conditions and normalized to the native positions at 0° during passive flexion. Wilcoxon signed-rank tests were used to compare the normalized AP translation between the native condition, and after implantation of a CR/CS and a PS TKA design pairwise at 5° flexion intervals for passive flexion and 5 % gait cycle intervals for stair ascent ($p \leq 0.05$). Furthermore, the projections of the MFC and LFC of three exemplary specimens are shown for the full range of flexion of both loading profiles in the native condition, and with both TKA designs at 5° flexion and 5% gait cycle intervals, respectively.

Four specimens showed joint luxation or exceeded the travel limits of the joint motion simulator during one of the applied loading scenarios and were therefore removed from the data analysis.

3. Results

3.1. Anterior–Posterior Range of Motion and Position During Passive Flexion and Stair Ascent

Figure 4 shows boxplots of the normalized AP ROM medially and laterally. The boxplots include the median normalized AP ROM, the first and third quartiles, and the range. Outliers are shown with dots. Significant differences ($p \leq 0.05$) are marked with an asterisk.

In the native condition, the median medial AP ROM was 0.14 during passive flexion and slightly lower with 0.13 during stair ascent. The median lateral AP ROM showed a higher variability and was greater than the medial ROM for both loading profiles. Furthermore, there was a significant difference ($p = 0.024$) between the AP ROM during passive flexion (0.17) and during stair ascent (0.18). After cruciate ligament resection, the median AP ROM was generally smaller compared to the native condition. The median medial AP ROM was significantly higher ($p = 0.013$) at 0.10 during stair ascent, compared to 0.05 during passive flexion. The median lateral AP ROM was higher than the median medial AP ROM with 0.11 during passive flexion and 0.14 during stair ascent. After implantation of the CR/CS TKA design, both the medial and lateral median AP ROM were significantly different between passive flexion and stair ascent ($p = 0.013$ and $p = 0.033$). Compared to the condition without cruciate ligaments, the median medial AP ROM increased slightly during passive flexion (0.08) and remained the same during stair ascent (0.10). The median lateral AP ROM increased during both passive flexion (0.12) and stair ascent (0.17) and was greater than the medial AP ROM for both loading profiles. After implantation of the PS TKA design, the medial and lateral AP ROM were higher compared to all other conditions. The median medial AP ROM was 0.17 during passive flexion and 0.18 during stair ascent, whereas the median lateral AP ROM was 0.28 and 0.30, respectively.

Bioengineering **2024**, *11*, 1064

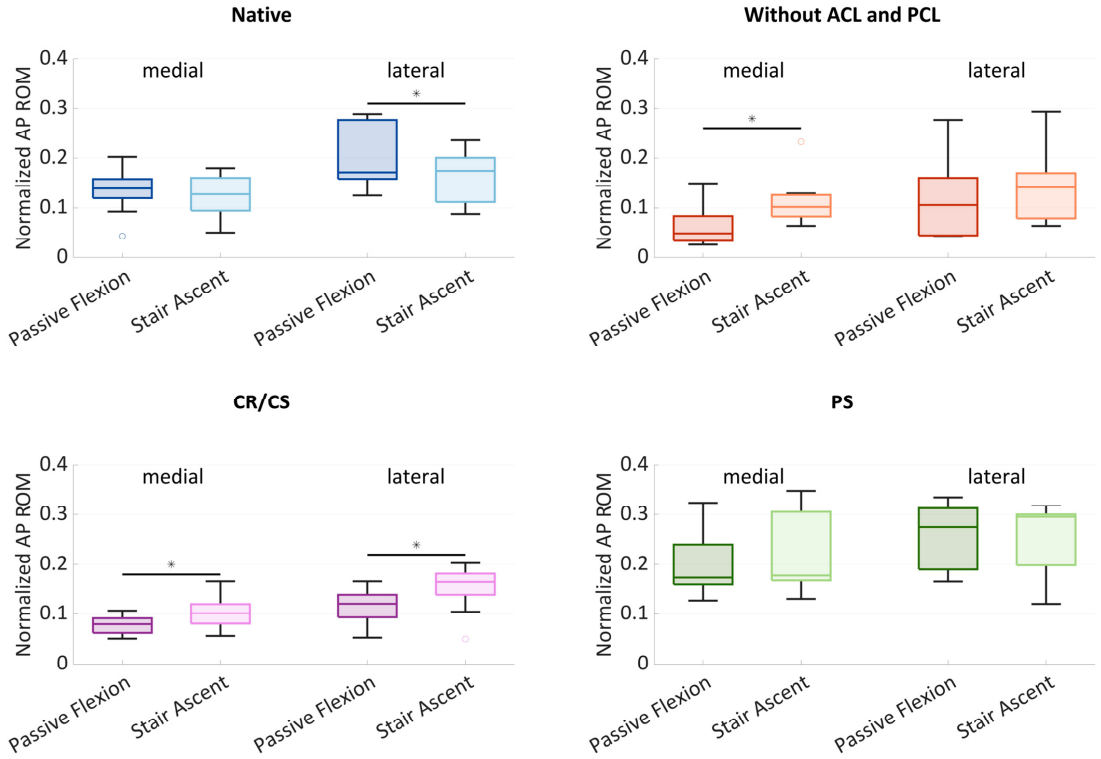

Figure 4. Normalized medial and lateral anterior–posterior (AP) range of motion (ROM) during passive flexion and stair ascent ($n = 9$) in the native condition (blue), after resection of the cruciate ligaments (red) and after implantation of the CR/CS (purple) and PS (green) total knee arthroplasty (TKA) design. Significant differences are marked with an asterisk ($p \leq 0.05$).

In all conditions, a generally higher AP ROM was found laterally, which can be interpreted as a medial pivoting kinematic. In addition, the lateral variability was greater in the native condition and without cruciate ligaments, which may be due to a more or less pronounced medial pivoting characteristic.

Figure 5 shows the projections of the MFC and LFC of all specimens at 14° of flexion and at flexion angles between 15° and 90° in 5° increments on a normalized tibia for all loading profiles and conditions, illustrating the condylar motion patterns of the specimens.

In the native condition, the medial condyles ranged around the posterior third of the tibia, mainly between 0.5 and 0.15 for both passive flexion and stair ascent. The lateral condyles not only showed a difference in AP ROM between passive flexion and stair ascent, but also a difference in position. During passive flexion, the lateral condyles were mainly between 0.5 and 0.1, but slightly more posterior between 0.4 and 0 during stair ascent. After resection of the cruciate ligaments, the projections of both condyles resulted in a high density of points during passive flexion, ranging mainly between 0.4 and 0.2 medially and between 0.5 and 0.15 laterally. In contrast, during stair ascent, the projections of the MFC and LFC showed a high variability and were mainly located between 0.5 and −0.05 medially, and slightly more posterior, between 0.4 and −0.05 laterally. After implantation of the CR/CS TKA design, the projections of the medial condyles were located more anterior than in the native condition and after cruciate ligament resection during both activities, ranging mainly between 0.6 and 0.3 during passive flexion and between 0.65 and 0.3 during stair ascent. The projections of the lateral condyles were also located more anterior

Bioengineering **2024**, *11*, 1064

than in the native condition, especially during stair ascent (0.6–0.1). After implantation of the PS TKA design, the anterior border of the point pattern was approximately in the same position as for the CR/CS TKA design for both condyles and loading profiles. In contrast, the posterior border of the point pattern was located more posteriorly compared to the CR/CS design. The pattern during passive flexion and stair ascent was comparable, ranging mainly between 0.6 and 0.2 medially and between 0.5 and 0 laterally.

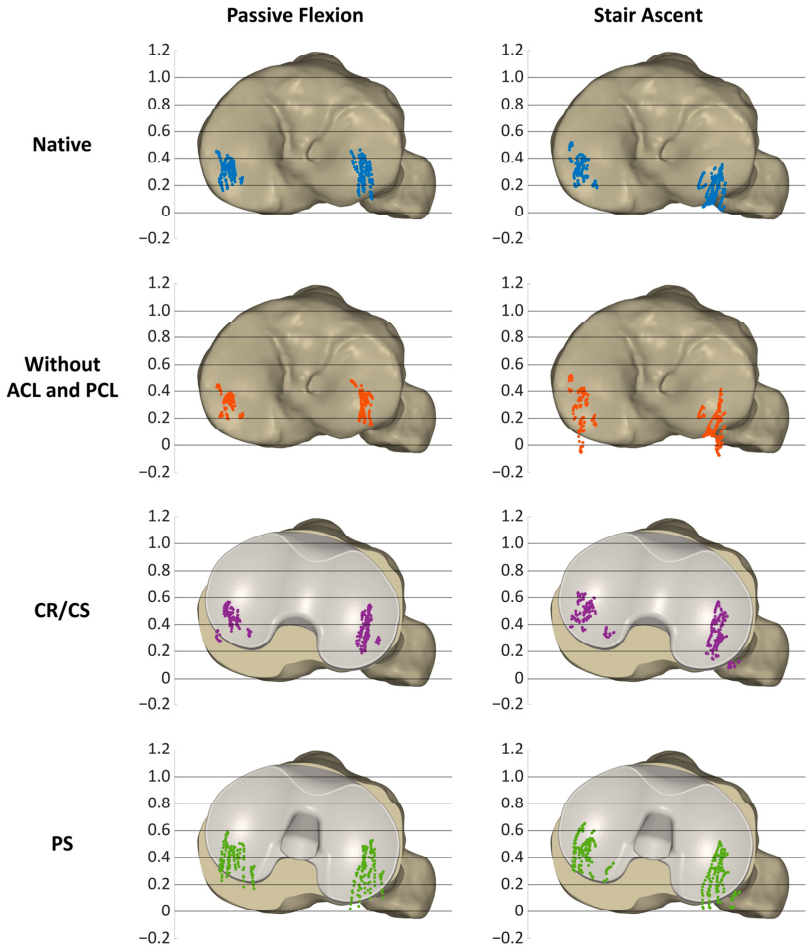

Figure 5. Projections of the native medial and lateral flexion facet centers (MFC and LFC) of all specimens (n = 9) and all timepoints during passive flexion and stair ascent on a normalized tibia.

3.2. AP Translation in the Native Condition and After TKA

Figure 6 shows the mean normalized medial and lateral AP translation and standard deviation during passive flexion and stair ascent in the native condition and after implantation of the CR/CS and PS TKA designs. Statistical significance is presented in Table 1. For clarity, the condition without cruciate ligaments is not illustrated in this section.

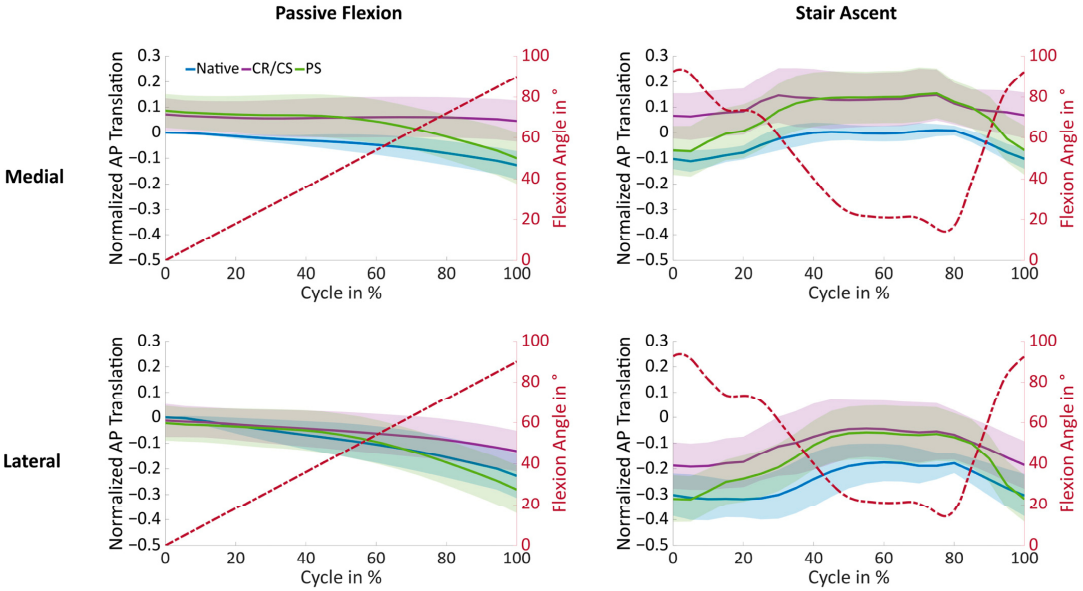

Figure 6. Mean normalized medial and lateral AP translation and standard deviation versus the movement cycle for passive flexion and stair ascent (n = 9) in the native condition (blue) and after implantation of the CR/CS (purple) and PS (green) TKA design.

Table 1. Statistical significances ($p \leq 0.05$) of the normalized medial and lateral AP translation between the native condition and the CR/CS TKA design, the native condition and the PS TKA design, and the CR/CS and PS TKA design during passive flexion and stair ascent (n = 9). ns = not significant. M = medial. L = lateral.

	Passive Flexion							Stair Ascent					
Flexion	**Native vs. CR/CS**		**Native vs. PS**		**CR/CS vs. PS**		**% Cycle (Flexion)**	**Native vs. CR/CS**		**Native vs. PS**		**CR/CS vs. PS**	
	M	**L**	**M**	**L**	**M**	**L**		**M**	**L**	**M**	**L**	**M**	**L**
0°	0.024	ns	0.018	ns	ns	ns	**0 (92.6°)**	0.013	0.024	ns	ns	0.009	0.009
5°	0.024	ns	0.018	ns	ns	ns	**5 (91.4°)**	0.009	0.018	ns	ns	0.009	0.009
10°	0.018	ns	0.024	ns	ns	ns	**10 (81.4°)**	0.009	0.018	ns	ns	0.009	0.009
15°	0.018	ns	0.024	ns	ns	ns	**15 (73.7°)**	0.009	0.009	0.044	ns	0.009	0.009
20°	0.024	ns	0.024	ns	ns	ns	**20 (73.5°)**	0.013	0.009	0.044	ns	0.009	0.009
25°	0.024	ns	0.033	ns	ns	ns	**25 (70.5°)**	0.013	0.009	ns	0.033	0.009	0.009
30°	0.024	ns	0.033	ns	ns	ns	**30 (61.1°)**	0.013	0.009	0.024	0.018	0.013	0.009
35°	0.024	ns	0.024	ns	ns	ns	**35 (50.5°)**	0.013	0.009	0.024	0.013	ns	0.013
40°	0.033	ns	0.024	ns	ns	ns	**40 (40.1°)**	0.013	0.009	0.013	0.009	ns	0.044
45°	0.024	ns	0.033	ns	ns	ns	**45 (30.4°)**	0.033	0.013	0.013	0.009	ns	ns
50°	0.024	ns	0.033	ns	ns	0.033	**50 (23.7°)**	0.024	0.013	0.013	0.009	ns	ns
55°	0.018	ns	0.033	ns	ns	0.024	**55 (21.7°)**	0.013	0.013	0.013	0.013	ns	ns
60°	0.013	ns	0.044	ns	0.024	0.013	**60 (21.1°)**	0.013	0.013	0.013	0.018	ns	ns
65°	0.013	ns	0.044	ns	0.013	0.009	**65 (21.3°)**	0.013	0.018	0.013	0.018	ns	ns
70°	0.009	ns	ns	ns	0.009	0.009	**70 (20.6°)**	0.013	0.013	0.013	0.013	ns	ns
75°	0.009	ns	ns	ns	0.009	0.009	**75 (15.6°)**	0.013	0.013	0.013	0.013	ns	ns
80°	0.009	0.044	ns	ns	0.009	0.009	**80 (16.9°)**	0.013	0.013	0.013	0.018	ns	ns
85°	0.009	0.033	ns	ns	0.009	0.009	**85 (38.7°)**	0.018	0.018	0.018	0.024	ns	ns
90°	0.009	0.024	ns	ns	0.009	0.009	**90 (62.5°)**	0.013	0.013	0.033	ns	0.018	0.024
							95 (83.7°)	0.013	0.018	ns	ns	0.009	0.009
							100 (92.5°)	0.013	0.024	ns	ns	0.009	0.009

In the native condition, posterior femoral rollback was observed both medially and laterally during passive flexion. After implantation, the medial condyle showed a more anterior position compared to the native knee over the entire range of flexion. The differences in position between the native condition and the CR/CS TKA design remained statistically significant over the entire range of flexion, whereas the differences between the native condition and the PS TKA design were significant only up to 65° of flexion, and then showed almost the same position in the anterior–posterior direction. The lateral condyle generally showed more posterior femoral translation than the medial condyle across all conditions. Furthermore, for the lateral condyle no significant differences were found between the native condition and the PS TKA design over the entire range of flexion. In contrast, the AP position of the CR/CS TKA design differed significantly from the native condition beyond 80° of flexion.

During stair ascent, both condyles showed significant differences in the AP position with the CR/CS TKA design compared to the native condition over the entire range of motion, whereas the PS TKA design differed only at flexion angles below 80°. At flexion angles above 60°, the PS TKA design induced significantly more posterior femoral rollback with both loading profiles. This shows that both loading profiles are capable of revealing differences between the two TKA designs. As expected, no TKA design was superior in recreating the mean native AP translation, which may be due to the high variability in the native knee kinematics and the need for individual selection of the TKA design to restore the individual physiological knee function. Therefore, the kinematic patterns of three exemplary specimens were investigated in more detail in the following.

3.3. Individual Kinematic Patterns

Figures 7–9 show the projections of the flexion axis and the MFC and LFC of three different specimens throughout the full range of motion for both loading profiles in the native condition and after implantation of the CR/CS and PS TKA designs at 5° flexion and 5% gait cycle intervals, respectively, and thereby reflect the individual condylar motion. The colors represent the respective flexion angle in 5° intervals. The 0° flexion is colored in dark blue and 90° flexion is colored in red. Gait intervals are colored based on the corresponding flexion angle. For consistency, tibia sizes are still standardized. Therefore, 0 and 1 correspond to the most posterior and anterior positions, respectively, regardless of the different tibia sizes.

Figure 7 illustrates the condylar motion of specimen S1 at various conditions and loading profiles. In the native condition, the medial condyle showed approximately the same kinematic pattern for both loading profiles. In contrast, the lateral condyle was positioned approximately 0.2 more posteriorly during stair ascent. With the CR/CS TKA design, the medial condyle shifted approximately 0.1 anteriorly during both loading profiles compared to the native condition. During passive flexion, the lateral condyle showed the same position throughout the range of flexion as in the native condition. During stair ascent, the lateral condyle shifted approximately 0.2 anteriorly for the entire range of motion compared to the native condition, and thus, resulted in the same position as during passive flexion. With the PS TKA design, in extension, the medial and lateral condyles were in the same position as with the CR/CS TKA design for both loading profiles. In flexion, both condyles showed a greater femoral rollback compared to the CR/CS TKA design and the native condition. The most posterior position of the medial and lateral condyles was similar for both loading profiles.

In this specimen, the CR/CS TKA design was superior in recreating the native kinematic pattern, but not the exact kinematics, including the exact AP position and translation. Furthermore, comparable kinematic patterns were observed between the passive flexion and stair ascent after implantation of the TKA components.

Bioengineering **2024**, *11*, 1064

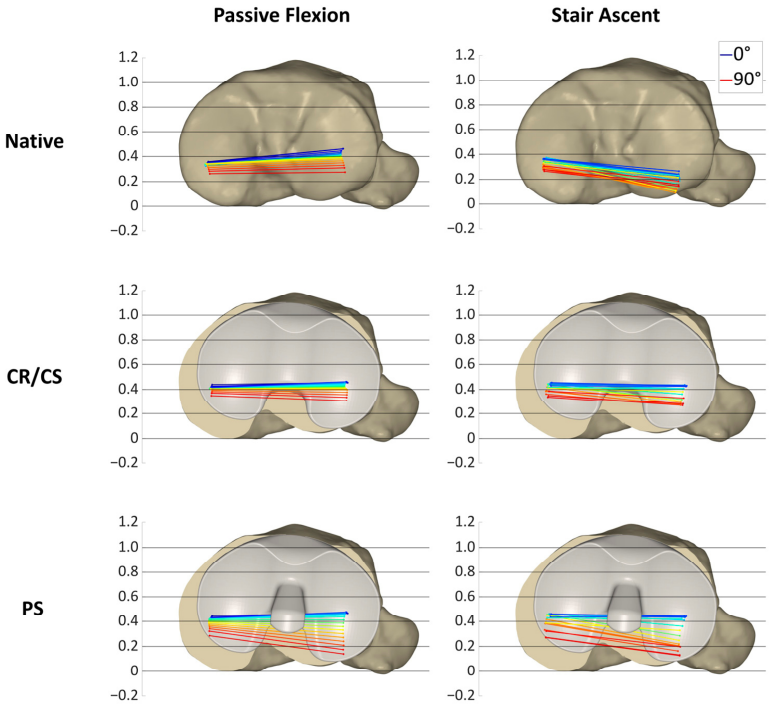

Figure 7. Projection of the flexion axis and the MFC and LFC for specimen S1, showing the individual condylar motion during passive flexion (0°–90° flexion) and stair ascent (16°–93° flexion) for the native condition and after implantation of the CR/CS and PS TKA designs. The colors represent the respective flexion angle in 5° intervals, from dark blue (0°) through green and yellow to red (90°).

In Figure 8, the condylar motion of specimen S2 is presented for various conditions and loading profiles. As for specimen S1, the medial condyle showed approximately the same kinematic pattern for both loading profiles in the native condition, whereas the lateral condyle was positioned more posteriorly during stair ascent. With the CR/CS TKA design, the medial condyle shifted approximately 0.1 anteriorly in extension during both loading profiles compared to the native condition and showed almost no change in position throughout the range of flexion. During passive flexion, the lateral condyle was located approximately in the same position as in the native condition in extension, but exhibited less posterior femoral rollback in flexion. During stair ascent, the lateral condyle shifted approximately 0.15 anteriorly in extension, and it also exhibited considerably less posterior femoral rollback in flexion compared to the native condition. After the implantation of the PS TKA design, the medial and lateral condyles in extension were located almost in the same position as with the CR/CS TKA design for both loading profiles. In flexion, both condyles showed a considerably higher femoral rollback compared to the CR/CS TKA design, but less femoral rollback than in the native condition. The most posterior position of the medial condyle was similar for both loading profiles, but more posterior for the lateral condyle during stair ascent.

For this specimen, the PS TKA design was superior in recreating the posterior femoral rollback as observed in the native kinematic pattern. Furthermore, comparable kinematic patterns were observed between passive flexion and stair ascent after implantation of the TKA components.

Bioengineering **2024**, *11*, 1064

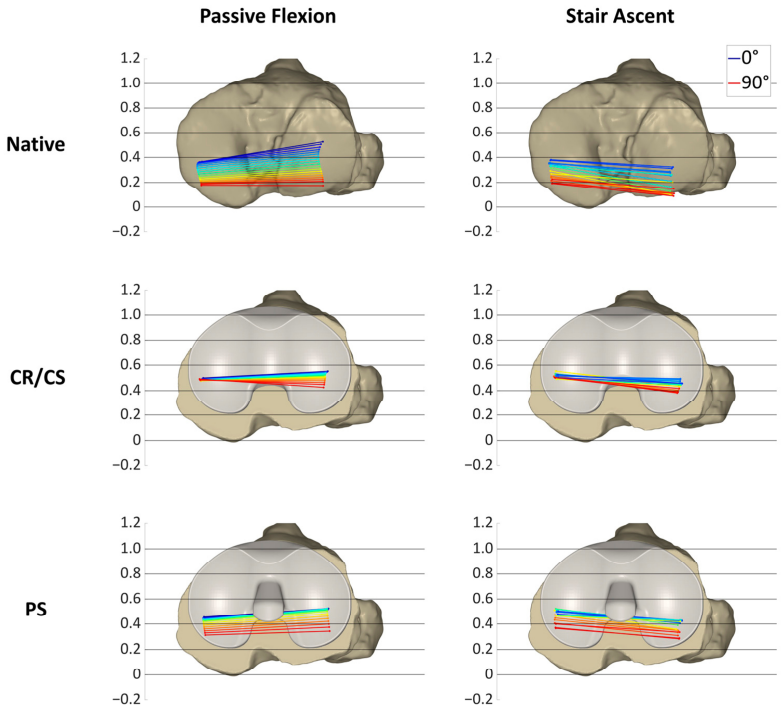

Figure 8. Projection of the flexion axis and the MFC and LFC for specimen S2, showing the individual condylar motion during passive flexion (0°–90° flexion) and stair ascent (16°–93° flexion) for the native condition and after implantation of the CR/CS and PS TKA designs. The colors represent the respective flexion angle in 5° intervals, from dark blue (0°) through green and yellow to red (90°).

Figure 9 shows the condylar motion of specimen S3 at various conditions and loading profiles. In the native condition, the medial condyle showed approximately the same kinematic pattern for both loading profiles, whereas the lateral condyle was positioned more posteriorly and exhibited less femoral rollback during stair ascent. This resulted in a medial pivoting characteristic for passive flexion and a more parallel rollback for stair ascent. With the CR/CS TKA design, the medial condyle shifted approximately 0.1 anteriorly during both loading profiles compared to the native condition. In extension, the lateral condyle showed the same position as in the native condition during passive flexion and was shifted approximately 0.1 anteriorly during stair ascent. Furthermore, the medial and lateral AP ROM during passive flexion was slightly reduced compared to the native condition, whereas the AP ROM during stair ascent remained almost the same. As for the other specimens, with the PS TKA design, in extension, the medial and lateral condyles were in the same position for both loading profiles as with the CR/CS TKA design. In flexion, both condyles showed a considerably higher femoral rollback compared to the CR/CS TKA design and a slightly higher femoral rollback compared to the native condition. As for specimen S1, the most posterior position of the medial and lateral condyles was similar for both loading profiles.

In this specimen, the native kinematic pattern was intermediate between the kinematic patterns of the two different TKA designs. Therefore, both TKA designs are suitable and do not alter the native kinematic pattern substantially.

Bioengineering **2024**, *11*, 1064

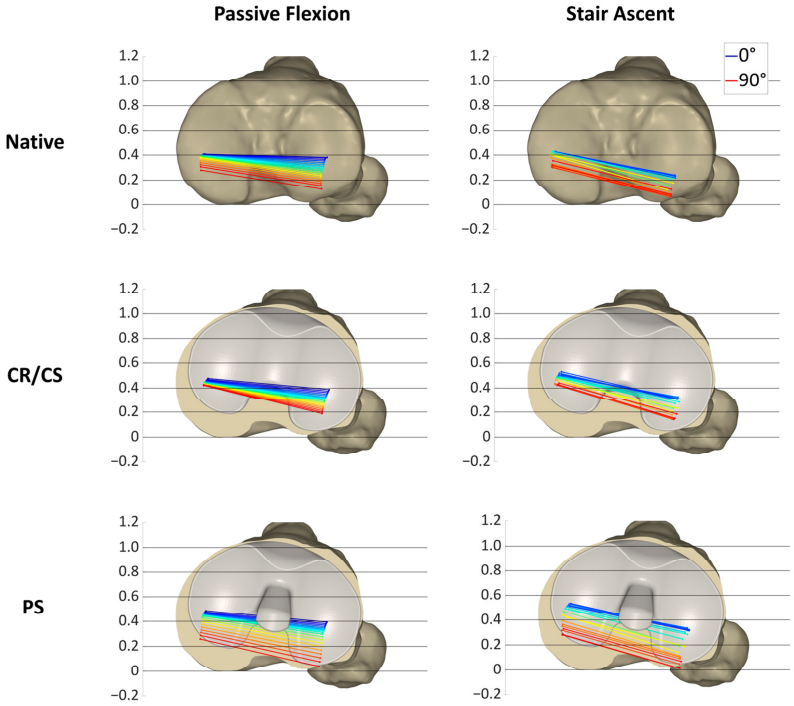

Figure 9. Projection of the flexion axis and the MFC and LFC for specimen S3, showing the individual condylar motion during passive flexion (0°–90° flexion) and stair ascent (16°–93° flexion) for the native condition and after implantation of the CR/CS and PS TKA designs. The colors represent the respective flexion angle in 5° intervals, from dark blue (0°) through green and yellow to red (90°).

4. Discussion

The main objective of the present study was to compare the AP range of motion and position of the medial and lateral femoral condyles during passive flexion and a complex activity of daily living, in the native condition, after resection of the cruciate ligaments and after implantation of the CR/CS and PS TKA designs. Passive knee flexion and stair ascent did not result in the same AP range of motion for each condition, but showed comparable condylar motion patterns, especially after TKA. As a secondary objective, we investigated whether differences in AP translation between the two different TKA designs can be detected during passive flexion and a complex activity of daily living, and if one design is superior in recreating the AP translation of the native knee. We found significant differences between the TKA designs with both loading profiles, with the PS TKA design showing a higher posterior translation of the femur in flexion. As expected, no design was superior in restoring the mean native AP translation throughout the range of motion. However, when looking at individual specimens, we found that either one of the TKA designs was superior in recreating the individual native kinematic pattern, or that both TKA designs were suitable and did not substantially alter the native kinematic pattern.

To our knowledge, this is the first study that has compared the kinematic patterns of different loading scenarios before and after total knee arthroplasty in the same knees with the same measuring technology in a highly controlled setting. Comparing the same knees at different conditions eliminates the problem of differences between cohorts. In addition, the controlled application of forces along reliable axes is an important aspect to ensure a valid comparison of different conditions in the same knees. Furthermore, using the same definitions while describing kinematics is essential to eliminate potential variations

in the results and interpretation of movement [23,24]. This study projected the flexion facet centers (FFCs) of the native femur onto the tibial plane and thereby visualized the kinematic pattern at different conditions. The projection of the FFCs is a widely used method for approximating the tibiofemoral contact situation and is valid for describing the kinematic behavior of the knee [25,26]. However, the projection of the native FFCs after implantation does not reflect the contact situation but the motion that the patient may feel. Another important aspect is the use of the same flexion angle range to compare the AP range of motion and the general kinematic pattern between the loading profiles. This overcomes the influence of the flexion angle on the AP translation, and therefore, only the influence of the loading situation is evaluated [27,28].

The hypothesis that passive and complex loading scenarios show a comparable range of motion in the AP direction, especially after TKA, could not be completely confirmed. In the native condition, the medial condyle showed a comparable AP range of motion and position with both loading profiles. In contrast, the AP range of motion of the lateral condyle revealed significant differences between passive flexion and the stair ascent loading profile in the native condition. Furthermore, the projection of the flexion facet centers showed that the tibiofemoral contact situation also differed between the loading profiles. The lateral condyle was located more posterior during stair ascent than during passive flexion. After cruciate ligament resection, the medial AP range of motion was significantly greater during stair ascent than during passive flexion. In addition, the projections of the MFC and LFC revealed large differences between the general kinematic patterns. During passive flexion, many of the projected points were clustered in one spot, meaning that the condyles were barely moving. This is probably due to the loss of the natural femoral rollback following cruciate ligament resection [29]. Therefore, the AP range of motion was considerably smaller than in the native condition. In contrast, during stair ascent, the projected points showed a large variance. This could be due to the varying degrees of destabilization of the specimens after cruciate ligament resection in combination with the complex loading scenario [20,30,31]. After implantation of the CR/CS TKA design, there were significant differences in the AP range of motion between the loading profiles, both medially and laterally. In contrast, no differences between the loading profiles were found after the implantation of the PS TKA design. This might be due to the higher guidance of the PS TKA design. A previous study of Belvedere et al. also found fewer differences between passive movement and complex activities with a more constraining TKA design [16]. The projection of the MFC and LFC with both TKA designs showed a comparable condylar motion pattern between passive flexion and stair ascent. In addition, a stabilization of the joint with a more anterior position of both condyles during the entire range of flexion was observed during stair ascent compared to the condition after resection of the cruciate ligaments. This demonstrates the generally good performance of the TKA designs and the ability to compare the general motion patterns between passive and complex loading scenarios after TKA. The reason for the large differences in the motion patterns between the loading profiles before TKA could be the high native slope of the specimens and the geometry of the lateral tibial plateau under the influence of the load situation. During stair ascent, the load is considerably higher than during passive flexion, even with load reduced loading profiles. Giffin et al. showed that axial loading in combination with a high tibial slope resulted in a more posterior position of the femoral condyles on the tibia plateau [32]. Furthermore, the complex loading scenarios including AP shear forces combined with the tibial slope may also influence the AP position of the femoral condyles on the tibial plateau. This could explain the more posterior position of the femoral condyles during stair ascent compared to passive flexion before the implantation of the TKA components. However, when looking at the individual specimens, it could be observed that despite the differences between passive and complex loading scenarios, the same TKA design would be chosen to closely mimic the native kinematic pattern.

The hypothesis that with the post-cam TKA design, the femoral posterior translation is higher compared to the TKA design without a post-cam mechanism could be confirmed.

At flexion angles above 60°, the PS TKA design induced significantly more posterior femoral rollback for both loading profiles, showing the impact and function of the post-cam mechanism. This demonstrates that both loading profiles were capable of revealing differences between the two TKA designs.

As expected, neither TKA design was superior in restoring the mean native AP translation of both condyles over the entire range of motion. In contrast, when looking at the individual specimens, the CR/CS TKA design was superior in restoring the overall native kinematic pattern in specimen S1, whereas the PS TKA design was superior in specimen S2. This indicates the necessity for individual kinematic analyses and the possibility to select a TKA design out of a comprehensive knee platform to address subject-specific functional needs and thereby restore the physiological knee function. However, neither the exact AP position of the native femoral condyles nor the exact AP translation was restored in these specimens. Given the still relatively high rate of 80% of patients who are satisfied with the results of their TKA, we believe that it is not necessary to exactly restore the native kinematics, but to avoid large differences and restore the general kinematic pattern as observed in the individual specimens. For example, a patient with no femoral rollback in the native condition, but a high femoral rollback after implantation, may not feel comfortable. This is particularly important for characteristic kinematics, such as those in specimens S1 and S2. For specimen S3, both TKA designs may be appropriate as they do not substantially alter the native kinematics. However, as these are only assumptions, further research and clinical studies are needed to identify the relevant parameters that are essential for the restoration of function and patient satisfaction. Furthermore, the extent to which native kinematics should be mimicked needs to be clarified, as they may already be altered due to osteoarthritis. Future studies should also consider the influence of different alignment techniques, soft-tissue balance, tibial slope, and physiological muscle loading to gain a better understanding of the differences in knee kinematics before and after TKA.

The main strength of the present study is the precise measurements of the kinematics under different conditions and loading scenarios in the same knees, which eliminates the problem of large individual and technical differences. However, several limitations should be considered when interpreting the results of this study. First, this study investigated only a small number of human cadaveric specimens that may show variations in soft tissue properties compared to living patients. However, the comparison of passive and complex activities with different implant designs in the same knees is not possible in vivo due to ethical reasons. Second, the applied loading profile used to simulate the complex activity was based on published data on instrumented knee implants [22,33]. This loading profile is also used in complex wear testing and is considered to realistically simulate patient movement under load conditions encountered during daily activities [34]. However, the data were recorded using an ultra-congruent implant design, which may limit their applicability to the intact knee. Therefore, although the applied loading profile resembles an activity of daily living, it does not fully represent the knee movement in all its complexity. However, in the absence of alternatives, the proposed standardized loads appear to be the most appropriate. In addition, the loads were reduced by 75% to avoid specimen damage considering the absence of muscle activity. This is a practice that has been used by others in previous cadaver studies [31,35]. Third, physiological muscle loading was not present and the patellar mechanism was only partially simulated. However, it is assumed that the weight-bearing rather than the muscle contraction has an influence on the tibiofemoral kinematics [18]. Fourth, only flexion angles until 90° were investigated, and kinematic patterns at higher flexion angles may differ. However, the majority of activities of daily living are performed at flexion angles below 90° [36]. Fifth, it was not possible to change the order of the different test conditions. Therefore, time-dependent effects cannot be completely eliminated. Nevertheless, the limited number of tests and the resulting short test duration should minimize these effects [37]. Finally, this study was conducted using a specific TKA design and the results may not be applicable to other TKA designs.

5. Conclusions

This study showed that neither TKA design was superior in restoring the mean native AP translation of both condyles throughout the complete range of passive flexion and stair ascent, but that both CR/CS and PS TKA designs may be suitable to restore the individual native kinematic pattern. Moreover, it was shown that passive and complex loading scenarios do not result in exactly the same kinematic pattern, but lead to the same choice of implant design if one design is superior in restoring the general kinematic behavior of the native individual knee. Therefore, this study highlights the importance of individual kinematic analyses to select the appropriate TKA design for a specific patient.

Author Contributions: Conceptualization, S.A.B., S.K., J.G., P.E.M., W.M.M., B.R. and T.M.G.; methodology, S.A.B. and S.K.; software, S.A.B.; validation, S.A.B. and S.K.; formal analysis, S.A.B.; investigation, S.A.B., S.K. and J.F.; resources, S.A.B., S.K., J.G., P.E.M., W.M.M., B.R. and T.M.G.; data curation, S.A.B.; writing—original draft preparation, S.A.B.; writing—review and editing, S.K., J.F., J.G., P.E.M., W.M.M., B.R. and T.M.G.; visualization, S.A.B. and J.F.; supervision, T.M.G.; project administration, T.M.G.; funding acquisition, T.M.G. All authors have read and agreed to the published version of the manuscript.

Funding: The study was funded by B. Braun Aesculap AG, Tuttlingen, Germany. The funders had no role in the design of the study; in the collection, analyses, or interpretation of the data; and in writing the manuscript, or in the decision to publish the results.

Institutional Review Board Statement: The study was conducted in accordance with the Declaration of Helsinki and approved by the Ethics Committee of the Ludwig Maximilian University of Munich (#20-0856, 9 November 2020).

Informed Consent Statement: Not applicable.

Data Availability Statement: The data presented in this study are available on request from the corresponding author. The data are not publicly available due to ethical and privacy considerations associated with human cadaveric donor material.

Acknowledgments: The authors would like to thank Ana-Laura Puente-Reyna, Brigitte Altermann, and Josef-Benedikt Weiß for their valuable support in this study.

Conflicts of Interest: Five of the authors (S.A.B., S.K., J.F., B.R., and T.M.G.) are employees of B. Braun Aesculap AG, Tuttlingen, Germany. J.G., P.E.M., and W.M.M. are paid consultants at B. Braun Aesculap AG. The funders had no role in the design of the study; in the collection, analyses, or interpretation of the data; and in writing the manuscript, or in the decision to publish the results.

References

1. Geng, R.; Li, J.; Yu, C.; Zhang, C.; Chen, F.; Chen, J.; Ni, H.; Wang, J.; Kang, K.; Wei, Z.; et al. Knee osteoarthritis: Current status and research progress in treatment (Review). *Exp. Ther. Med.* **2023**, *26*, 481. [CrossRef] [PubMed]
2. Smith, P.N.; Gill, D.R.; McAuliffe, M.J.; McDougall, C.; Stoney, J.D.; Vertullo, C.J.; Wall, C.J.; Corfield, S.; Page, R.; Cuthbert, A.R.; et al. *Hip, Knee and Shoulder Arthroplasty: 2023 Annual Report*; Australian Orthopaedic Association National Joint Replacement Registry, AOA: Adelaide, Australia, 2023. [CrossRef]
3. Grimberg, A.; Lützner, J.; Melsheimer, O.; Morlock, M.; Steinbrück, A. *Endoprothesenregister Deutschland (EPRD) Jahresbericht 2023*; Hamburg University of Technology: Hamburg, Germany, 2023. [CrossRef]
4. Bourne, R.B.; Chesworth, B.M.; Davis, A.M.; Mahomed, N.N.; Charron, K.D.J. Patient satisfaction after total knee arthroplasty: Who is satisfied and who is not? *Clin. Orthop. Relat. Res.* **2010**, *468*, 57–63. [CrossRef]
5. Dunbar, M.J.; Richardson, G.; Robertsson, O. I can't get no satisfaction after my total knee replacement: Rhymes and reasons. *Bone Joint J.* **2013**, *95*, 148–152. [CrossRef] [PubMed]
6. Gunaratne, R.; Pratt, D.N.; Banda, J.; Fick, D.P.; Khan, R.J.K.; Robertson, B.W. Patient Dissatisfaction Following Total Knee Arthroplasty: A Systematic Review of the Literature. *J. Arthroplasty* **2017**, *32*, 3854–3860. [CrossRef] [PubMed]
7. Angerame, M.R.; Holst, D.C.; Jennings, J.M.; Komistek, R.D.; Dennis, D.A. Total Knee Arthroplasty Kinematics. *J. Arthroplasty* **2019**, *34*, 2502–2510. [CrossRef]
8. Wada, K.; Hamada, D.; Takasago, T.; Kamada, M.; Goto, T.; Tsuruo, Y.; Sairyo, K. Intraoperative analysis of the kinematics of the native knee including two-dimensional translation of the femur using a navigation system: A cadaveric study. *J. Med. Investig.* **2019**, *66*, 367–371. [CrossRef]

9. Postolka, B.; Taylor, W.R.; List, R.; Fucentese, S.F.; Koch, P.P.; Schütz, P. ISB clinical biomechanics award winner 2021: Tibio-femoral kinematics of natural versus replaced knees—A comparison using dynamic videofluoroscopy. *Clin. Biomech.* **2022**, *96*, 105667. [CrossRef]
10. Lützner, J.; Beyer, F.; Lützner, C.; Riedel, R.; Tille, E. Ultracongruent insert design is a safe alternative to posterior cruciate-substituting total knee arthroplasty: 5-year results of a randomized controlled trial. *Knee Surg. Sports Traumatol. Arthrosc.* **2022**, *30*, 3000–3006. [CrossRef]
11. Kim, T.W.; Lee, S.M.; Seong, S.C.; Lee, S.; Jang, J.; Lee, M.C. Different intraoperative kinematics with comparable clinical outcomes of ultracongruent and posterior stabilized mobile-bearing total knee arthroplasty. *Knee Surg. Sports Traumatol. Arthrosc.* **2016**, *24*, 3036–3043. [CrossRef]
12. Hinarejos, P.; Leal-Blanquet, J.; Fraile-Suari, A.; Sánchez-Soler, J.; Torres-Claramunt, R.; Monllau, J.C. Increased posterior translation but similar clinical outcomes using ultracongruent instead of posterior stabilized total knee arthroplasties in a prospective randomized trial. *Knee Surg. Sports Traumatol. Arthrosc.* **2022**, *30*, 3041–3048. [CrossRef]
13. Kono, K.; Dorthe, E.W.; Tomita, T.; Tanaka, S.; Angibaud, L.; D'Lima, D.D. Intraoperative knee kinematics measured by computer-assisted navigation and intraoperative ligament balance have the potential to predict postoperative knee kinematics. *J. Orthop. Res.* **2022**, *40*, 1538–1546. [CrossRef] [PubMed]
14. Gasparutto, X.; Bonnefoy-Mazure, A.; Attias, M.; Dumas, R.; Armand, S.; Miozzari, H. Comparison between passive knee kinematics during surgery and active knee kinematics during walking: A preliminary study. *PLoS ONE* **2023**, *18*, e0282517. [CrossRef] [PubMed]
15. Belvedere, C.; Tamarri, S.; Ensini, A.; Durante, S.; Ortolani, M.; Leardini, A. Can Computer-Assisted Total Knee Arthroplasty Support the Prediction of Postoperative Three-Dimensional Kinematics of the Tibiofemoral and Patellofemoral Joints at the Replaced Knee? *J. Knee Surg.* **2021**, *34*, 1014–1025. [CrossRef] [PubMed]
16. Belvedere, C.; Tamarri, S.; Notarangelo, D.P.; Ensini, A.; Feliciangeli, A.; Leardini, A. Three-dimensional motion analysis of the human knee joint: Comparison between intra- and post-operative measurements. *Knee Surg. Sports Traumatol. Arthrosc.* **2013**, *21*, 2375–2383. [CrossRef] [PubMed]
17. Fritzsche, H.; Beyer, F.; Postler, A.; Lützner, J. Different intraoperative kinematics, stability, and range of motion between cruciate-substituting ultracongruent and posterior-stabilized total knee arthroplasty. *Knee Surg. Sports Traumatol. Arthrosc.* **2018**, *26*, 1465–1470. [CrossRef]
18. Grassi, A.; Pizza, N.; Lopomo, N.F.; Marcacci, M.; Capozzi, M.; Marcheggiani Muccioli, G.M.; Colle, F.; Zaffagnini, S. No differences in knee kinematics between active and passive flexion-extension movement: An intra-operative kinematic analysis performed during total knee arthroplasty. *J. Exp. Orthop.* **2020**, *7*, 12. [CrossRef]
19. Morooka, T.; Okuno, M.; Seino, D.; Iseki, T.; Fukunishi, S.; Kobashi, S.; Yoshiya, S. Intraoperative kinematic analysis of posterior stabilized total knee arthroplasty with asymmetric helical post-cam design. *Eur. J. Orthop. Surg. Traumatol.* **2019**, *29*, 675–681. [CrossRef]
20. Brendle, S.A.; Krueger, S.; Grifka, J.; Müller, P.E.; Grupp, T.M. A New Methodology for the Accurate Measurement of Tibiofemoral Kinematics in Human Cadaveric Knees: An Evaluation of the Anterior–Posterior Laxity Pre- and Post-Cruciate Ligament Resection. *Life* **2024**, *14*, 877. [CrossRef]
21. Grood, E.S.; Suntay, W.J. A joint coordinate system for the clinical description of three-dimensional motions: Application to the knee. *J. Biomech. Eng.* **1983**, *105*, 136–144. [CrossRef]
22. Bergmann, G.; Bender, A.; Graichen, F.; Dymke, J.; Rohlmann, A.; Trepczynski, A.; Heller, M.O.; Kutzner, I. Standardized loads acting in knee implants. *PLoS ONE* **2014**, *9*, e86035. [CrossRef]
23. Sauer, A.; Kebbach, M.; Maas, A.; Mihalko, W.M.; Grupp, T.M. The Influence of Mathematical Definitions on Patellar Kinematics Representations. *Materials* **2021**, *14*, 7644. [CrossRef] [PubMed]
24. Wu, G.; Cavanagh, P.R. ISB recommendations for standardization in the reporting of kinematic data. *J. Biomech.* **1995**, *28*, 1257–1261. [CrossRef] [PubMed]
25. Hull, M.L. Errors in using fixed flexion facet centers to determine tibiofemoral kinematics increase fourfold for multi-radius femoral component designs with early versus late decreases in the radius of curvature. *Knee* **2022**, *35*, 183–191. [CrossRef] [PubMed]
26. Scarvell, J.M.; Smith, P.N.; Refshauge, K.M.; Galloway, H.R.; Woods, K.R. Comparison of kinematic analysis by mapping tibiofemoral contact with movement of the femoral condylar centres in healthy and anterior cruciate ligament injured knees. *J. Orthop. Res.* **2004**, *22*, 955–962. [CrossRef]
27. Iwaki, H.; Pinskerova, V.; Freeman, M.A. Tibiofemoral movement 1: The shapes and relative movements of the femur and tibia in the unloaded cadaver knee. *J. Bone Joint Surg. Br.* **2000**, *82*, 1189–1195. [CrossRef]
28. Walker, P.S.; Arno, S.; Borukhoy, I.; Bell, C.P. Characterising knee motion and laxity in a testing machine for application to total knee evaluation. *J. Biomech.* **2015**, *48*, 3551–3558. [CrossRef]
29. Jerosch, J. *Knieendoprothetik: Indikationen Operationstechnik Nachbehandlung Begutachtung*; Springer: Berlin/Heidelberg, Germany, 1999; ISBN 9783662081228.
30. Dennis, D.A.; Mahfouz, M.R.; Komistek, R.D.; Hoff, W. In vivo determination of normal and anterior cruciate ligament-deficient knee kinematics. *J. Biomech.* **2005**, *38*, 241–253. [CrossRef]

31. Borque, K.A.; Gold, J.E.; Incavo, S.J.; Patel, R.M.; Ismaily, S.E.; Noble, P.C. Anteroposterior Knee Stability During Stair Descent. *J. Arthroplasty* **2015**, *30*, 1068–1072. [CrossRef]
32. Giffin, J.R.; Stabile, K.J.; Zantop, T.; Vogrin, T.M.; Woo, S.L.-Y.; Harner, C.D. Importance of tibial slope for stability of the posterior cruciate ligament deficient knee. *Am. J. Sports Med.* **2007**, *35*, 1443–1449. [CrossRef]
33. Kutzner, I.; Heinlein, B.; Graichen, F.; Bender, A.; Rohlmann, A.; Halder, A.; Beier, A.; Bergmann, G. Loading of the knee joint during activities of daily living measured in vivo in five subjects. *J. Biomech.* **2010**, *43*, 2164–2173. [CrossRef] [PubMed]
34. Schwiesau, J.; Fritz, B.; Kutzner, I.; Bergmann, G.; Grupp, T.M. CR TKA UHMWPE wear tested after artificial aging of the vitamin E treated gliding component by simulating daily patient activities. *Biomed Res. Int.* **2014**, *2014*, 567374. [CrossRef] [PubMed]
35. Willing, R.; Moslemian, A.; Yamomo, G.; Wood, T.; Howard, J.; Lanting, B. Condylar-Stabilized TKR May Not Fully Compensate for PCL-Deficiency: An In Vitro Cadaver Study. *J. Orthop. Res.* **2019**, *37*, 2172–2181. [CrossRef] [PubMed]
36. Taylor, W.R.; Schütz, P.; Bergmann, G.; List, R.; Postolka, B.; Hitz, M.; Dymke, J.; Damm, P.; Duda, G.; Gerber, H.; et al. A comprehensive assessment of the musculoskeletal system: The CAMS-Knee data set. *J. Biomech.* **2017**, *65*, 32–39. [CrossRef] [PubMed]
37. Dandridge, O.; Garner, A.; Jeffers, J.R.T.; Amis, A.A.; Cobb, J.P.; van Arkel, R.J. Validity of repeated-measures analyses of in vitro arthroplasty kinematics and kinetics. *J. Biomech.* **2021**, *129*, 110669. [CrossRef]

4.3 Publication III: Constraint of different knee implant designs under anterior–posterior shear forces and internal–external rotation moments in human cadaveric knees

Authors:	Saskia A. Brendle, Sven Krueger, Joachim Grifka, Peter E. Müller, William M. Mihalko, Berna Richter, Thomas M. Grupp
Journal:	Bioengineering – Special Issue: Joint Biomechanics and Implant Design
Volume:	12
Pages:	17
Year:	2025
DOI:	https://doi.org/10.3390/bioengineering12010087
Impact factor:	3.8 (according to InCites Journal Citation Reports 2023)

bioengineering

MDPI

Article

Constraint of Different Knee Implant Designs Under Anterior–Posterior Shear Forces and Internal–External Rotation Moments in Human Cadaveric Knees

Saskia A. Brendle [1,2,*], Sven Krueger [1], Joachim Grifka [3], Peter E. Müller [2], William M. Mihalko [4], Berna Richter [1] and Thomas M. Grupp [1,2]

[1] Research & Development, Aesculap AG, 78532 Tuttlingen, Germany
[2] Department of Orthopaedic and Trauma Surgery, Musculoskeletal University Center Munich (MUM), Campus Grosshadern, LMU Munich, 81377 Munich, Germany
[3] Department of Orthopaedics, Asklepios Klinikum, 93077 Bad Abbach, Germany
[4] Campbell Clinic Department of Orthopaedic Surgery & Biomedical Engineering, University of Tennessee Health Science Center, Memphis, TN 38104, USA
* Correspondence: saskia.brendle@aesculap.de

Abstract: Instability remains one of the most common indications for revision after total knee arthroplasty. To gain a better understanding of how an implant will perform in vivo and support surgeons in selecting the most appropriate implant design for an individual patient, it is crucial to evaluate the implant constraint within clinically relevant ligament and boundary conditions. Therefore, this study investigated the constraint of three different implant designs (symmetrical implants with and without a post-cam mechanism and an asymmetrical medial-stabilized implant) under anterior–posterior shear forces and internal–external rotation moments at different flexion angles in human cadaveric knees using a six-degrees-of-freedom joint motion simulator. Both symmetrical designs showed no significant differences between the anterior–posterior range of motion of the medial and lateral condyles. In contrast, the medial-stabilized implant exhibited less anterior–posterior translation medially than laterally, without constraining the medial condyle to a fixed position. Furthermore, the post-cam implant design showed a significantly more posterior position of the femoral condyles in flexion compared to the other designs. The results show that despite the differences in ligament situations and individual implant positioning, specific characteristics of each implant design can be identified, reflecting the different geometries of the implant components.

Keywords: knee; biomechanics; cadaveric study; anterior–posterior stability; TKA design

Academic Editor: Ryan Willing

Received: 20 December 2024
Revised: 13 January 2025
Accepted: 16 January 2025
Published: 19 January 2025

Citation: Brendle, S.A.; Krueger, S.; Grifka, J.; Müller, P.E.; Mihalko, W.M.; Richter, B.; Grupp, T.M. Constraint of Different Knee Implant Designs Under Anterior–Posterior Shear Forces and Internal–External Rotation Moments in Human Cadaveric Knees. *Bioengineering* **2025**, *12*, 87. https://doi.org/10.3390/bioengineering12010087

1. Introduction

In total knee arthroplasty (TKA), various implant designs are available which generate different kinematic profiles and envelopes of stability [1]. Symmetrical implants with different conformities, with or without a post-cam mechanism, are most commonly used and have been established for decades, with promising long-term results [2,3]. In comparison, the medial-pivot implant design is a more recent innovation and has not been studied in depth. With this design, the motion is guided by a highly congruent medial compartment, which behaves similarly to a ball in socket and creates a fixed medial pivot point [4]. In addition, there is a new generation of medial-stabilized implants with less medial conformity that have been designed to closely mimic the kinematic pattern of the healthy knee, with no fixed pivot point [3,5–7].

To date, many in vivo and in vitro studies have focused on comparing the resulting kinematics of different implant designs [8–16]. However, since instability remains one of the most common indications for revision after total knee arthroplasty [2,17–20], it is important to select the implant design for each patient individually, not only to meet the individual patient's needs in terms of kinematics [9], but also to ensure an adequate envelope of stability. For this reason, it is important to understand how much stability a particular implant design provides at different flexion angles to select the appropriate design for each individual patient in a more personalized approach. To accurately compare the anterior–posterior constraint of different implant designs, it is essential to have a highly controlled environment and precise application of forces. Additionally, it is crucial to test not only the implant itself but also its behavior under clinically relevant boundary conditions that the surrounding ligament conditions will provide. While some in vivo studies allow for controlled application of forces by arthrometers [21–26], others are conducted by applying manual force [27], which has limited reproducibility. Moreover, in vivo studies do not provide the opportunity to test different implant designs within the same ligamentous situation [21–26,28]. In contrast, biomechanical in vitro studies offer a high degree of accuracy and control, as well as the ability to measure the constraint of different implant designs within the same ligamentous situation [9,29,30]. However, no studies to date have thoroughly investigated the anterior–posterior position and range of motion of the femoral condyles under anterior–posterior shear forces and internal–external rotational moments with various implant designs in the same knees [30–32]. Furthermore, each TKA design exhibits unique characteristics, and not all cruciate-retaining (CR), cruciate-sacrificing (CS), medial-stabilized (MS), or posterior-stabilized (PS) designs share the same properties. For this reason, it is imperative to conduct detailed analyses of each newly developed design to assist surgeons in selecting the most appropriate implant design to address the specific needs of individual patients.

Therefore, the objective of this study was to investigate the constraint of symmetrical implants with and without a post-cam mechanism, as well as an asymmetrical medial-stabilized implant design during anterior–posterior shear forces and internal–external rotational moments at various flexion angles in human cadaveric knees. The hypothesis was that the symmetrical TKA designs have the same anterior–posterior range of motion medially and laterally despite the differences in the individual ligamentous situations. We anticipated that, with the medial-stabilized TKA design, the medial condyle would exhibit less anterior–posterior translation compared to the lateral condyle, without constraining the medial condyle to a fixed position. Furthermore, we hypothesized that, with the post-cam TKA design, the femoral condyles would be located more posterior in flexion compared to the other TKA designs.

2. Materials and Methods

2.1. Specimen Preparation

Thirteen fresh-frozen human cadaveric lower right extremities (three females and ten males) were used in this study. The donors had a mean age of 67 ± 10 years and a mean body mass index of 23.3 ± 8.0 kg/m^2. The specimens were screened for pre-existing knee disorders, surgical interventions, and other relevant pathologies. Ethical approval was obtained from the ethics committee of the Ludwig Maximilian University of Munich (No. 20-0856).

Before the experiment, each specimen was thawed for 24 h at 7 °C and then prepared for testing based on a methodology recently published by Brendle et al. [29]. The proximal and distal segments of the joint were skeletonized, while care was taken to preserve soft tissue surrounding the knee joint capsule. GOM measuring points (1.5 mm, Carl Zeiss GOM Metrology GmbH, Braunschweig, Germany) were attached to the skeletonized parts of the

bones, and 3D fittings of femur and tibia were performed by aligning segmented CT scans (Mimics 24.0, Materialise, Leuven, Belgium) to 3D point clouds of each bone (ARAMIS 12M, Carl Zeiss GOM Metrology GmbH, Braunschweig, Germany). Afterwards, the 3D fitting information, containing the 3D point cloud to CT scan information, was saved and the bones were cut and embedded in custom-made aluminum pots for mounting in a six-degrees-of-freedom joint motion simulator. For this purpose, the femur was aligned with the axes of the upper actuator of the joint motion simulator and the tibia was embedded at 0° flexion.

After initial preparation, the specimens underwent cruciate-sacrificing total knee arthroplasty [9] by an experienced knee surgeon using the oneKNEE® TKA system (Aesculap AG, Tuttlingen, Germany), which allows the use of a femoral component with or without a post-cam mechanism (PS or CR/CS) with the same bone cuts. Furthermore, the system has the option to utilize a symmetrical tibial inlay with medium conformity without a post-cam mechanism (CR/CS), a symmetrical tibial inlay with medium conformity and a post-cam mechanism (PS), or an asymmetrical medial-stabilized tibial inlay with higher conformity medial and lower conformity lateral (MS) fixed to the same tibial component (Figure 1). The components were implanted using mechanical alignment and 0° tibial slope. After implantation, the position of the implants in relation to the bones was measured (ARAMIS 12M, Carl Zeiss GOM Metrology GmbH, Braunschweig, Germany) [9].

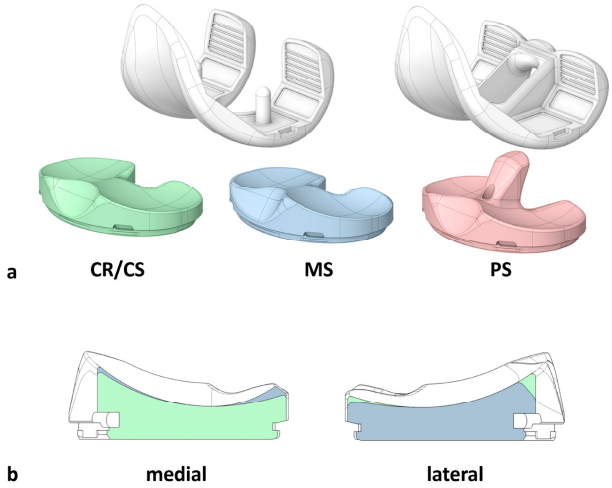

Figure 1. (**a**) Illustration of the total knee arthroplasty (TKA) components. The CR/CS femoral component (left) can be used with a symmetrical inlay with medium conformity without a post-cam mechanism (CR/CS, green) or an asymmetrical medial-stabilized inlay with higher conformity medial and lower conformity lateral (MS, blue). The PS femoral component (right) can be used with a symmetrical inlay with medium conformity and a post-cam mechanism (PS, red). All inlay designs can be fixed to the same tibial component, which is not illustrated in this Figure. (**b**) Schematic illustration of a cross-section through the dwell point of the medial and lateral compartments of the CR/CS (green) and MS (blue) inlay designs. The medial compartment of the MS design has steeper anterior and posterior ramps compared to the CR/CS design. The lateral compartment of the MS design has a flatter posterior ramp compared to the CR/CS design. In the shown cross-sections, the PS design has the same characteristics as the CR/CS design and is therefore not presented separately.

2.2. Experimental Testing

Testing was performed on a six-degrees-of-freedom joint motion simulator (VIVO, Advanced Mechanical Technologies Inc., Watertown, MA, USA), which allows independent control of each degree-of-freedom in either force or displacement mode. The forces and

motions are expressed in accordance with the Grood and Suntay conventions [33]. After mounting the specimen, the absolute joint position of the specimen was transferred to the joint motion simulator by projecting the previously generated 3D fitting information of the segmented CT scans onto the residual bones using the remaining measuring points. In this way, the 3D information of the complete femur and tibia were available even after the bones were cut. Subsequently, each specimen was subjected to dynamic testing. In order to characterize the constraint of the implant designs in each knee, cyclic anterior–posterior shear forces of ±80 N and internal–external rotation moments of ±5 Nm were sequentially applied as a ramp profile for four cycles at 0, 30, 45, 60, and 90° of flexion while maintaining an axial compression force of 200 N and all other forces and moments at 0 N/Nm. The applied loads were chosen to reflect those used in clinical assessment of joint laxity [34] and were within the range of forces used in comparable studies [35–37]. Each loading protocol was applied to the CR/CS, MS, and PS TKA designs. Thereby, the CR/CS and MS implant designs were tested in a randomized order in each specimen. The PS implant design was always tested last. For all conditions, the knee capsule was opened using a medial parapatellar approach and closed with surgical sutures (Number 1 Vicryl, B. Braun, Melsungen, Germany). During testing, the relative position of femur and tibia were tracked by the joint motion simulator. The passive tension of the patella tendon was simulated by a spring sutured to the quadriceps tendon with an increasing force of up to 50 N at 90° flexion. Furthermore, the specimens were kept moist with sodium chloride solution to mitigate the effects of tissue drying during testing. Figure 2 illustrates the entire testing process.

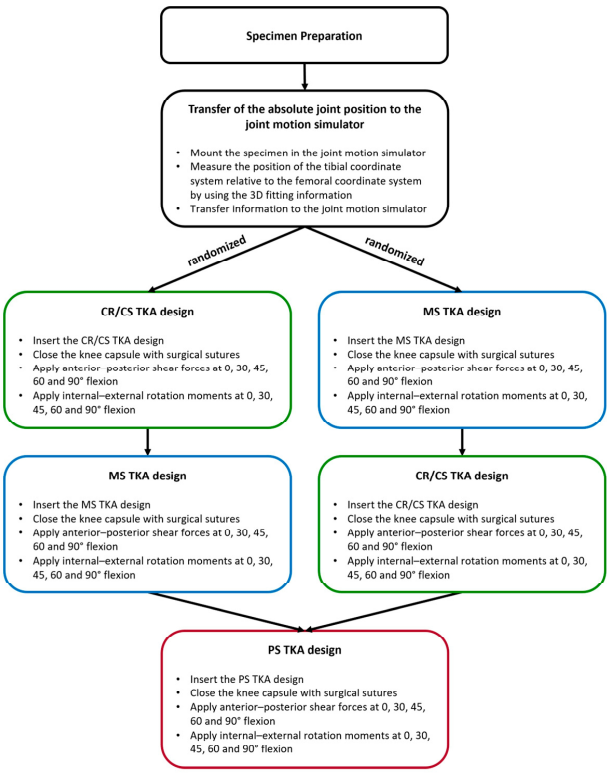

Figure 2. Illustration of the key steps of the testing process. TKA = total knee arthroplasty. CR/CS = symmetrical TKA design without a post-cam mechanism. MS = asymmetrical medial-stabilized TKA design. PS = symmetrical TKA design with a post-cam mechanism.

2.3. Data Analysis

The data from a single cycle of each experiment were evaluated with custom MATLAB scripts (Version R2023a, MathWorks Inc., Natick, MA, USA) [29]. The flexion axis and the centers of the medial and lateral condyles of the femoral component were projected onto the tibial plane at various flexion angles (0, 30, 45, 60, and 90°) at the first time reaching the maximum or minimum force or moment, representing the positions of the femoral condyles on the tibial plateau (Figure 3). The positions were normalized to the anterior–posterior width of the implanted tibial plateau of the respective tibia to minimize the effect of the implant component size. Thus, irrespective of the different tibia size, 0 and 1 correspond to the most posterior and most anterior position on the tibial plateau, respectively, as illustrated in Figure 3. Furthermore, the normalized anterior–posterior range of motion of the medial and lateral condyles was calculated for all implant designs as the difference between the positions at maximum and minimum force or moment.

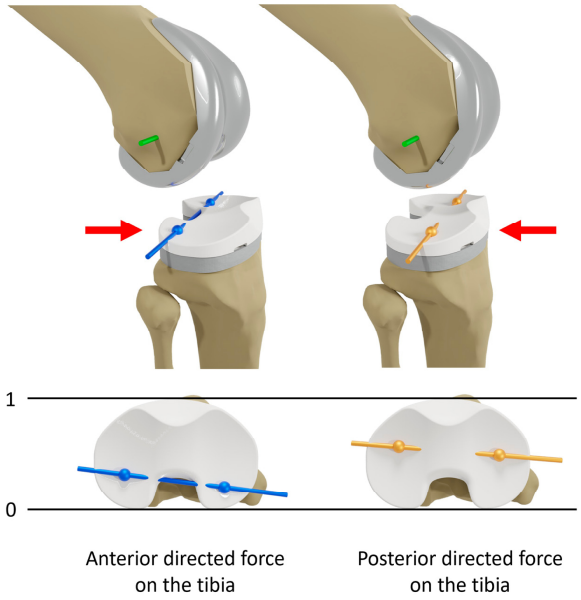

Figure 3. Illustration of the projections of the flexion axis (**green**) and the centers of the medial and lateral condyles of the femoral component on the tibial plane at 45° flexion under maximum anterior (**blue**) and posterior (**orange**) directed force on the tibia. Red errors indicate the direction of shear force applied on the tibia. The projections represent the positions of the medial and lateral femoral condyles on the normalized tibial plateau. Irrespective of the different tibia sizes, 0 and 1 correspond to the most posterior and most anterior position on the tibial plateau, respectively.

Statistical analyses were performed in Minitab (Version 21.2, Minitab GmbH, Munich, Germany). Wilcoxon-signed rank tests [38] were used to compare the position at maximum anterior/posterior shear force and internal/external rotation moment, respectively, between the different TKA designs pairwise at various flexion angles. Furthermore, the normalized anterior–posterior range of motion was compared between the medial and lateral condyles, as well as between the different TKA designs at various flexion angles during anterior–posterior (AP) shear forces and internal–external (IE) rotation moments. The level of significance was set at $p \leq 0.05$. Some specimens exceeded the range of motion of the joint motion simulator during testing and were therefore excluded from data analysis ($n = 2$ for AP shear forces and $n = 3$ for IE rotation moments).

3. Results

3.1. Anterior–Posterior Shear Forces

Figure 4 shows the projection of the flexion axis and the centers of the medial and lateral condyles of the femoral component onto the tibial plane during anterior–posterior shear forces applied on the tibia at 45° flexion with a CR/CS, MS, and PS TKA design exemplary for one specimen. The posterior translation of the femoral condyles at maximum anterior directed force (positive) is colored in blue, whereas the anterior translation of the femoral condyles at maximum posterior directed force (negative) is colored in orange. With the CR/CS and the PS TKA designs, the femoral condyles exhibited a parallel translation with less anterior displacement for the PS TKA design at maximum negative force. In contrast, with the MS TKA design, the medial condyle showed less posterior translation than the lateral condyle, due to the higher constraint of the medial compartment.

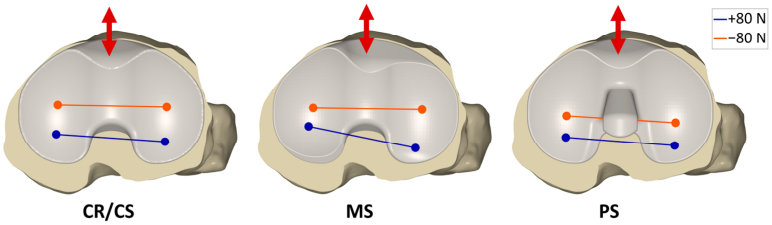

Figure 4. Projections of the flexion axis and the centers of the medial and lateral condyles of the femoral component onto the tibial plane with ±80 N anterior (+) and posterior (−) shear force applied on the tibia at 45° flexion, showing the condylar motion with a CR/CS, MS, and PS TKA design exemplary for one specimen. The colors represent the respective force on the tibia. Blue = 80 N; orange = −80 N.

Figure 5 shows the normalized medial and lateral anterior–posterior range of motion during anterior–posterior shear forces with the CR/CS, MS, and PS TKA designs for all specimens. Furthermore, it illustrates the anterior–posterior positions of the medial and lateral femoral condyles at maximum anterior and posterior shear forces, respectively, with the different TKA designs at various flexion angles for all specimens with boxplots on a normalized tibia. Boxplots include the median AP positions, the first and third quartiles, and the range. Outliers are displayed as dots, and significant differences between the values ($p \leq 0.05$) are marked with an asterisk. In addition, median values and statistical significances are presented in Table A1 for the AP range of motion, and in Table A2 for the AP positions at maximum anterior and posterior shear forces, respectively.

As already observed for the exemplary specimen, the CR/CS design demonstrated a greater medial AP range of motion compared to the MS and PS designs, with significant differences at all flexion angles. Furthermore, the MS and PS designs significantly differed at 0, 30, and 90° flexion, with a smaller medial AP range of motion for the PS design at 90°. Laterally, the PS design had the smallest AP range of motion compared to the other designs and significantly differed from the CR/CS design at all flexion angles. For all designs, the smallest medial and lateral AP ranges were observed at 0° flexion, with the MS design showing a significantly smaller medial AP range of motion than the symmetrical designs. For the MS design, the medial AP range of motion was generally smaller than the lateral AP range of motion with significant differences at 45, 60, and 90° flexion. The CR/CS and PS designs also exhibited a smaller medial AP range of motion at 30 and 45° flexion but showed almost identical medial and lateral ranges at 60 and 90° flexion. Furthermore, the variance between the individual specimens was greatest in mid-flexion.

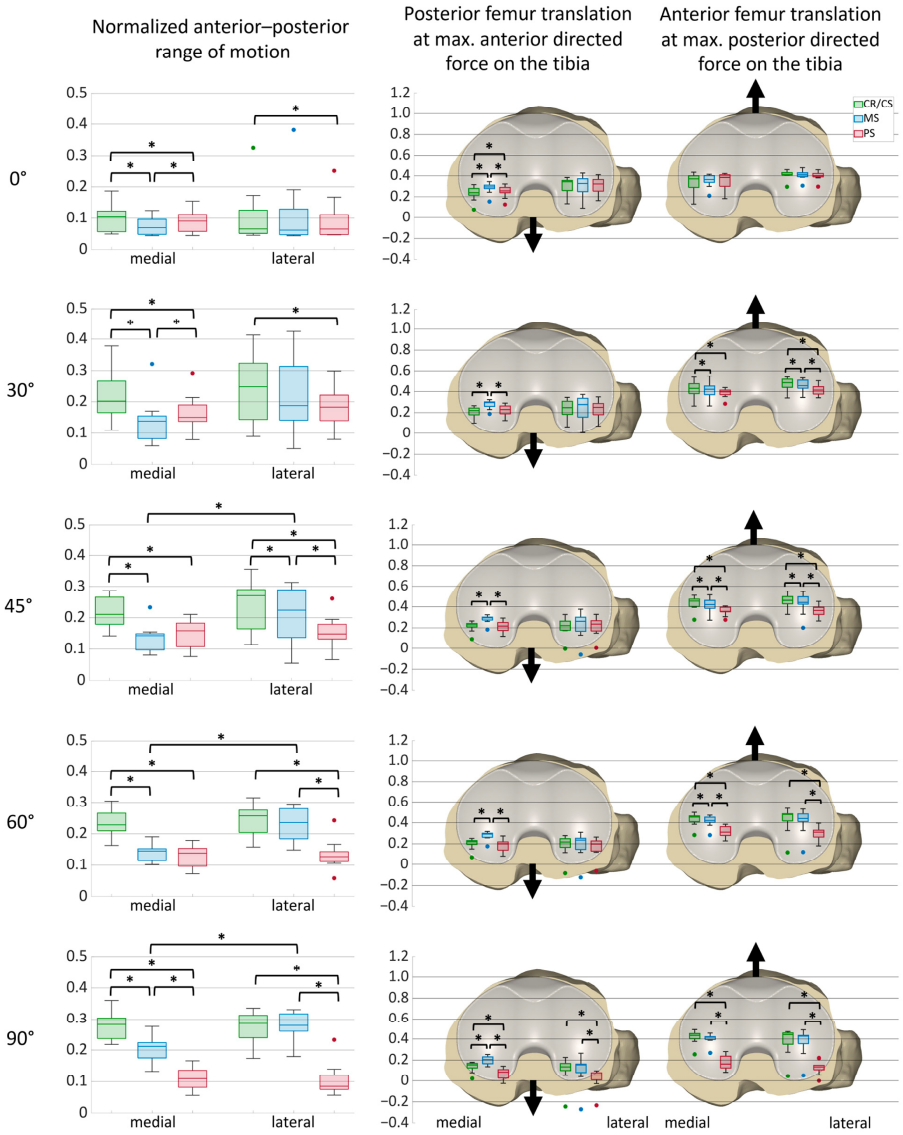

Figure 5. Anterior–posterior range of motion during anterior–posterior shear forces at different flexion angles and anterior–posterior positions of the medial and lateral femoral condyles at maximum anterior and posterior shear forces, respectively, at different flexion angles on a normalized tibia ($n = 11$). The anterior–posterior range of motion and the positions are normalized to an anterior–posterior tibia width of 1. Significant differences are marked with an asterisk ($p \leq 0.05$). Posterior femur translation = anterior directed force on the tibia; anterior femur translation = posterior directed force on the tibia. Green = CR/CS; blue = MS; red = PS.

During anterior directed force on the tibia, the medial condyle was positioned significantly more anterior with the MS design than with the CR/CS and PS designs at all flexion angles. From 30° of flexion, the medial and lateral condyles were positioned at approximately the same height with the symmetrical designs. In contrast, with the MS design, the medial condyle was positioned more anteriorly than the lateral condyle. For all

TKA designs, the position of the condyles shifted posteriorly at higher flexion angles. At 90° flexion, the femoral condyles were positioned significantly more posterior with the PS design than with the CR/CS and MS designs.

During posterior directed force on the tibia, the lateral condyle was positioned more anterior than the medial condyle with all TKA designs at 0 and 30° of flexion, and were approximately at the same height at 45° flexion. From 30°, both femoral condyles were positioned significantly more posterior with the PS design than with the CR/CS design. In addition, from 45° of flexion, the femoral condyles were positioned significantly more posterior with the PS design compared to the MS design. Furthermore, the position of the CR/CS and MS designs revealed significant differences at 30, 45, and 60° flexion, with a more posterior position of the MS design. With the PS design, the femoral condyles shifted posteriorly with flexion. In contrast, the median position of the femoral condyles remained approximately the same throughout the range of flexion with the CR/CS and MS designs.

3.2. Internal–External Rotation Moments

Figure 6 shows the projection of the flexion axis and the centers of the medial and lateral condyles of the femoral component onto the tibial plane during internal–external rotation moments applied on the tibia at 45° flexion with a CR/CS, MS, and PS TKA design exemplary for one specimen. The internal rotation of the femoral condyles at maximum external rotation moment (positive) is shown in blue, whereas the external rotation of the femoral condyles at maximum internal rotation moment (negative) is shown in orange. With the CR/CS and the PS TKA designs, the medial and lateral condyles exhibited approximately the same anterior–posterior range of motion during internal–external rotation moments, resulting in a rotation around the center of the tibia with a small medial offset. In contrast, with the MS TKA design, the medial condyle showed less anterior–posterior translation compared to the lateral condyle, resulting in a rotation around the medial compartment of the tibia.

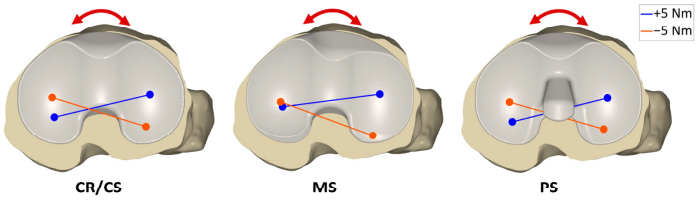

Figure 6. Projections of the flexion axis and the centers of the medial and lateral condyles of the femoral component onto the tibial plane with ±5 Nm internal (−) and external (+) rotation moment applied on the tibia at 45° flexion, showing the condylar motion with a CR/CS, MS, and PS TKA design exemplary for one specimen. The colors represent the respective moment on the tibia. Blue = +5 Nm; orange = −5 Nm.

Figure 7 shows the normalized medial and lateral anterior–posterior range of motion during internal–external rotation moments with the different TKA designs for all specimens. In addition, it presents the anterior–posterior positions of the medial and lateral femoral condyles at maximum internal and external rotation moments, respectively, with a CR/CS, MS, and PS TKA design at various flexion angles for all specimens with boxplots on a normalized tibia. Boxplots include the median AP positions, the first and third quartiles, and the range. Outliers are displayed as dots, and significant differences between the values ($p \leq 0.05$) are marked with an asterisk. Additionally, median values and statistical significances are presented in Table A3 for the AP range of motion and in Table A4 for the AP positions at maximum internal and external rotation moments.

Bioengineering **2025**, *12*, 87

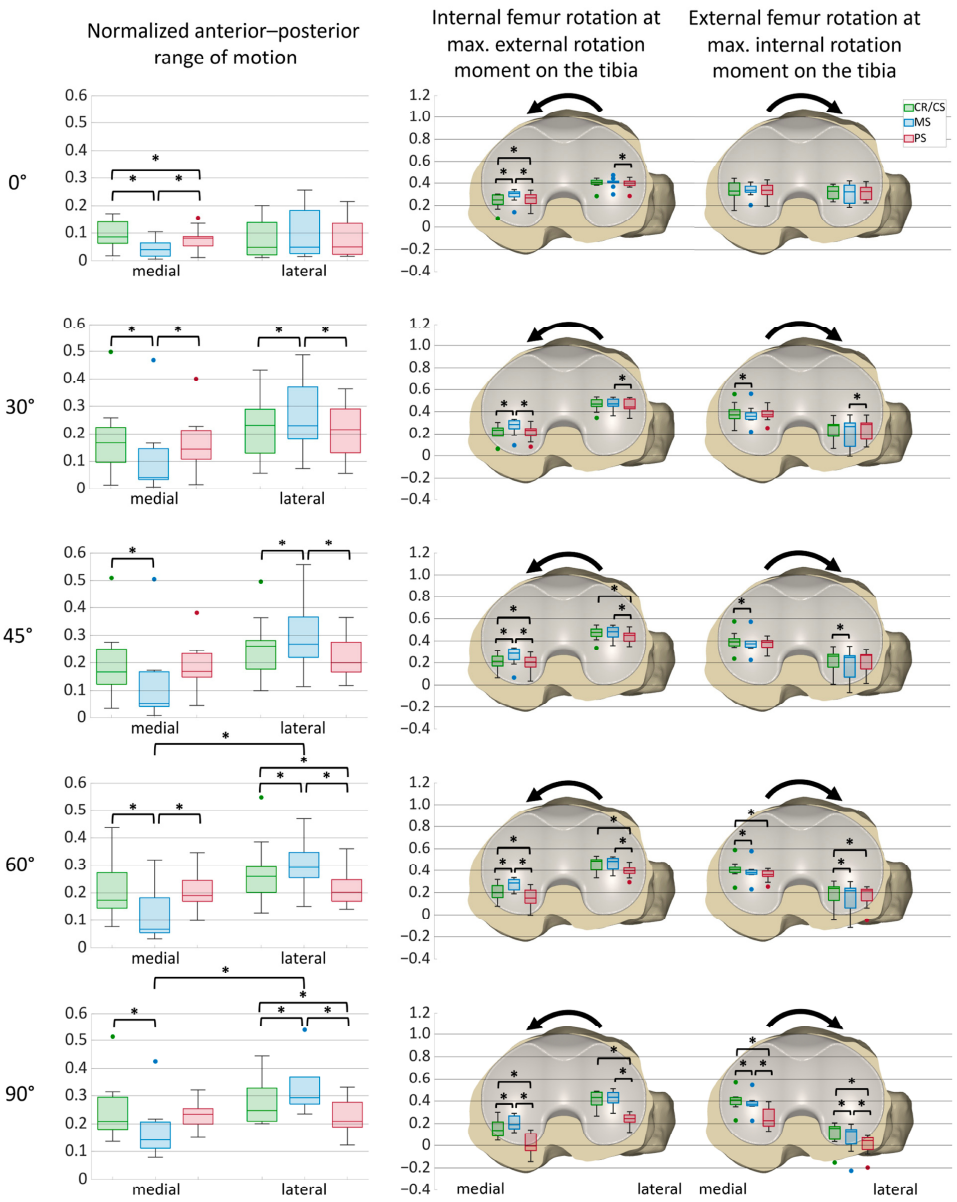

Figure 7. Anterior–posterior range of motion during internal–external rotation moments at different flexion angles and anterior–posterior positions of the medial and lateral femoral condyles at maximum internal and external rotation moments, respectively, at different flexion angles on a normalized tibia (n = 10). The anterior–posterior range of motion and the positions are normalized to an anterior–posterior tibia width of 1. Significant differences are marked with an asterisk ($p \leq 0.05$). Internal femur rotation = external rotation moments on the tibia; external femur rotation = internal rotation moments on the tibia. Green = CR/CS; blue = MS; red = PS.

As observed for the exemplary specimen, the symmetrical designs exhibited approximately the same AP range of motion medially and laterally, whereas the MS design showed smaller ranges medially with significant differences at 60 and 90° flexion. Furthermore,

the MS design showed a significantly smaller medial AP range of motion compared to the CR/CS design at all flexion angles. In contrast, the lateral condyle showed a significantly larger AP range of motion with the MS design compared to the CR/CS and PS designs at 30, 45, 60, and 90° flexion. For all designs, the smallest medial and lateral AP ranges were observed at 0° flexion.

During external rotation moment, the medial condyle was positioned significantly more anterior with the MS design than with the CR/CS and PS designs at all flexion angles. Furthermore, with the PS design, the position of the medial condyle differed significantly from that obtained with the CR/CS design at 0, 45, 60, and 90° of flexion, with a more anterior position at 0° flexion and a more posterior position at 45, 60, and 90° of flexion. The lateral condyle was located more posterior with the PS design and differed significantly from the MS (all flexion angles) and the CR/CS (45, 60, and 90° flexion) designs. In addition, the median position of the medial condyle shifted posteriorly through the range of flexion with all TKA designs, whereas the median position of the lateral condyle stayed nearly unchanged with the CR/CS and MS designs and was considerably more posterior with the PS design.

During internal rotation moment, both femoral condyles were positioned significantly more posterior with the MS design compared to the CR/CS design at 45, 60, and 90° flexion. Furthermore, the median position of the lateral condyle shifted posteriorly through the range of flexion for all TKA designs. In contrast, the median position of the medial condyle remained almost the same with the CR/CS and MS designs but was considerably more posterior with the PS design. At 60° flexion, both femoral condyles were significantly more posterior with the PS design compared to the CR/CS design. In addition, at 90° flexion, the femur was positioned significantly more posterior with the PS design compared to both the CR/CS and MS designs.

4. Discussion

To gain a better understanding of how an implant will perform in vivo and select the most appropriate implant design to address a patient's individual needs, it is crucial to evaluate the differences in constraint not only for isolated implant components, but within clinically relevant ligament and boundary conditions [39]. Therefore, the objective of this study was to investigate the constraints of three different implant designs out of a newly developed comprehensive knee platform during anterior–posterior shear forces and internal–external rotation moments at various flexion angles in human cadaveric knees. We confirmed the first hypothesis that the symmetrical TKA designs have the same anterior–posterior range of motion medially and laterally. During both anterior–posterior shear forces and internal–external rotation moments, the medial and lateral anterior–posterior ranges showed no significant differences for the CR/CS and PS TKA designs, despite the differences in the individual ligamentous situations. In contrast, with the medial-stabilized TKA design, the medial condyle exhibited significantly less anterior–posterior translation compared to the lateral condyle, but still allowed sliding and did not constrain the medial condyle to a fixed position when subjected to anterior–posterior shear forces, confirming the second hypothesis. In addition, as expected, the femoral condyles were located significantly more posterior with the post-cam TKA design compared to the other TKA designs in flexion.

Each implant design has a different constraint based on its geometry and associated behavior when subjected to different forces and moments. In this study, the constraint under anterior–posterior shear forces and internal–external rotational moments was investigated. This constraint comprises several aspects: the anterior–posterior range of motion and the maximum possible anterior and posterior translation of the medial and lateral femoral condyles on the tibial plateau. Clinically, it is important to understand the constraint of

different implants, as it essentially defines the envelope for kinematics. However, the individual kinematics of different patients may vary within this envelope [9]. Ideally, the implant design should allow the individuals physiological kinematics while providing stability. An excessive highly constrained implant may compromise the physiological kinematics of a particular patient, whereas a constraint that is too low may cause variations in translation, resulting in an unstable situation in some patients. Thus, each patient has individual needs, and greater stability does not necessarily correlate with higher patient satisfaction [22,24–26]. In the following paragraphs, the various aspects of the implant constraints are discussed.

For all designs, the smallest anterior–posterior range of motion was found in extension, with a considerable increase at 30° flexion. Due to the normalized anterior–posterior range of motion and the specific implant designs used in this study, the results cannot be directly compared with those of other studies. However, previous studies also found a significant increase in AP laxity between 0° and 30° of flexion in the native condition, as well as with different CR, CS, and ultracongruent (UC) designs [27,30]. Furthermore, Shalhoub et al. [40] and Minoda et al. [41] showed that the tibiofemoral gaps significantly increase until 30° of flexion, which also represents an increase in laxity. Therefore, these findings reflect the influence of the natural ligamentous situation of the knee in mid-flexion and demonstrate the importance of evaluating the differences in constraint not only for isolated implant components but within real ligamentous supported conditions. In motion, mid-flexion instability can lead to phenomena such as paradoxical anterior sliding of the femur. However, this was not observed for the TKA designs of the present study [9].

For both symmetrical designs, there were no significant differences between the medial and lateral AP range of motion. However, during AP shear forces, both femoral condyles exhibited a considerably higher AP range of motion with the CR/CS design than with the PS design at all flexion angles, but comparable ranges until 45° flexion during internal–external rotation moments. With the MS design, the AP range of motion of the lateral condyle was similar to the CR/CS design during anterior–posterior shear forces but was higher during internal–external rotation moments. In contrast, the medial condyle exhibited a smaller AP range of motion with the MS design than with the CR/CS design during both anterior–posterior shear forces and internal rotation moments. This is attributed to the greater conformity provided by the steeper anterior and posterior ramps of the medial tibial compartment in the MS design. Nevertheless, the MS design still allowed sliding of the femoral condyle on the tibial plateau. This is a major difference to previous medial-stabilized and medial-pivot designs, which show almost no movement of the medial condyle during various activities and therefore create a fixed medial pivot point with minimal variation between patients due to the high conforming medial compartment of the tibia [28].

When analyzing the maximum posterior translation of the femoral condyles under various conditions, it could be observed that, during both anterior shear forces and external rotation moments, the MS design allowed less posterior translation of the medial condyle compared to the CR/CS and PS designs, and was therefore positioned more anteriorly at all flexion angles. This can be explained by the steeper posterior ramp of the medial compartment of the MS inlay. In contrast, as a result of the flatter posterior ramp of the lateral compartment of the MS design, the lateral condyle showed a higher posterior translation compared to the CR/CS design during internal–external rotation moments. In flexion, both femoral condyles achieved the most posterior position with the PS design, due to the intervention of the post-cam mechanism. Furthermore, it can be observed that the PS design showed the smallest variation. This is probably due to the higher guidance of the PS design compared to the CR/CS and MS designs. For one specimen, the lateral femoral condyle was generally positioned more posteriorly than observed for the other specimens,

during both anterior and posterior shear forces and internal and external rotation moments with all implant designs. Therefore, outliers exist for the maximum anterior and posterior positions, but not for the anterior–posterior range of motion.

Analysis of the maximum anterior translation of the femoral condyles showed that the CR/CS design allowed the greatest anterior translation of the medial condyle during both posterior shear forces and internal rotation moments. In comparison, with the MS design, the medial condyle showed considerably less anterior translation and was therefore located more posterior than with the CR/CS design at all flexion angles. In a previous study, Kour et al. [28] investigated the positions of the medial and lateral condyles of three different TKA designs (CR, MS, and PS) on the tibial plateau during activities of daily living using mobile biplane fluoroscopy. In addition to the high constraint of the medial compartment of the tibia in the MS design, they found that the lateral condyle shifted more anterior with the MS design compared to the PS and CR designs during some of the activities. This is not expected with the MS design tested in this study. The most anterior position of the lateral condyle was similar for the CR/CS and MS designs during external rotation moments, and slightly more posterior for the MS design when subjected to posterior shear forces. Thus, the lateral compartment of the MS design has the same constraint as the CR/CS design in the anterior direction and therefore provides the same stability. A similar behavior is expected during activities of daily living, since the envelope of kinematics is prescribed by the constraint. With the PS design, the femoral condyles were positioned more posterior compared to the other designs, especially in flexion, as the post-cam mechanism forces the femur to translate posteriorly with flexion and prevents anterior translation when subjected to posterior shear forces or internal–external rotation moments. A study by Scott et al. [23] revealed a greater mid-flexion laxity characterized by a higher anterior translation of the femur in patients with PS implants than in patients with MS implants, as the post-cam mechanism used for stabilization in PS implants usually only intervenes at flexion angles beyond 45° [42] and does not prevent anterior translation of the femoral component prior to that. However, this could not be observed in the present study due to an earlier post-cam intervention as for most of the PS designs. This demonstrates that not every design of the same type has identical characteristics. Consequently, it is crucial to characterize each newly developed design, as each one has a unique geometry and therefore specific features that are essential to understand. To gain a broader understanding of the different implant designs and the influence of various factors on the overall performance and stability, future studies should also investigate the constraint when using different alignment techniques, soft-tissue balance, and tibial slope.

To the best of our knowledge, this is the first study that has compared the constraint of different implant designs in the same knees in a highly controlled environment. By examining the different TKA designs in the same knees, the variability between different cohorts can be eliminated. Furthermore, precise application of forces along reliable axes avoids false conclusions due to variations in the treatment of the different conditions and ensures a valid comparison of the different TKA designs [9,29]. Nevertheless, several limitations should be taken into account when interpreting the results of the present study. First, this study investigated only a small number of human cadaveric specimens, which may have different soft tissue characteristics from living patients. However, comparing different TKA designs in the same knees under highly controlled conditions is not possible in vivo. Second, physiological muscle loading was not applied, and the patellar mechanism was only passively simulated. Third, the constraint of the TKA designs was only investigated until 90° of flexion, and the results at higher flexion angles may differ. However, most of the activities of daily living are covered with flexion angles of up to 90° [43]. Fourth, the projection of the centers of the medial and lateral femoral condyles onto the tibial plane

was used to analyze the anterior–posterior position and range of motion. This is a valid and widely used method to approximate the tibiofemoral contact pattern, especially for single-radius implant designs such as the CR/CS femoral component in the present study. However, the PS femoral component slightly changes its radius of curvature in flexion. For a better comparison of the position of the femoral condyles between the different implant designs in the same ligamentous situation, we chose to always project the CR/CS centers onto the tibial plane. This results in small inaccuracies when approximating the tibiofemoral contact pattern of the PS design in flexion. However, since the present study only investigated flexion angles up to 90°, the error should be limited and not change the general characteristic behavior [44]. Fifth, the PS TKA design was always tested last since the femoral component had to be replaced. For this reason, time-dependent effects cannot be completely excluded. However, the limited number of tests and the short test duration should mitigate these effects [45]. Finally, this study was performed using oneKNEE® TKA components, and the results may not be applicable to other TKA designs.

5. Conclusions

This study investigated the constraints of three different implant designs from a newly developed comprehensive knee platform during anterior–posterior shear forces and internal–external rotation moments at various flexion angles in human cadaveric knees. It was found that, despite the differences in ligament situations and individual implant positioning, specific characteristics of the individual implant designs can be identified, reflecting the different geometries of the implant components. The results help to understand how much stability a particular implant design provides at different flexion angles under clinically relevant conditions and may therefore assist in selecting the most appropriate implant design to address the specific needs of individual patients.

Author Contributions: Conceptualization, S.A.B., S.K., J.G., P.E.M., W.M.M., B.R. and T.M.G.; methodology, S.A.B. and S.K.; software, S.A.B.; validation, S.A.B. and S.K.; formal analysis, S.A.B.; investigation, S.A.B. and S.K.; resources, S.A.B., S.K., J.G., P.E.M., W.M.M., B.R. and T.M.G.; data curation, S.A.B.; writing—original draft preparation, S.A.B.; writing—review and editing, S.K., J.G., P.E.M., W.M.M., B.R. and T.M.G.; visualization, S.A.B.; supervision, T.M.G.; project administration, T.M.G.; funding acquisition, T.M.G. All authors have read and agreed to the published version of the manuscript.

Funding: The study was funded by B. Braun Aesculap AG, Tuttlingen, Germany. The funders had no role in the design of the study, in the collection, analyses or interpretation of the data, in writing the manuscript or in the decision to publish the results.

Institutional Review Board Statement: The study was conducted in accordance with the Declaration of Helsinki and approved by the Ethics Committee of the Ludwig Maximilian University of Munich (#20-0856, 9 November 2020).

Informed Consent Statement: Not applicable.

Data Availability Statement: The data presented in this study are available on request from the corresponding author. The data are not publicly available due to ethical and privacy considerations associated with human cadaveric donor material.

Acknowledgments: The authors would like to thank Ana-Laura Puente-Reyna, Brigitte Altermann, and Josef-Benedikt Weiß for their valuable support in this study.

Conflicts of Interest: Four of the authors (S.A.B., S.K., B.R., and T.M.G.) are employees of B. Braun Aesculap AG, Tuttlingen, Germany. J.G., P.E.M., and W.M.M. are paid consultants at B. Braun Aesculap AG. The funders had no role in the design of the study, in the collection, analyses, or interpretation of the data, in writing the manuscript, or in the decision to publish the results.

Bioengineering **2025**, *12*, 87

Appendix A

Table A1. Median values and statistical significance of the normalized medial and lateral anterior–posterior range of motion during anterior–posterior shear forces at various flexion angles (n = 11). CR/CS = symmetrical implant design without a post-cam mechanism; MS = asymmetrical medial-stabilized implant design; PS = symmetrical implant design with a post-cam mechanism; * $p < 0.05$. Bold indicates statistical significance.

Flexion Angle	Condyle	Median			*p*-Value			*p*-Value Medial vs. Lateral		
		CR/CS	MS	PS	CR/CS vs. MS	CR/CS vs. PS	MS vs. PS	CR/CS	MS	PS
0° flexion	Medial	0.10	0.07	0.09	**0.005** *	**0.037** *	**0.005** *	0.756	0.824	1.000
	Lateral	0.07	0.06	0.07	0.563	**0.037** *	0.824			
30° flexion	Medial	0.20	0.14	0.15	**0.004** *	**0.004** *	**0.045** *	0.505	0.056	0.505
	Lateral	0.25	0.19	0.18	0.056	**0.009** *	0.197			
45° flexion	Medial	0.21	0.14	0.16	**0.004** *	**0.004** *	0.197	0.398	**0.029** *	0.625
	Lateral	0.27	0.22	0.15	**0.037** *	**0.007** *	**0.045** *			
60° flexion	Medial	0.23	0.15	0.14	**0.004** *	**0.004** *	0.505	0.351	**0.005** *	0.563
	Lateral	0.26	0.24	0.13	0.266	**0.005** *	**0.004** *			
90° flexion	Medial	0.28	0.21	0.11	**0.004** *	**0.004** *	**0.004** *	0.965	**0.004** *	0.266
	Lateral	0.28	0.28	0.08	0.756	**0.004** *	**0.004** *			

Table A2. Median values and statistical significance of the normalized medial and lateral anterior–posterior position during maximum anterior and posterior shear forces, respectively, at various flexion angles (n = 11). CR/CS = symmetrical implant design without a post-cam mechanism; MS = asymmetrical medial-stabilized implant design; PS = symmetrical implant design with a post-cam mechanism; * $p < 0.05$. Bold indicates statistical significance.

Flexion Angle	Position	Condyle	Median			*p*-Value		
			CR/CS	MS	PS	CR/CS vs. MS	CR/CS vs. PS	MS vs. PS
0° flexion	Anterior force	Medial	0.24	0.29	0.26	**0.005** *	**0.023** *	**0.009** *
		Lateral	0.34	0.33	0.32	0.965	0.505	0.824
	Posterior force	Medial	0.37	0.36	0.38	0.120	0.197	0.100
		Lateral	0.41	0.41	0.40	0.756	0.398	0.100
30° flexion	Anterior force	Medial	0.22	0.30	0.23	**0.004** *	0.168	**0.007** *
		Lateral	0.25	0.28	0.25	0.563	0.756	0.563
	Posterior force	Medial	0.43	0.42	0.40	**0.045** *	**0.018** *	0.056
		Lateral	0.48	0.46	0.41	**0.037** *	**0.005** *	**0.007** *
45° flexion	Anterior force	Medial	0.23	0.29	0.22	**0.004** *	0.689	**0.005** *
		Lateral	0.22	0.26	0.23	0.625	0.625	0.266
	Posterior force	Medial	0.46	0.42	0.36	**0.014** *	**0.007** *	**0.011** *
		Lateral	0.46	0.44	0.36	**0.011** *	**0.004** *	**0.011** *
60° flexion	Anterior force	Medial	0.22	0.29	0.20	**0.004** *	0.142	**0.004** *
		Lateral	0.22	0.23	0.20	0.625	0.068	0.056
	Posterior force	Medial	0.45	0.42	0.31	**0.029** *	**0.004** *	**0.005** *
		Lateral	0.48	0.44	0.31	0.142	**0.005** *	**0.005** *
90° flexion	Anterior force	Medial	0.15	0.20	0.08	**0.005** *	**0.004** *	**0.004** *
		Lateral	0.14	0.15	0.06	0.894	**0.005** *	**0.007** *
	Posterior force	Medial	0.43	0.42	0.16	0.083	**0.004** *	**0.004** *
		Lateral	0.44	0.43	0.14	0.351	**0.004** *	**0.004** *

Table A3. Median values and statistical significance of the normalized medial and lateral anterior–posterior range of motion during internal-external rotation moments at various flexion angles (n = 10). CR/CS = symmetrical implant design without a post-cam mechanism; MS = asymmetrical medial-stabilized implant design; PS = symmetrical implant design with a post-cam mechanism; * $p < 0.05$. Bold indicates statistical significance.

Flexion Angle	Condyle	Median			*p*-Value			*p*-Value Medial vs. Lateral		
		CR/CS	MS	PS	CR/CS vs. MS	CR/CS vs. PS	MS vs. PS	CR/CS	MS	PS
0° flexion	Medial	0.09	0.04	0.08	**0.006** *	**0.041** *	**0.006** *	0.476	0.308	1.000
	Lateral	0.05	0.05	0.05	0.067	1.00	0.154			
30° flexion	Medial	0.17	0.04	0.14	**0.006** *	0.541	**0.019** *	0.308	0.083	0.308
	Lateral	0.23	0.23	0.22	**0.032** *	0.308	**0.011** *			
45° flexion	Medial	0.17	0.05	0.17	**0.006** *	0.919	0.053	0.185	0.067	0.262
	Lateral	0.26	0.27	0.20	**0.014** *	0.053	**0.011** *			
60° flexion	Medial	0.17	0.07	0.19	**0.006** *	0.919	**0.006** *	0.154	**0.014** *	0.308
	Lateral	0.26	0.29	0.20	**0.006** *	**0.041** *	**0.008** *			
90° flexion	Medial	0.21	0.14	0.23	**0.006** *	0.541	0.067	0.126	**0.025** *	0.541
	Lateral	0.25	0.29	0.21	**0.006** *	**0.041** *	**0.008** *			

Table A4. Median values and statistical significance of the normalized medial and lateral anterior–posterior position during maximum internal and external rotation moments, respectively, at various flexion angles (n = 10). CR/CS = symmetrical implant design without a post-cam mechanism; MS = asymmetrical medial-stabilized implant design; PS = symmetrical implant design with a post-cam mechanism; * $p < 0.05$. Bold indicates statistical significance.

Flexion Angle	Position	Condyle	Median			*p*-Value		
			CR/CS	MS	PS	CR/CS vs. MS	CR/CS vs. PS	MS vs. PS
0° flexion	External moment	Medial	0.25	0.31	0.27	**0.006** *	**0.032** *	**0.006** *
		Lateral	0.41	0.41	0.40	0.760	0.221	**0.032** *
	Internal moment	Medial	0.33	0.34	0.34	0.683	0.541	0.683
		Lateral	0.33	0.32	0.32	0.541	0.185	0.760
30° flexion	External moment	Medial	0.23	0.29	0.23	**0.008** *	0.221	**0.006** *
		Lateral	0.47	0.47	0.44	0.610	0.083	**0.025** *
	Internal moment	Medial	0.37	0.36	0.37	**0.041** *	0.919	0.083
		Lateral	0.28	0.27	0.29	0.053	1.000	**0.041** *
45° flexion	External moment	Medial	0.21	0.29	0.21	**0.011** *	**0.041** *	**0.006** *
		Lateral	0.48	0.48	0.45	0.683	**0.011** *	**0.006** *
	Internal moment	Medial	0.39	0.38	0.39	**0.006** *	0.262	0.359
		Lateral	0.26	0.25	0.27	**0.011** *	0.760	0.083
60° flexion	External moment	Medial	0.20	0.29	0.15	**0.008** *	**0.006** *	**0.006** *
		Lateral	0.49	0.49	0.40	0.185	**0.006** *	**0.006** *
	Internal moment	Medial	0.41	0.38	0.36	**0.006** *	**0.019** *	0.610
		Lateral	0.24	0.22	0.22	**0.006** *	**0.019** *	0.308
90° flexion	External moment	Medial	0.14	0.19	0.00	**0.008** *	**0.006** *	**0.006** *
		Lateral	0.43	0.43	0.24	0.067	**0.006** *	**0.006** *
	Internal moment	Medial	0.41	0.37	0.22	**0.014** *	**0.006** *	**0.008** *
		Lateral	0.16	0.13	0.04	**0.006** *	**0.006** *	**0.011** *

References

1. Movassaghi, K.; Patel, A.; Ghulam-Jelani, Z.; Levine, B.R. Modern Total Knee Arthroplasty Bearing Designs and the Role of the Posterior Cruciate Ligament. *Arthroplast. Today* **2023**, *21*, 101130. [CrossRef] [PubMed]

2. Grimberg, A.; Lützner, J.; Melsheimer, O.; Morlock, M.; Steinbrück, A. *Endoprothesenregister Deutschland (EPRD) Jahresbericht 2023*; EPRD Deutsche Endoprothesenregister gGmbH: Berlin, Germany, 2023. [CrossRef]
3. *American Joint Replacement Registry (AJRR): 2024 Annual Report*; American Academy of Orthopaedic Surgeons: Rosemont, IL, USA, 2024.
4. Sabatini, L.; Risitano, S.; Parisi, G.; Tosto, F.; Indelli, P.F.; Atzori, F.; Massè, A. Medial Pivot in Total Knee Arthroplasty: Literature Review and Our First Experience. *Clin. Med. Insights Arthritis Musculoskelet. Disord.* **2018**, *11*, 1179544117751431. [CrossRef] [PubMed]
5. Gray, H.A.; Guan, S.; Thomeer, L.T.; Schache, A.G.; de Steiger, R.; Pandy, M.G. Three-dimensional motion of the knee-joint complex during normal walking revealed by mobile biplane x-ray imaging. *J. Orthop. Res.* **2019**, *37*, 615–630. [CrossRef]
6. Postolka, B.; Schütz, P.; Fucentese, S.F.; Freeman, M.A.R.; Pinskerova, V.; List, R.; Taylor, W.R. Tibio-femoral kinematics of the healthy knee joint throughout complete cycles of gait activities. *J. Biomech.* **2020**, *110*, 109915. [CrossRef] [PubMed]
7. Freeman, M.A.R.; Pinskerova, V. The movement of the knee studied by magnetic resonance imaging. *Clin. Orthop. Relat. Res.* **2003**, *410*, 35–43. [CrossRef] [PubMed]
8. Steinbrück, A.; Schröder, C.; Woiczinski, M.; Fottner, A.; Pinskerova, V.; Müller, P.E.; Jansson, V. Femorotibial kinematics and load patterns after total knee arthroplasty: An in vitro comparison of posterior-stabilized versus medial-stabilized design. *Clin. Biomech. (Bristol, Avon)* **2016**, *33*, 42–48. [CrossRef] [PubMed]
9. Brendle, S.A.; Krueger, S.; Fehrenbacher, J.; Grifka, J.; Müller, P.E.; Mihalko, W.M.; Richter, B.; Grupp, T.M. Kinematic Patterns of Different Loading Profiles Before and After Total Knee Arthroplasty: A Cadaveric Study. *Bioengineering* **2024**, *11*, 1064. [CrossRef]
10. Hinarejos, P.; Leal-Blanquet, J.; Fraile-Suari, A.; Sánchez-Soler, J.; Torres-Claramunt, R.; Monllau, J.C. Increased posterior translation but similar clinical outcomes using ultracongruent instead of posterior stabilized total knee arthroplasties in a prospective randomized trial. *Knee Surg. Sports Traumatol. Arthrosc.* **2022**, *30*, 3041–3048. [CrossRef] [PubMed]
11. Kim, T.W.; Lee, S.M.; Seong, S.C.; Lee, S.; Jang, J.; Lee, M.C. Different intraoperative kinematics with comparable clinical outcomes of ultracongruent and posterior stabilized mobile-bearing total knee arthroplasty. *Knee Surg. Sports Traumatol. Arthrosc.* **2016**, *24*, 3036–3043. [CrossRef]
12. Massin, P.; Boyer, P.; Sabourin, M. Less femorotibial rotation and AP translation in deep-dished total knee arthroplasty. An intraoperative kinematic study using navigation. *Knee Surg. Sports Traumatol. Arthrosc.* **2012**, *20*, 1714–1719. [CrossRef]
13. Postolka, B.; Taylor, W.R.; List, R.; Fucentese, S.F.; Koch, P.P.; Schütz, P. ISB clinical biomechanics award winner 2021: Tibio-femoral kinematics of natural versus replaced knees—A comparison using dynamic videofluoroscopy. *Clin. Biomech. (Bristol, Avon)* **2022**, *96*, 105667. [CrossRef]
14. Koster, L.A.; Kaptein, B.L.; van der Linden-van der Zwaag, E.H.M.J.; Nelissen, R.G.H.H. Knee kinematics are not different between asymmetrical and symmetrical tibial baseplates in total knee arthroplasty: A fluoroscopic analysis of step-up and lunge motions. *Knee Surg. Sports Traumatol. Arthrosc.* **2024**, *32*, 1253–1263. [CrossRef] [PubMed]
15. Dupraz, I.; Thorwächter, C.; Grupp, T.M.; Hammerschmid, F.; Woiczinski, M.; Jansson, V.; Müller, P.E.; Steinbrück, A. Impact of femoro-tibial size combinations and TKA design on kinematics. *Arch. Orthop. Trauma Surg.* **2022**, *142*, 1197–1212. [CrossRef] [PubMed]
16. Gray, H.A.; Guan, S.; Young, T.J.; Dowsey, M.M.; Choong, P.F.; Pandy, M.G. Comparison of posterior-stabilized, cruciate-retaining, and medial-stabilized knee implant motion during gait. *J. Orthop. Res.* **2020**, *38*, 1753–1768. [CrossRef] [PubMed]
17. Smith, P.N.; Gill, D.R.; McAuliffe, M.J.; McDougall, C.; Stoney, J.D.; Vertullo, C.J.; Wall, C.J.; Corfield, S.; Page, R.; Cuthbert, A.R.; et al. *Hip, Knee and Shoulder Arthroplasty: 2023 Annual Report*; Australian Orthopaedic Association National Joint Replacement Registry, AOA: Sydney, Australia, 2023. [CrossRef]
18. Krackow, K.A. Instability in total knee arthroplasty: Loose as a goose. *J. Arthroplast.* **2003**, *18*, 45–47. [CrossRef]
19. Sharkey, P.F.; Lichstein, P.M.; Shen, C.; Tokarski, A.T.; Parvizi, J. Why are total knee arthroplasties failing today--has anything changed after 10 years? *J. Arthroplast.* **2014**, *29*, 1774–1778. [CrossRef]
20. Wilson, C.J.; Theodoulou, A.; Damarell, R.A.; Krishnan, J. Knee instability as the primary cause of failure following Total Knee Arthroplasty (TKA): A systematic review on the patient, surgical and implant characteristics of revised TKA patients. *Knee* **2017**, *24*, 1271–1281. [CrossRef] [PubMed]
21. Jang, S.W.; Kim, M.S.; Koh, I.J.; Sohn, S.; Kim, C.; In, Y. Comparison of Anterior-Stabilized and Posterior-Stabilized Total Knee Arthroplasty in the Same Patients: A Prospective Randomized Study. *J. Arthroplast.* **2019**, *34*, 1682–1689. [CrossRef]
22. Wautier, D.; Thienpont, E. Changes in anteroposterior stability and proprioception after different types of knee arthroplasty. *Knee Surg. Sports Traumatol. Arthrosc.* **2017**, *25*, 1792–1800. [CrossRef]
23. Scott, D.F.; Hellie, A.A. Mid-Flexion, Anteroposterior Stability of Total Knee Replacement Implanted with Kinematic Alignment: A Randomized, Quantitative Radiographic Laxity Study with Posterior-Stabilized and Medial-Stabilized Implants. *J. Bone Jt. Surg. Am.* **2023**, *105*, 9–19. [CrossRef] [PubMed]
24. Jones, C.W.; Jacobs, H.; Shumborski, S.; Talbot, S.; Redgment, A.; Brighton, R.; Walter, W.L. Sagittal Stability and Implant Design Affect Patient Reported Outcomes After Total Knee Arthroplasty. *J. Arthroplast.* **2020**, *35*, 747–751. [CrossRef] [PubMed]

25. De Groot, J.D.; Brokelman, R.B.G.; Lammers, P.G.; van Stralen, G.M.J.; Kooijman, C.M.; Hokwerda, S.T. Performance of medial pivot, posterior stabilized and rotating platform total knee arthroplasty based on anteroposterior stability and patient-reported outcome measures; a multicentre double-blinded randomized controlled trial of 210 knees. *Arch. Orthop. Trauma Surg.* **2024**, *144*, 2327–2335. [CrossRef] [PubMed]
26. Edelstein, A.I.; Bhatt, S.; Wright-Chisem, J.; Sullivan, R.; Beal, M.; Manning, D.W. The Effect of Implant Design on Sagittal Plane Stability: A Randomized Trial of Medial- versus Posterior-Stabilized Total Knee Arthroplasty. *J. Knee Surg.* **2020**, *33*, 452–458. [CrossRef] [PubMed]
27. Lützner, J.; Firmbach, F.-P.; Lützner, C.; Dexel, J.; Kirschner, S. Similar stability and range of motion between cruciate-retaining and cruciate-substituting ultracongruent insert total knee arthroplasty. *Knee Surg. Sports Traumatol. Arthrosc.* **2015**, *23*, 1638–1643. [CrossRef]
28. Kour, R.Y.N.; Guan, S.; Dowsey, M.M.; Choong, P.F.; Pandy, M.G. Kinematic function of knee implant designs across a range of daily activities. *J. Orthop. Res.* **2023**, *41*, 1217–1227. [CrossRef]
29. Brendle, S.A.; Krueger, S.; Grifka, J.; Müller, P.E.; Grupp, T.M. A New Methodology for the Accurate Measurement of Tibiofemoral Kinematics in Human Cadaveric Knees: An Evaluation of the Anterior–Posterior Laxity Pre- and Post-Cruciate Ligament Resection. *Life* **2024**, *14*, 877. [CrossRef] [PubMed]
30. Willing, R.; Moslemian, A.; Yamomo, G.; Wood, T.; Howard, J.; Lanting, B. Condylar-Stabilized TKR May Not Fully Compensate for PCL-Deficiency: An In Vitro Cadaver Study. *J. Orthop. Res.* **2019**, *37*, 2172–2181. [CrossRef] [PubMed]
31. Borque, K.A.; Gold, J.E.; Incavo, S.J.; Patel, R.M.; Ismaily, S.E.; Noble, P.C. Anteroposterior Knee Stability During Stair Descent. *J. Arthroplast.* **2015**, *30*, 1068–1072. [CrossRef] [PubMed]
32. Walker, P.S.; Borukhov, I.; LiArno, S. Obtaining anatomic motion and laxity characteristics in a total knee design. *Knee* **2022**, *35*, 133–141. [CrossRef]
33. Grood, E.S.; Suntay, W.J. A joint coordinate system for the clinical description of three-dimensional motions: Application to the knee. *J. Biomech. Eng.* **1983**, *105*, 136–144. [CrossRef]
34. Daniel, D.M.; Malcom, L.L.; Losse, G.; Stone, M.L.; Sachs, R.; Burks, R. Instrumented measurement of anterior laxity of the knee. *J. Bone Jt. Surg. Am.* **1985**, *67*, 720–726. [CrossRef]
35. Bull, A.M.J.; Kessler, O.; Alam, M.; Amis, A.A. Changes in knee kinematics reflect the articular geometry after arthroplasty. *Clin. Orthop. Relat. Res.* **2008**, *466*, 2491–2499. [CrossRef] [PubMed]
36. Reynolds, R.J.; Walker, P.S.; Buza, J. Mechanisms of anterior-posterior stability of the knee joint under load-bearing. *J. Biomech.* **2017**, *57*, 39–45. [CrossRef] [PubMed]
37. Walker, P.S.; Arno, S.; Borukhoy, I.; Bell, C.P. Characterising knee motion and laxity in a testing machine for application to total knee evaluation. *J. Biomech.* **2015**, *48*, 3551–3558. [CrossRef] [PubMed]
38. King, A.P.; Eckersley, R.J. Inferential Statistics III: Nonparametric Hypothesis Testing. In *Statistics for Biomedical Engineers and Scientists*; Elsevier: Amsterdam, The Netherlands, 2019; pp. 119–145, ISBN 9780081029398.
39. Willing, R.; Walker, P.S. Measuring the sensitivity of total knee replacement kinematics and laxity to soft tissue imbalances. *J. Biomech.* **2018**, *77*, 62–68. [CrossRef] [PubMed]
40. Shalhoub, S.; Moschetti, W.E.; Dabuzhsky, L.; Jevsevar, D.S.; Keggi, J.M.; Plaskos, C. Laxity Profiles in the Native and Replaced Knee-Application to Robotic-Assisted Gap-Balancing Total Knee Arthroplasty. *J. Arthroplast.* **2018**, *33*, 3043–3048. [CrossRef] [PubMed]
41. Minoda, Y.; Nakagawa, S.; Sugama, R.; Ikawa, T.; Noguchi, T.; Hirakawa, M. Midflexion Laxity After Implantation Was Influenced by the Joint Gap Balance Before Implantation in TKA. *J. Arthroplast.* **2015**, *30*, 762–765. [CrossRef] [PubMed]
42. Arnout, N.; Vanlommel, L.; Vanlommel, J.; Luyckx, J.P.; Labey, L.; Innocenti, B.; Victor, J.; Bellemans, J. Post-cam mechanics and tibiofemoral kinematics: A dynamic in vitro analysis of eight posterior-stabilized total knee designs. *Knee Surg. Sports Traumatol. Arthrosc.* **2015**, *23*, 3343–3353. [CrossRef] [PubMed]
43. Taylor, W.R.; Schütz, P.; Bergmann, G.; List, R.; Postolka, B.; Hitz, M.; Dymke, J.; Damm, P.; Duda, G.; Gerber, H.; et al. A comprehensive assessment of the musculoskeletal system: The CAMS-Knee data set. *J. Biomech.* **2017**, *65*, 32–39. [CrossRef] [PubMed]
44. Hull, M.L. Errors in using fixed flexion facet centers to determine tibiofemoral kinematics increase fourfold for multi-radius femoral component designs with early versus late decreases in the radius of curvature. *Knee* **2022**, *35*, 183–191. [CrossRef] [PubMed]
45. Dandridge, O.; Garner, A.; Jeffers, J.R.T.; Amis, A.A.; Cobb, J.P.; van Arkel, R.J. Validity of repeated-measures analyses of in vitro arthroplasty kinematics and kinetics. *J. Biomech.* **2021**, *129*, 110669. [CrossRef] [PubMed]

5 Additional content

The new methodology developed within this dissertation allows the exploration of additional aspects, beyond those covered in the three publications of this thesis, to gain a more comprehensive understanding of the biomechanics of the native knee. In order to highlight the advantages and importance of the new methodology, some of these aspects are briefly presented in the following sections.

5.1 Additional content I: Tibiofemoral gaps of human cadaveric knees before and after sacrificing both cruciate ligaments

Presented at the congress of the 'European Society of Biomechanics' in Maastricht, 2023 (71).

Introduction

Implant alignment and the resulting knee stability are crucial factors that affect short- and long-term outcomes of total knee arthroplasty (TKA) (72). While the goal of gap balancing is to create equal and symmetric flexion and extension gaps to obtain correct soft tissue balance, it was shown that gaps in the native knee are neither equal nor symmetric through the arc of flexion (73). However, tibiofemoral gaps of native knees are so far measured after tibial-cut and resection of the anterior cruciate ligament (ACL), while the "true" native gaps are mostly unknown. Therefore, the objective of this study was to quantify the tibiofemoral gaps of native knees at different flexion angles prior to tibia and ACL resection and to investigate changes after sacrificing both cruciate ligaments.

Materials and methods

Eleven fresh-frozen human cadaveric knees were tested on a six-degrees-of-freedom joint motion simulator (Advanced Mechanical Technologies Inc., Watertown, USA) by applying 100 N distraction force for 25 s at different flexion angles (0°, 30°, 45°, 60° and 90°) and different stages of resection (native knee and after resection of the cruciate ligaments) with all other forces/moments maintained at 0 N/Nm. Before testing, femur and tibia of each specimen underwent a complex 3D fitting process (ARAMIS 12M, Carl Zeiss GOM Metrology GmbH, Braunschweig, Germany) using segmented CT scans containing landmark-based femoral and tibial coordinate systems (Figure 5a). During testing, the relative position of femoral and tibial coordinate systems was tracked by the joint motion simulator. This allowed subsequent positioning of the segmented CT scans relative to each other to measure the tibiofemoral gaps

medially and laterally along the mechanical axis of the tibia (Figure 5b). Measured gaps were normalized to the native medial gaps at 0° flexion to enable comparison of the specimens. Mean standardized gaps and standard deviations were calculated across the eleven specimens.

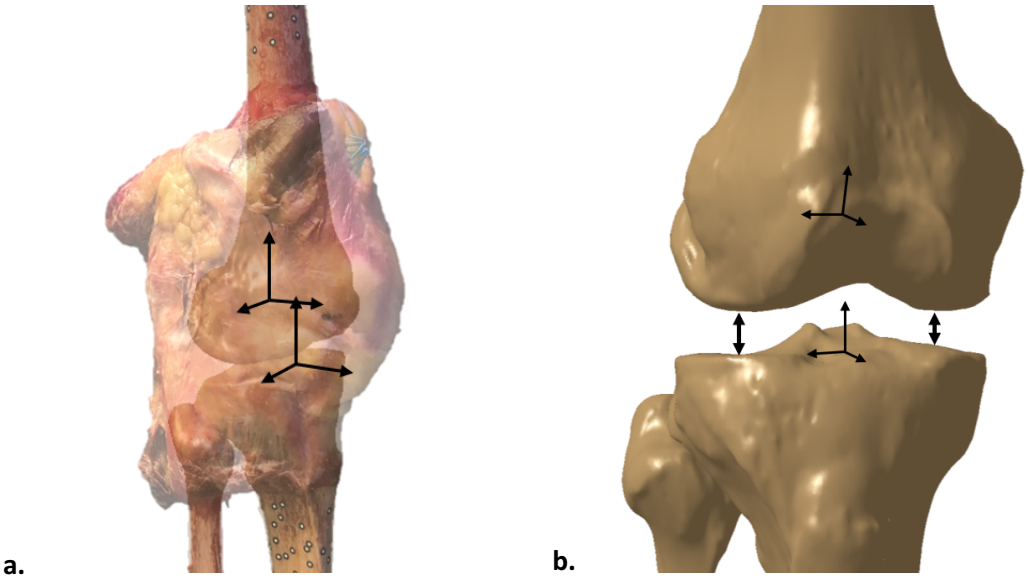

a. b.

Figure 5. (a) Specimen with 3D fitted segmented CT scans. (b) Exemplary gap measurement within the positioned CT scans.

Results

Native medial and lateral gaps were tightest in extension, increased mostly until 30° flexion, then only showed a small increase until 60° and a slight decrease again at 90° (Figure 6). The lateral native gap was larger than the medial gap throughout the complete range of flexion. After resection of the cruciate ligaments, the gaps increased on both, the medial and lateral sides. In contrast to the native knees, the gaps continued increasing until 90° flexion.

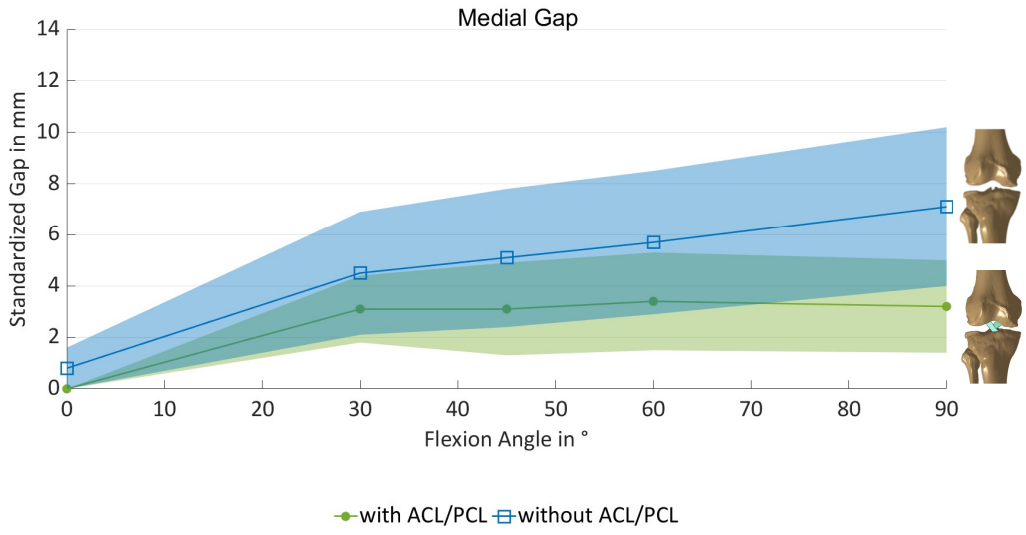

a.

b.

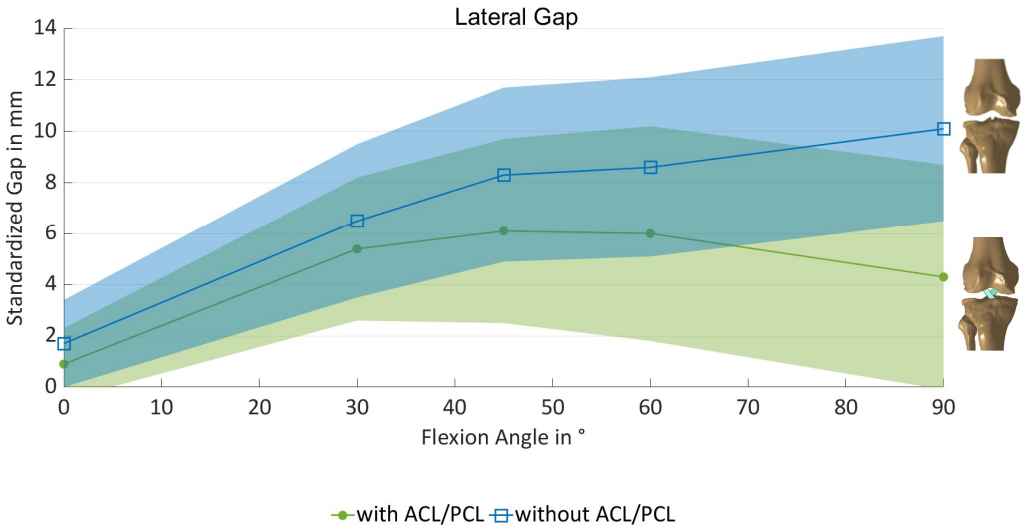

Figure 6. Mean standardized (a) medial and (b) lateral gaps (n = 11) and standard deviations throughout the range of flexion (0° to 90°) in the native (green) and cruciate sacrificed (ACL & PCL, blue) knees.

Discussion

It was shown that the tibiofemoral gaps in native knees, prior to tibia-cut and ACL resection, are neither equal nor symmetric with a markable increase until 30° flexion. This may affect knee stability in mid-flexion after gap balanced TKA. Furthermore, sacrificing both cruciate ligaments resulted in a greater flexion-extension mismatch than in native knees.

5.2 Additional content II: Condylar motion of human cadaveric knees before and after sacrificing both cruciate ligaments

Presented at the congress of the 'International Society for Technology in Arthroplasty' in New York, 2023 (74).

Introduction

Even though knee prostheses have improved greatly and became one of the most reliable joint replacements, numerous studies point out that only approximately 80% of patients are satisfied with the results of their total knee arthroplasty (TKA) (25). It is hypothesized that recreating native knee kinematics is beneficial regarding patient satisfaction after TKA (36). However, it is not clear whether all native knees show the same kinematic pattern and would therefore be suitable for the same TKA design. For this reason, the aim of this study was to characterize the condylar motion of native knees and to investigate changes after sacrificing the anterior cruciate

ligament (ACL) and posterior cruciate ligament (PCL), respectively, in order to identify different implant requirements.

Materials and methods

In this *in vitro* study, nine fresh-frozen human cadaveric knees were tested on a six-degrees-of-freedom joint motion simulator (Advanced Mechanical Technologies Inc., Watertown, USA). The neutral path of motion of each knee was recorded by applying continuous knee flexion and extension from 0° to 90° with 50 N compression force at different stages of resection (native, after resection of the ACL and after resection of both cruciate ligaments), with all other forces/moments maintained at 0 N/Nm. Prior to each resection stage, the knee capsule was opened using a medial parapatellar approach and closed by sutures. In order to track the relative position of femur and tibia during testing, each specimen underwent a complex 3D fitting process (ARAMIS 12M, Carl Zeiss GOM Metrology GmbH, Braunschweig, Germany) using segmented CT scans containing landmark-based femoral and tibial coordinate systems. Knowledge of the relative positions of femoral and tibial coordinate systems and their according bone geometries allowed the projection of the flexion axis and medial and lateral flexion facet centers (MFC and LFC) onto the tibial plane at different flexion angles and therefore the measurement of condylar motion throughout the arc of flexion. Anterior-posterior (AP) translation of the MFC and LFC of each specimen was calculated and normalized to the native medial AP position at 0° flexion.

Results

AP translation of the MFC and LFC and consequently condylar motion varied between the specimens and stages of resection. Specimen P08, for example, showed similar AP translation of the MFC and the LFC, resulting in a symmetrical femoral rollback in the native condition (Figure 7a). Femoral rollback decreased after sacrificing the ACL and disappeared mostly after sacrificing both cruciate ligaments (Figure 8). In contrast, specimen P12 showed almost no posterior translation of the MFC, whereas a large posterior translation was observed for the LFC (Figure 7b). Consequently, a medial pivot was present in the native condition and was maintained after sacrificing the cruciate ligaments (Figure 9).

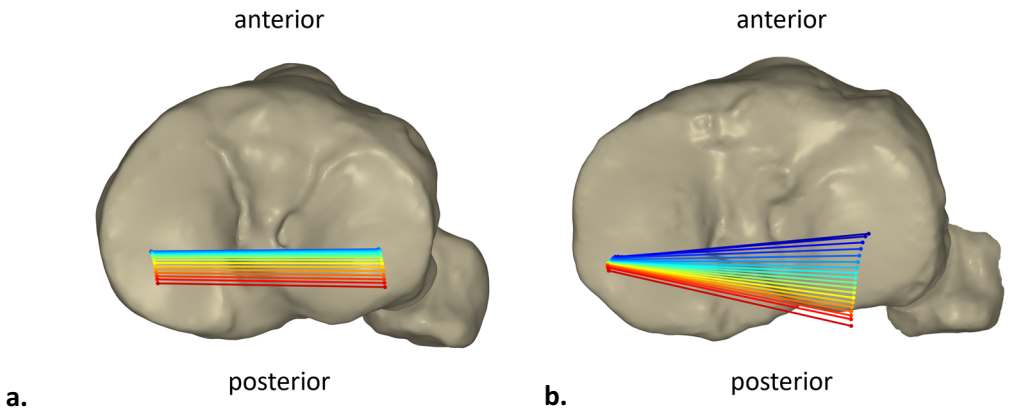

Figure 7. Projection of the flexion axis and medial and lateral flexion facet centers onto the tibial plane at different flexion angles showing condylar motion throughout the arc of flexion of (a) specimen P08 and (b) P12 in the native condition. The colors represent the respective flexion angle in 5° intervals, from dark blue (0°) through green and yellow to red (90°).

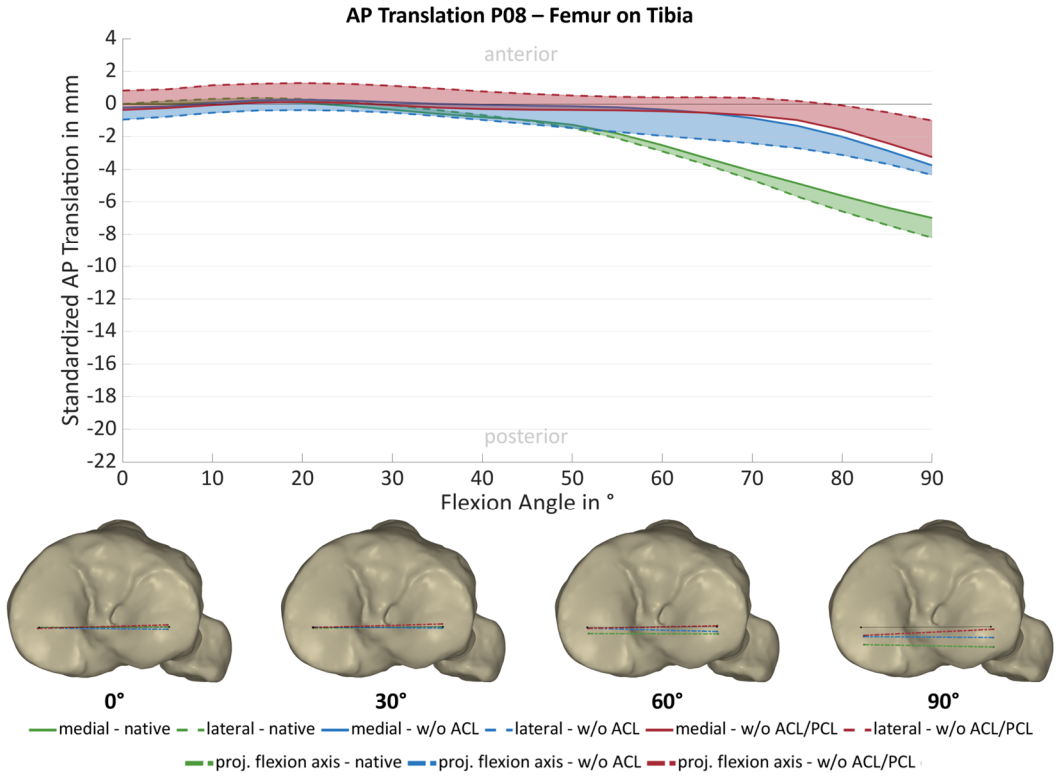

Figure 8. AP translation of the MFC and LFC of specimen P08, normalized to the native medial AP position at 0° flexion. Specimen P08 showed similar AP translation of the MFC (green line) and the LFC (dashed green line), resulting in a femoral rollback in the native condition. Femoral rollback decreased after sacrificing the ACL (blue) and disappeared mostly after sacrificing both cruciate ligaments (red).

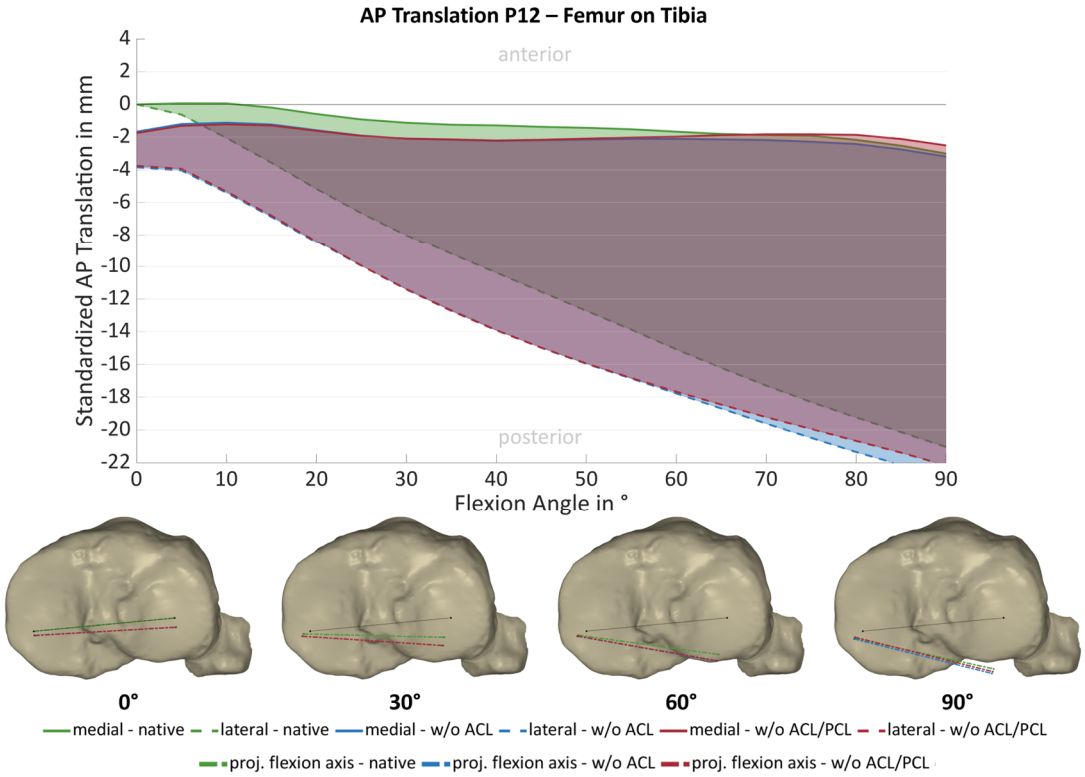

Figure 9. AP translation of the MFC and LFC of specimen P12, normalized to the native medial AP position at 0° flexion. Specimen P12 showed almost no AP translation of the MFC (green line), whereas a large AP translation was observed for the LFC (dashed green line). Consequently, a medial pivot was present in the native condition (green) and was maintained after sacrificing the cruciate ligaments (without ACL – blue, without ACL/PCL – red).

Discussion

It was shown that the condylar motion of native knees and the effect of ACL and PCL resection varies greatly and therefore each knee has individual requirements regarding implant design and alignment to mimic native knee kinematics. A further study will investigate which implant designs best replicate the specimens' native knee kinematics.

5.3 Additional content III: Condylar motion patterns during passive knee flexion are not only a results of osteoarthrosis

Presented at the congress of the 'Orthopaedic Research Society' in Long Beach, 2024 (75).

Introduction

Although total knee arthroplasty (TKA) has improved considerably and became one of the most reliable joint replacement procedures, numerous studies indicate that approximately 20% of

patients are dissatisfied with the results of their TKA (25). It has been hypothesized that restoration of the native knee kinematics may improve patient satisfaction following TKA (36). However, it is not clear whether all native knees show the same kinematic behaviour and, therefore, would be suitable for the same type of TKA design. In addition, it is currently unknown whether specific kinematic patterns are the result of a particular level of osteoarthrosis. For this reason, the aim of this study was to characterize the condylar motion of native knees and to investigate whether the kinematic behavior is related to the osteoarthrosis level.

Materials and methods

Within the scope of this *in vitro* study, thirteen fresh-frozen human cadaveric knees were tested on a six-degrees-of-freedom joint motion simulator (Advanced Mechanical Technologies Inc., Watertown, USA). To record the neutral path of motion of each knee, the knees were continuously flexed and extended from 0° to 90° with a compressive force of 50 N, while all other forces/moments were maintained at 0 N/Nm. Before testing, the femur and tibia of each specimen underwent a complex 3D fitting process (ARAMIS 12M, Carl Zeiss GOM Metrology GmbH, Braunschweig, Germany) using segmented CT scans containing landmark-based femoral and tibial coordinate systems. Tracking the relative positions of the femoral and tibial coordinate systems and their corresponding bone geometries during testing allowed the projection of the flexion axis and the medial and lateral flexion facet centres (MFC and LFC) onto the tibial plane at different flexion angles. The resulting condylar motion is characterized by the anterior-posterior (AP) translation of the MFC and the rotation of the projected flexion axis when flexing the knee from 0° to 90°. After testing, the knee capsule was opened using a medial parapatellar approach and the osteoarthrosis level was determined by an experienced knee surgeon. To better visualize cartilage distributions and defects on the femoral condyles, 3D scans of each femur were acquired and matched to the segmented CT scans.

Results

The condylar motion which is described by the AP translation of the MFC and the rotation of the projected flexion axis varied between the specimens (Figure 10). However, two main kinematic pattern groups could be identified. In group 1, the posterior translation of the MFC was associated with a small rotational movement (< 5°), resulting in a symmetrical femoral rollback (Figure 11a). In contrast, group 2 showed a posterior translation of the MFC combined with a higher rotation (> 5°, Figure 11b). This pattern can be described as medial pivoting. In two specimens, the medial pivot was more prominent than in the main group (P10 and P12). Furthermore, four different osteoarthrosis levels of the femoral condyles were determined

based on the experienced knee surgeon's assessment and evaluation of the 3D scans: 1. Slight degeneration medial and lateral (Figure 12), 2. Moderate degeneration medial and lateral, 3. More medial than lateral degeneration, 4. More lateral than medial degeneration. Neither group of kinematic patterns is associated with a specific osteoarthrosis level.

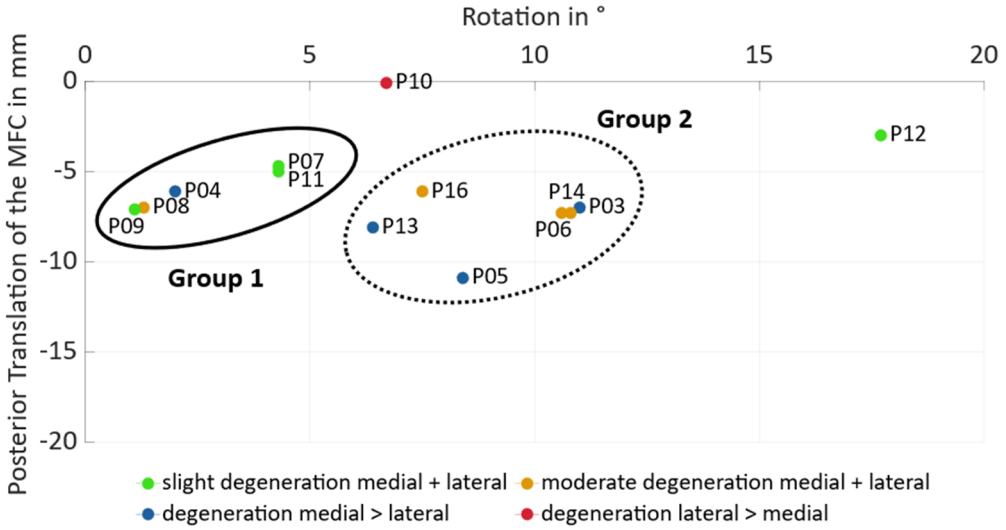

Figure 10. Posterior translation of the MFC vs. rotation of the projected flexion axis of different specimens during passive knee flexion from 0° to 90° based on level of osteoarthrosis and kinematic pattern group. Group 1 shows a symmetrical femoral rollback, whereas group 2 displays a medial pivot.

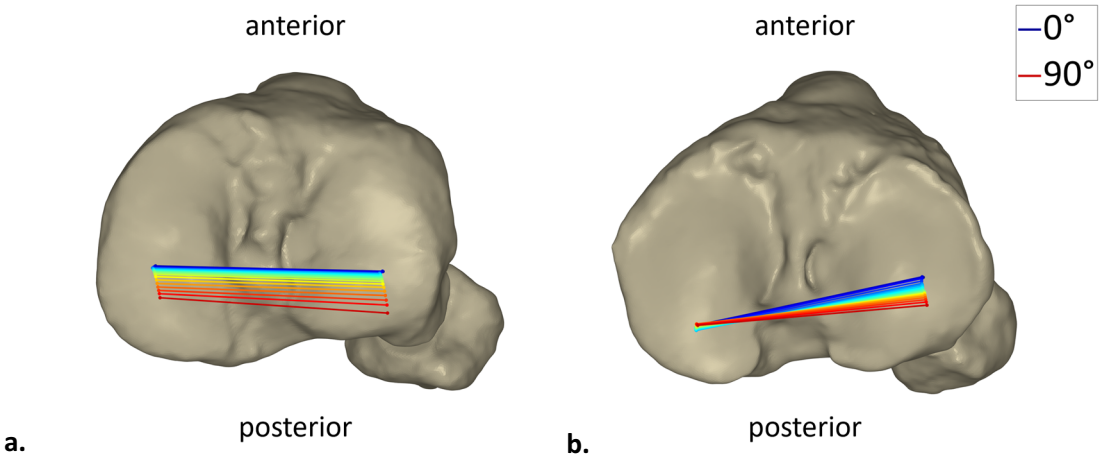

Figure 11. Projection of the flexion axis and flexion facet centers onto the tibial plane at different flexion angles resulting in (a) a symmetrical femoral rollback and (b) a medial pivot.

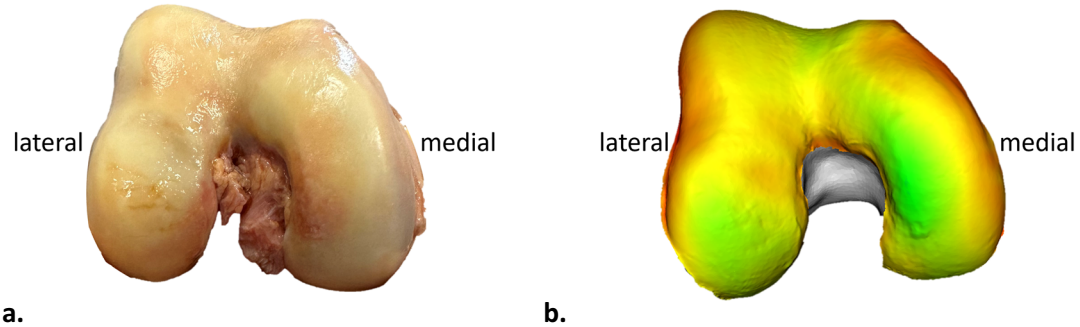

a. **b.**

Figure 12. (a) Femoral condyles and (b) matched 3D scan of femoral condyles of specimen P11 showing slight degeneration medial and lateral with cartilage swelling on the medial distal condyle. The thickness of the cartilage layer decreases from green to red.

Discussion

It has been shown that the condylar motion of native knees can be divided into two main groups, with no kinematic pattern associated with a specific level of osteoarthrosis. This suggests that different kinematic patterns are not only a result of osteoarthrosis. Consequently, each knee has unique implant design and alignment requirements to mimic native knee kinematics. However, severe progredient osteoarthrosis was not investigated in this study. Therefore, no conclusions can be drawn about the kinematic behavior in this condition. A further study will investigate which implant designs best replicate the specimens' individual native knee kinematics.

References

1. Schünke M. Prometheus. 5. vollständig überarbeitete Auflage. Stuttgart, New York:Georg Thieme Verlag;2018.

2. Standring S, Anhand N, Gray H, editors. Gray's Anatomy: The anatomical basis of clinical practice. 42nd edition. Amsterdam:Elsevier;2021.

3. Arnold WH, Bechmann IJ, Böckers A, Bräuer L, Dehghani F, Deller T et al. Anatomie: Das Lehrbuch : Sobotta. 2. Auflage. München:Elsevier;2019.

4. Affatato S. Biomechanics of the knee. In: Affatato S, editor. Surgical techniques in total knee arthroplasty (TKA) and alternative procedures. Amsterdam, Boston, Cambridge: Elsevier/WP Woodhead Publishing; 2015. p. 17–35 (Woodhead Publishing series in biomaterials; number 87).

5. Hirschmann MT, Müller W. Complex function of the knee joint: the current understanding of the knee. Knee Surg Sports Traumatol Arthrosc. 2015;23(10):2780–8.

6. Mora JC, Przkora R, Cruz-Almeida Y. Knee osteoarthritis: pathophysiology and current treatment modalities. J Pain Res. 2018;11:2189–96.

7. Global burden of 369 diseases and injuries in 204 countries and territories, 1990-2019: a systematic analysis for the Global Burden of Disease Study 2019. Lancet. 2020;396(10258):1204–22.

8. Yang G, Wang J, Liu Y, Lu H, He L, Ma C et al. Burden of Knee Osteoarthritis in 204 Countries and Territories, 1990-2019: Results From the Global Burden of Disease Study 2019. Arthritis Care Res (Hoboken). 2023;75(12):2489–500.

9. Langworthy M, Dasa V, Spitzer AI. Knee osteoarthritis: disease burden, available treatments, and emerging options. Ther Adv Musculoskelet Dis. 2024;16:1759720X241273009.

10. Fuchs J, Kuhnert R, Scheidt-Nave C. 12-Monats-Prävalenz von Arthrose in Deutschland; 2017.

11. Gao J, Xing D, Dong S, Lin J. The primary total knee arthroplasty: a global analysis. J Orthop Surg Res. 2020;15(1):190.

12. Bruyère O, Honvo G, Veronese N, Arden NK, Branco J, Curtis EM et al. An updated algorithm recommendation for the management of knee osteoarthritis from the European Society for Clinical and Economic Aspects of Osteoporosis, Osteoarthritis and Musculoskeletal Diseases (ESCEO). Semin Arthritis Rheum. 2019;49(3):337–50.

13. Dupraz I, Thorwächter C, Grupp TM, Hammerschmid F, Woiczinski M, Jansson V et al. Impact of femoro-tibial size combinations and TKA design on kinematics. Arch Orthop Trauma Surg. 2022;142(6):1197–212.

14. Gray HA, Guan S, Young TJ, Dowsey MM, Choong PF, Pandy MG. Comparison of posterior-stabilized, cruciate-retaining, and medial-stabilized knee implant motion during gait. J Orthop Res. 2020;38(8):1753–68.

15. Hamilton LD, Shelburne KB, Rullkoetter PJ, Barnes CL, Mannen EM. Kinematic Performance of Medial Pivot Total Knee Arthroplasty. J Arthroplasty. 2024;39(6):1595-1601.e7.

16. Postolka B, Taylor WR, List R, Fucentese SF, Koch PP, Schütz P. ISB clinical biomechanics award winner 2021: Tibio-femoral kinematics of natural versus replaced knees - A comparison using dynamic videofluoroscopy. Clin Biomech (Bristol, Avon). 2022;96:105667.

17. Steinbrück A, Schröder C, Woiczinski M, Fottner A, Pinskerova V, Müller PE et al. Femorotibial kinematics and load patterns after total knee arthroplasty: An in vitro comparison of posterior-stabilized versus medial-stabilized design. Clin Biomech (Bristol, Avon). 2016;33:42–8.

18. Grimberg A, Kirschner S, Lützner J, Melsheimer O, Morlock M, Steinbrück A. Endoprothesenregister Deutschland (EPRD) Jahresbericht 2024. 2024.

19. Lewis PL, Gill DR, McAuliffe MJ, McDougall C, Stoney JD, Vertullo CJ et al. Hip, Knee and Shoulder Arthroplasty: 2024 Annual Report. Australian Orthopaedic Association National Joint Replacement Registry, AOA. 2024.

20. American Academy of Orthopaedic Surgeons (AAOS), editor. American Joint Replacement Registry (AJRR): 2024 Annual Report. Rosemont, IL;2024.

21. Sabatini L, Risitano S, Parisi G, Tosto F, Indelli PF, Atzori F et al. Medial Pivot in Total Knee Arthroplasty: Literature Review and Our First Experience. Clin Med Insights Arthritis Musculoskelet Disord. 2018;11:1179544117751431.

22. Gray HA, Guan S, Thomeer LT, Schache AG, Steiger R de, Pandy MG. Three-dimensional motion of the knee-joint complex during normal walking revealed by mobile biplane x-ray imaging. J Orthop Res. 2019;37(3):615–30.

23. Postolka B, Schütz P, Fucentese SF, Freeman MAR, Pinskerova V, List R et al. Tibio-femoral kinematics of the healthy knee joint throughout complete cycles of gait activities. J Biomech. 2020;110:109915.

24. Iwaki H, Pinskerova V, Freeman MA. Tibiofemoral movement 1: the shapes and relative movements of the femur and tibia in the unloaded cadaver knee. J Bone Joint Surg Br. 2000;82(8):1189–95.

25. Bourne RB, Chesworth BM, Davis AM, Mahomed NN, Charron KDJ. Patient satisfaction after total knee arthroplasty: who is satisfied and who is not? Clin Orthop Relat Res. 2010;468(1):57–63.

26. Bryan S, Goldsmith LJ, Davis JC, Hejazi S, MacDonald V, McAllister P et al. Revisiting patient satisfaction following total knee arthroplasty: a longitudinal observational study. BMC Musculoskelet Disord. 2018;19(1):423.

27. Dunbar MJ, Richardson G, Robertsson O. I can't get no satisfaction after my total knee replacement: rhymes and reasons. Bone Joint J. 2013;95-B(11 Suppl A):148–52.

28. Gandhi R, Davey JR, Mahomed NN. Predicting patient dissatisfaction following joint replacement surgery. J Rheumatol. 2008;35(12):2415–8.

29. Gunaratne R, Pratt DN, Banda J, Fick DP, Khan RJK, Robertson BW. Patient Dissatisfaction Following Total Knee Arthroplasty: A Systematic Review of the Literature. J Arthroplasty. 2017;32(12):3854–60.

30. Kahlenberg CA, Nwachukwu BU, McLawhorn AS, Cross MB, Cornell CN, Padgett DE. Patient Satisfaction After Total Knee Replacement: A Systematic Review. HSS J. 2018;14(2):192–201.

31. Singh M, Harary J, Schilling PL, Moschetti WE. Patient Satisfaction Is Nearly 90% After Total Knee Arthroplasty; We Are Better Than We Were. J Arthroplasty. 2024.

32. Noble PC, Conditt MA, Cook KF, Mathis KB. The John Insall Award: Patient expectations affect satisfaction with total knee arthroplasty. Clin Orthop Relat Res. 2006;452:35–43.

33. Halawi MJ, Jongbloed W, Baron S, Savoy L, Williams VJ, Cote MP. Patient Dissatisfaction After Primary Total Joint Arthroplasty: The Patient Perspective. J Arthroplasty. 2019;34(6):1093–6.

34. Klem N-R, Smith A, O'Sullivan P, Dowsey MM, Schütze R, Kent P et al. What Influences Patient Satisfaction after TKA? A Qualitative Investigation. Clin Orthop Relat Res. 2020;478(8):1850–66.

35. Jones CW, Jacobs H, Shumborski S, Talbot S, Redgment A, Brighton R et al. Sagittal Stability and Implant Design Affect Patient Reported Outcomes After Total Knee Arthroplasty. J Arthroplasty. 2020;35(3):747–51.

36. Angerame MR, Holst DC, Jennings JM, Komistek RD, Dennis DA. Total Knee Arthroplasty Kinematics. J Arthroplasty. 2019;34(10):2502–10.

37. Wada K, Hamada D, Takasago T, Kamada M, Goto T, Tsuruo Y et al. Intraoperative analysis of the kinematics of the native knee including two-dimensional translation of the femur using a navigation system : a cadaveric study. J Med Invest. 2019;66(3.4):367–71.

38. Pinskerova V, Vavrik P. Personalized Hip and Knee Joint Replacement: Knee Anatomy and Biomechanics and its Relevance to Knee Replacement. 1st ed. 2020. Cham:Springer International Publishing; Imprint Springer;2020. (Springer eBook Collection).

39. Kono K, Dorthe EW, Tomita T, Tanaka S, Angibaud L, D'Lima DD. Intraoperative knee kinematics measured by computer-assisted navigation and intraoperative ligament balance have the potential to predict postoperative knee kinematics. J Orthop Res. 2022;40(7):1538–46.

40. Grupp TM, Holderied M, Pietschmann MF, Schröder C, Islas Padilla AP, Schilling C et al. Primary stability of unicompartmental knee arthroplasty under dynamic flexion movement in human femora. Clin Biomech (Bristol, Avon). 2017;41:39–47.

41. Grupp TM, Pietschmann MF, Holderied M, Scheele C, Schröder C, Jansson V et al. Primary stability of unicompartmental knee arthroplasty under dynamic compression-shear loading in human tibiae. Clin Biomech (Bristol, Avon). 2013;28(9-10):1006–13.

42. Willing R, Moslemian A, Yamomo G, Wood T, Howard J, Lanting B. Condylar-Stabilized TKR May Not Fully Compensate for PCL-Deficiency: An In Vitro Cadaver Study. J Orthop Res. 2019;37(10):2172–81.

43. Bauer L, Woiczinski M, Thorwächter C, Müller PE, Holzapfel BM, Niethammer TR et al. Influence of kinematic alignment on femorotibial kinematics in medial stabilized TKA design compared to mechanical alignment. Arch Orthop Trauma Surg. 2023;143(7):4339–47.

44. Walker PS, Arno S, Borukhoy I, Bell CP. Characterising knee motion and laxity in a testing machine for application to total knee evaluation. J Biomech. 2015;48(13):3551–8.

45. Reynolds RJ, Walker PS, Buza J. Mechanisms of anterior-posterior stability of the knee joint under load-bearing. J Biomech. 2017;57:39–45.

46. Yang H, Bayoglu R, Renani MS, Behnam Y, Navacchia A, Clary C et al. Validation and sensitivity of model-predicted proximal tibial displacement and tray micromotion in cementless total knee arthroplasty under physiological loading conditions. J Mech Behav Biomed Mater. 2020;109:103793.

47. Bull AMJ, Kessler O, Alam M, Amis AA. Changes in knee kinematics reflect the articular geometry after arthroplasty. Clin Orthop Relat Res. 2008;466(10):2491–9.

48. Ghosh KM, Blain AP, Longstaff L, Rushton S, Amis AA, Deehan DJ. Can we define envelope of laxity during navigated knee arthroplasty? Knee Surg Sports Traumatol Arthrosc. 2014;22(8):1736–43.

49. C Millar S, Arnold JB, B Solomon L, Thewlis D, Fraysse F. Development and evaluation of a method to define a tibial coordinate system through the fitting of geometric primitives. Int Biomech. 2021;8(1):12–8.

50. Hancock CW, Winston MJ, Bach JM, Davidson BS, Eckhoff DG. Cylindrical axis, not epicondyles, approximates perpendicular to knee axes. Clin Orthop Relat Res. 2013;471(7):2278–83.

51. Brendle SA, Krueger S, Grifka J, Müller PE, Grupp TM. A New Methodology for the Accurate Measurement of Tibiofemoral Kinematics in Human Cadaveric Knees: An Evaluation of the Anterior–Posterior Laxity Pre- and Post-Cruciate Ligament Resection. Life. 2024;14(7):877.

52. Gasparutto X, Bonnefoy-Mazure A, Attias M, Dumas R, Armand S, Miozzari H. Comparison between passive knee kinematics during surgery and active knee kinematics during walking: A preliminary study. PLoS One. 2023;18(3):e0282517.

53. Belvedere C, Tamarri S, Ensini A, Durante S, Ortolani M, Leardini A. Can Computer-Assisted Total Knee Arthroplasty Support the Prediction of Postoperative Three-Dimensional Kinematics of the Tibiofemoral and Patellofemoral Joints at the Replaced Knee? J Knee Surg. 2021;34(9):1014–25.

54. Belvedere C, Tamarri S, Notarangelo DP, Ensini A, Feliciangeli A, Leardini A. Three-dimensional motion analysis of the human knee joint: comparison between intra- and post-operative measurements. Knee Surg Sports Traumatol Arthrosc. 2013;21(10):2375–83.

55. Fritzsche H, Beyer F, Postler A, Lützner J. Different intraoperative kinematics, stability, and range of motion between cruciate-substituting ultracongruent and posterior-stabilized total knee arthroplasty. Knee Surg Sports Traumatol Arthrosc. 2018;26(5):1465–70.

56. Grassi A, Pizza N, Lopomo NF, Marcacci M, Capozzi M, Marcheggiani Muccioli GM et al. No differences in knee kinematics between active and passive flexion-extension movement: an intra-operative kinematic analysis performed during total knee arthroplasty. J Exp Orthop. 2020;7(1):12.

57. Morooka T, Okuno M, Seino D, Iseki T, Fukunishi S, Kobashi S et al. Intraoperative kinematic analysis of posterior stabilized total knee arthroplasty with asymmetric helical post-cam design. Eur J Orthop Surg Traumatol. 2019;29(3):675–81.

58. Dupraz I, Renaudot R, Larrainzar-Garijo R, Ochs BG, McHugh G, Grupp TM. Defining Phenotypes in Total Knee Arthroplasty Based on Intra-Operative Kinematics: a Multi-Center Cohort of 3915 Patients.

59. Larrainzar-Garijo R, Murillo-Vizuete D, Garcia-Bogalo R, Escobar-Anton D, Horna-Castiñeiras L, Peralta-Molero JV. Dynamic Alignment Analysis in the Osteoarthritic Knee Using Computer Navigation. J Knee Surg. 2017;30(9):909–15.

60. Maderbacher G, Baier C, Springorum HR, Zeman F, Grifka J, Keshmiri A. Lower Limb Anatomy and Alignment Affect Natural Tibiofemoral Knee Kinematics: A Cadaveric Investigation. J Arthroplasty. 2016;31(9):2038–42.

61. Maderbacher G, Keshmiri A, Krieg B, Greimel F, Grifka J, Baier C. Kinematic component alignment in total knee arthroplasty leads to better restoration of natural tibiofemoral kinematics compared to mechanic alignment. Knee Surg Sports Traumatol Arthrosc. 2019;27(5):1427–33.

62. Krackow KA. Instability in total knee arthroplasty: loose as a goose. J Arthroplasty. 2003;18(3 Suppl 1):45–7.

63. Wilson CJ, Theodoulou A, Damarell RA, Krishnan J. Knee instability as the primary cause of failure following Total Knee Arthroplasty (TKA): A systematic review on the patient, surgical and implant characteristics of revised TKA patients. Knee. 2017;24(6):1271–81.

64. Jang SW, Kim MS, Koh IJ, Sohn S, Kim C, In Y. Comparison of Anterior-Stabilized and Posterior-Stabilized Total Knee Arthroplasty in the Same Patients: A Prospective Randomized Study. J Arthroplasty. 2019;34(8):1682–9.

65. Wautier D, Thienpont E. Changes in anteroposterior stability and proprioception after different types of knee arthroplasty. Knee Surg Sports Traumatol Arthrosc. 2017;25(6):1792–800.

66. Scott DF, Hellie AA. Mid-Flexion, Anteroposterior Stability of Total Knee Replacement Implanted with Kinematic Alignment: A Randomized, Quantitative Radiographic Laxity Study with Posterior-Stabilized and Medial-Stabilized Implants. J Bone Joint Surg Am. 2023;105(1):9–19.

67. Groot JD de, Brokelman RBG, Lammers PG, van Stralen GMJ, Kooijman CM, Hokwerda ST. Performance of medial pivot, posterior stabilized and rotating platform total knee arthroplasty based on anteroposterior stability and patient-reported outcome measures; a multicentre double-blinded randomized controlled trial of 210 knees. Arch Orthop Trauma Surg. 2024;144(5):2327–35.

68. Edelstein AI, Bhatt S, Wright-Chisem J, Sullivan R, Beal M, Manning DW. The Effect of Implant Design on Sagittal Plane Stability: A Randomized Trial of Medial- versus Posterior-Stabilized Total Knee Arthroplasty. J Knee Surg. 2020;33(5):452–8.

69. Kour RYN, Guan S, Dowsey MM, Choong PF, Pandy MG. Kinematic function of knee implant designs across a range of daily activities. J Orthop Res. 2023;41(6):1217–27.

70. Lützner J, Firmbach F-P, Lützner C, Dexel J, Kirschner S. Similar stability and range of motion between cruciate-retaining and cruciate-substituting ultracongruent insert total knee arthroplasty. Knee Surg Sports Traumatol Arthrosc. 2015;23(6):1638–43.

71. Brendle SA, Krueger S, Grifka J, Müller PE, Grupp TM. Tibiofemoral gaps of human cadaveric knees before and after sacrificing both cruciate ligaments. 28th Congress of the European Society of Biomechanics, Maastricht, Netherlands. 2023.

72. Dennis DA, Komistek RD, Kim RH, Sharma A. Gap balancing versus measured resection technique for total knee arthroplasty. Clin Orthop Relat Res. 2010;468(1):102–7.

73. Shalhoub S, Moschetti WE, Dabuzhsky L, Jevsevar DS, Keggi JM, Plaskos C. Laxity Profiles in the Native and Replaced Knee-Application to Robotic-Assisted Gap-Balancing Total Knee Arthroplasty. J Arthroplasty. 2018;33(9):3043–8.

74. Brendle SA, Krueger S, Grifka J, Müller PE, Grupp TM. Condylar motion of human cadaveric knees before and after sacrificing both cruciate ligaments. 34th Annual Congress of the International Society of Technology in Arthroplasty, New York, USA. 2023.

75. Brendle SA, Krueger S, Grifka J, Müller PE, Grupp TM. Condylar motion patterns during passive knee flexion are not only a result of osteoarthrosis. Annual Meeting of the Orthopaedic Research Society, Long Beach, USA. 2024.

Acknowledgements

First, I would like to thank my primary supervisor, Prof. Dr. med. habil. Dr.-Ing. Thomas M. Grupp, for his support throughout this thesis. I am immensely grateful for the incredible opportunity and all the inspiring conversations we have had over the past few years. Thanks also to my co-supervisors, Prof. Dr. med. Peter E. Müller and Prof. Dr. rer. biol. hum. Steffen Peldschus, for their always constructive criticism and invaluable feedback.

My appreciation also goes to my co-authors, Prof. Dr. med. Dr. h.c. mult. Joachim Grifka, Prof. William M. Mihalko MD PhD, Dr. Berna Richter and Janno Fehrenbacher, for their valuable input and feedback and for making the realization of the projects possible.

Furthermore, I would like to thank my colleagues in the biomechanical laboratory for creating such a wonderful working atmosphere and for their continuous support. Special thanks go to Sven Krüger for the close collaboration, endless discussions and all his support and valuable input. I would also like to thank Josef-Benedikt Weiß and Dr. Ana Laura Puente Reyna for their assistance over the years, and the team at the prototype workshop for the fast production of the endless number of test components.

Last but not least, I would like to thank my parents, grandparents, family and friends for their unconditional support, words of encouragement and for celebrating every successful step along the way with me. I am also very grateful to my partner Simon for always believing in me and supporting my goals. Your faith in me has been a great source of strength and motivation.